



UNIVERSITÀ DEGLI STUDI DI PARMA

**Department of Pharmacy
Laboratories of Biochemistry and Molecular Biology**

**PhD Program in
Biochemistry and Molecular Biology
XXVII cycle**

**Characterization of the human
O-phosphoethanolamine phospholyase,
an unconventional pyridoxal phosphate-
dependent β -lyase**

Coordinator:

Prof. Andrea Mozzarelli

Tutor:

Prof. Alessio Peracchi

**PhD student:
DAVIDE SCHIROLI**

2012-2014

INDEX:

Chapter 1: A subfamily of PLP-dependent enzymes specialized in handling terminal amines

Abstract.....	pg.10
Introduction.....	pg.11
-Nomenclature issues: subgroup-II aminotransferases, class-III aminotransferases or ω -aminotransferases?.....	pg.13
Chemical peculiarities of the reactions catalyzed by AT-II enzymes.....	pg.18
- Equilibria in ω -amine transaminase reactions.....	pg.18
- Specificity and dual-specificity issues.....	pg.22
Structural peculiarities of AT-II enzymes.....	pg.23
- AT-II vs. AT-I enzymes. Comparing the overall structures.....	pg.23
- AT-II vs. AT-I. Comparing the PLP-binding sites.....	pg.25
- The substrate binding site: a gateway system in α -KG-specific AT-II transaminases.....	pg.31
- The substrate binding site: P and O pockets in pyruvate-specific AT-II transaminases.....	pg.35
- An overview of substrate specificity in AT-II transaminases.....	pg.42

AT-II enzymes that are not aminotransferases.....pg.43

.....pg.43

Inferences on the evolution of AT-II enzymes.....pg.47

.....pg.47

Conclusions.....pg.53

.....pg.53

Purpose of the research.....pg.63

.....pg.63

Chapter 2: Strict reaction and substrate specificity of AGXT2L1, the human O-phosphoethanolamine phospho-lyase

Abstract.....pg.66

.....pg.66

Introduction.....pg.67

.....pg.67

Materials and methods.....pg.69

.....pg.69

-Materials.....pg.69

.....pg.69

-Enzymatic assays.....pg.69

.....pg.69

- Spectrophotometric measurements.....pg.70

.....pg.70

Results.....pg.72

.....pg.72

- Relatively unspecific inhibition of AGXT2L1 by anions.....pg.77

.....pg.77

- Spectroscopic screening of AGXT2L1 binding selectivity.....pg.77

- Aminotransferase activity of AGXT2L1.....pg.81

Discussion.....pg.84

-Evolution of AGXT2L1: of an aminotransferase a phospho-lyase made.....pg.84

-Determinants of binding selectivity in AGXT2L1.....pg.89

-Considerations on the biological role of AGXT2L1.....pg.90

Chapter 3: Kinetic characterization of the human O-phosphoethanolamine phospho-lyase reveals unconventional features of this specialized pyridoxal phosphate-dependent lyase

Abstract.....pg.98

Introduction.....pg.99

Results.....pg.102

-pH dependence of k_{cat} and K_Mpg.102

-pH dependence of the inhibition by selected anions.....pg.103

-Steady-state spectrophotometric and fluorometric analysis of the

interaction of PEA phospho-lyase with PEA, phosphate and 3-APP.....pg.105

-Multi- and single-wavelength pre-steady-state kinetics.....pg.109

-NaBH₄ reduction of different PLP species at the active site of PEA phospho-lyase.....pg.115

Discussion.....pg.118

-A noncovalent enzyme-substrate complex accumulates at the steady-state of the PEA phospho-lyase reaction.....pg.118

-PEA phospho-lyase as an example of selectivity-efficiency tradeoff.....pg.120

-The active site of PEA phospho-lyase is set to bind dianions.....pg.122

-Considerations on the inhibition of PEA phospho-lyase by phosphate.....pg.124

-Conclusions.....pg.126

Materials and methods.....pg.127

-Materials.....pg.127

-Enzymatic assays.....pg.127

-Inhibition studies.....	pg.127
-pH dependence analysis.....	pg.129
-Spectrophotometric measurements.....	pg.129
-Fluorometric measurements.....	pg.129
-Stopped-flow measurements.....	pg.130
-Singular value decomposition analysis.....	pg.131
-NaBH ₄ treatment of the enzyme-PEA complex.....	pg.132

Chapter 4: Enzyme-based fluorometric assay for the quantitative analysis of O-phosphoethanolamine in biological fluids

Abstract.....	pg.143
Introduction.....	pg.144
Materials and methods.....	pg.147
-Materials.....	pg.147
-Design of the resazurin-based fluorescence assay for PEA quantitation.....	pg.147
-Deproteinization methods.....	pg.148

-Expression and purification of ethanolamine kinase.....pg.148

-PEA and ³²P-PEA production.....pg.149

-Analytical thin layer chromatography.....pg.149

Results.....pg.150

-Optimization of buffer features and of reagent concentrations for the fluorometric PEA assay.....pg.150

-Fluorescence assay: range of linearity of the readout and test of the assay on plasma ultrafiltrate supplemented with PEA.....pg.151

-Assay with radioactive PEA: analysis of the deproteinization methods and of the fluorescence assay reaction, using ³²P-PEA.....pg.152

-Conclusions.....pg.155

A subfamily of PLP-dependent enzymes specialized in handling terminal amines

Davide Schiroli and Alessio Peracchi

From the Department of Life Sciences, Laboratory of Biochemistry, Molecular Biology and Bioinformatics, University of Parma, 43124 Parma, Italy

¹Corresponding author. Address: Department of Life Sciences, University of Parma, 43124 Parma, Italy. Phone: +39 0521905137 Fax: +39 0521905151. Email: alessio.peracchi@unipr.it

Keywords: pyridoxal-phosphate; ω -aminotransferases; dual-specificity; evolution of enzyme families

Abbreviations: PLP, pyridoxal 5'-phosphate; PMP, pyridoxamine 5'-phosphate; α -KG, α -ketoglutarate; GABA, γ -aminobutyrate; AT, aminotransferase; AT-I, Subgroup-I aminotransferases; AT-II, Subgroup-II aminotransferases; AspAT, Aspartate aminotransferase; AroAT, Aromatic aminotransferase ; ω -AT, ω -amine aminotransferase. Other abbreviations for specific aminotransferases are given in Table 1.

ABSTRACT

The present review focuses on a subfamily of pyridoxal phosphate (PLP)-dependent enzymes belonging to the broader fold-type I structural group and alternatively termed subgroup-II aminotransferases (P.K. Mehta, T.I. Hale, P. Christen, (1993) *Eur. J. Biochem.*, 214, 549-561) or class-III aminotransferases (V. Grishin, M.A. Phillips, E.J. Goldsmith, (1995) *Prot. Sci.* 4, 1291-1304). As the names suggest, this subgroup includes mainly transaminases, with just a few interesting exceptions. However, at variance with most other PLP-dependent enzymes, catalysts in this subfamily seem specialized at utilizing substrates whose amino group is not adjacent to a carboxylate group.

Subgroup-II aminotransferases are widespread in all organisms, where they play mostly catabolic roles. Furthermore, today several ω -transaminases in this group are being used as bioorganic tools for the asymmetric synthesis of chiral amines. We present here an overview of the biochemical and structural features of these enzymes, illustrating how they are distinctive and how they compare with those of the other fold-type I enzymes.

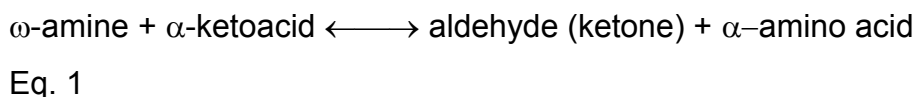
1. Introduction

Pyridoxal phosphate (PLP) arguably represents the most versatile organic cofactor in biology, being used by a variety of enzymes in all organisms [1-5]. PLP-dependent enzymes almost invariably catalyze reactions that involve amino compounds, since PLP can bind covalently to the amino group of the substrate and then act as an electrophile to stabilize different carbanionic intermediates [1, 4, 5]. Building on this shared mechanistic feature, PLP-dependent enzymes comprise, among others, transaminases, decarboxylases, racemases, aldolases, lyases, and enzymes that catalyze β - or γ -replacement reactions [1-5]. In spite of this functional diversity, all PLP-dependent enzymes structurally characterized to date can be grouped in just seven distinct structural families, or 'fold-types' [6-9], presumably corresponding to different evolutionary lineages. Of these, the so-called fold-type I is the most populated, functionally and structurally diverse and arguably the most evolutionarily ancient.

We focus herein on a subgroup of PLP-dependent enzymes belonging to the broader fold-type I family. Mehta, Christen and co-workers reported for the first time in 1993 a classification of aminotransferases (AT) in different subgroups, based on an algorithm that took into account sequence comparison, hydropathy patterns and secondary structure features of 51 ATs [2, 10, 11]. One of four identified subgroups (distinguished by roman numerals) included as prototypical enzymes ornithine δ -transaminase and γ -aminobutyrate (GABA) transaminase and was termed subgroup-II aminotransferases (AT-II; [2, 10-12]).

An updated list of AT-II is provided in Table 1. As suggested by the name, most enzymes in this subfamily are indeed aminotransferases, using either α -ketoglutarate (α -KG) or pyruvate as the preferred

amino group acceptor. The amino group donors instead are generally compounds where the amino group is located distal to a carboxylate and usually at the end of an alkyl chain. These compounds are conventionally called ω -amines, and their transamination leads to production of an aldehyde (or less frequently a ketone) as shown in Eq. 1.



The first ω -amine-specific transaminases (later shown to belong to AT-II) were described in the mid-1960s [13, 14], and their number has kept increasing over time, as summarized in a recent paper by Rausch et al. [15]. A great amount of biochemical, physiological, structural and applicative information has been accumulating on these enzymes, while at the same time studies have also identified some strictly related AT-II members that do not act as transaminases (Table 1).

In relation to this, we examine the literature and analyze sequences and three-dimensional structures trying to address some general points: What are the peculiar features of the reactions catalyzed by AT-II enzymes? What differentiates them structurally from the other enzymes of the fold type I? Are there structural properties that make the enzymes in this subfamily particularly apt at handling terminal amines? What features contribute to their substrate and reaction specificity? Our analysis also offers an overview of the evolution of these proteins, integrating it with the broader issue of the evolution of fold-type I enzymes.

1.1 - Nomenclature issues: subgroup-II aminotransferases, class-III aminotransferases or ω -aminotransferases?

To describe the group of enzymes in table 1, we will follow here the original designation of AT-II given by Mehta, Christen and co-workers [2, 10, 11]. However it is essential to note that just a couple of years after the first study by Mehta et al. [10], Grishin and coworkers re-named the very same subfamily of enzymes 'class III aminotransferases' [6]. The change arose due to those authors splitting subgroup I (identified by Mehta et al.) into two smaller subfamilies. While this operation was based on reasonable structural considerations, Grishin and coworkers quite arbitrarily proceeded to rename the new subfamilies "Class I" and "Class II", shifting up the roman numbering for all other subgroups [6].

The Grishin et al. classification has been adopted by some databases such as PROSITE [16]. Pfam [17] reunites the classes I and II (as defined by Grishin et al.) into a single family, but instead of reverting to the original Mehta et al nomenclature calls this family "Aminotransferases Class I and II", while it retains the definition "Class III aminotransferases" for the enzymes in Table 1

(<http://pfam.sanger.ac.uk/family?entry=PF00202>) [18].

Often the aminotransferases of the AT-II group are also collectively referred to as ω -amine ATs or simply ω -transaminases (ω -ATs; as noted above, the letter ω is meant to broadly denote compounds whose reactive amino group is not in α -position with respect to a carboxylate). [19-22] The name amine-TA is instead used referring to enzymes converting ketones into amines. These enzymes are especially important for organic synthesis and it is possible to find large literature about them [23], for this reason this group of AT-II enzymes is not extensively pre-

sented during this review (see chapter 2.1). The reader should be aware that while the AT-II (or “Class III AT” according to Grishin and coworkers) classification is based on sequence and structure criteria, the definition ω -amine ATs is functional, so the two denominations do not really overlap.

In particular, as noted, there are some AT-II members that are not aminotransferases at all (Table 1). On the other hand, at variance with the statements found in some authors (e.g., [22]), AT-II is not the only subgroup of PLP-dependent enzymes containing ATs that act on ω -amino-compounds. For example 2-aminoethylphosphonate-pyruvate AT (belonging to fold-type I, but not to AT-II; [24]) acts on a substrate that definitely qualifies as an ω -amine. Several ω -transaminases have also been identified belonging to fold-type IV; these enzymes are being used (much like some belonging to the AT-II subgroup; see section below) for both the asymmetric synthesis and resolution of chiral amines [22, 25].

Table 1: PLP-dependent enzyme belonging to the AT-II subgroup.

Enzyme name	Acronym ¹	Sequence ²	E.C.	Substrates	
				First (amino group donor)	Second (acceptor)
Aminotransferases					
γ -aminobutyrate AT	GABA-AT	GABT_HUMAN ³ GABT_ECOLI ³	2.6.1.19	γ -aminobutyrate (GABA)	α -KG
Ornithine AT	OAT	OAT_HUMAN	2.6.1.13	L-ornithine	α -KG
Acetyloronithine AT	ACOAT	ARGD_ECOLI	2.6.1.11	N ₂ -Acetyl-L-ornithine	α -KG

Succinylornithine AT	SOAT	4ADE	2.6.1.81	N ₂ -succinyl-L-ornithine	α-KG
L-lysine δ-aminotransferase	LAT	LAT_STRC ⁴ BAB13756 ⁴	2.6.1.36	L-lysine	α-KG
Putrescine AT	PUAT	NP_417544	2.6.1.29/ 2.6.1.82 ⁵	cadaverine, putrescine	α-KG
Diaminobutyrate AT	DABAAT	DAT_ACIBA	2.6.1.76	L-2,4-diaminobutyrate	α-KG
D-4-hydroxyphenylglycine AT	D-FGAT	AAQ82900	2.6.1.72	D-4-hydroxyphenylglycine	α-KG
Neamine AT	NEAT	Q53U08	2.6.1.93	Neomycin C, Neamine	α-KG
2'-deamino-2'-hydroxyneamine AT	DHNEAT	Q6L741	2.6.1.94	2'-deamino-2'-hydroxyneamine, Neamine	α-KG
3-aminobenzoate synthase	ABS	BAF92604	-	L-Glutamate ⁶	3-dehyd roshikimate
L-Glutamate 1-semialdehyde (GSA) aminomutase ⁷	GSA	GSA_ECOLI	5.4.3.8	glutamate 1-semialdehyde (GSA) ⁷	aminolevulinic acid (ALA)
β-alanine-pyruvate AT	βA-PAT	OAPT_PSEPU	2.6.1.18	β-Alanine	Pyruvate
γ-aminobutyrate-pyruvate AT	GABA-PAT	AFS28621	2.6.1.96	γ-aminobutyrate	Pyruvate, Glyoxylate
Putrescine-pyruvate AT	PU-PAT	AAG03688	--	Putrescine	Pyruvate
D-3-aminoisobutyrate pyruvate AT	AGXT2 ⁸	AGT2_RAT	2.6.1.40 /43/44 ⁸	(D)-3-aminoisobutyrate	Pyruvate, Glyoxylate
Taurine-pyruvate AT	TAU-PAT	TPA_BILWA	2.6.1.77	Taurine	Pyruvate
Fumonisin-pyruvate AT ¹²	FUMAT	ACS27061	-	fumonisin B ₁ , hydrolyzed fumonisin B ₁	Pyruvate
Dialkylglycine decarboxylase ⁹	DGDA	DGDA_BURCE	4.1.1.64	(Isopropylamine)	Pyruvate

7,8-diaminopelargonate AT	DAPA-AT	BIOA_ECOLI	2.6.1.62	S-adenosyl-L-methionine (SAM)	7-keto-8-aminopelargonic acid (KAPA) ¹⁰
Lysine-7,8-diaminopelargonate AT ¹³	K-DAPA-AT	Q8KZN0_BACIU		Lysine	7-keto-8-aminopelargonic acid (KAPA) ¹⁰
Amine-pyruvate AT ¹¹	ω -PAT	AEA39183	-	Various ω -amines	Pyruvate
β -amino acid AT ¹¹	β -AT	ABL7437	-	Various β -amino acids	Pyruvate, α -KG
3-Acetyloctanal transaminase ¹⁴	AcOCT-AT	L7ZI44_SERMA	--	?	3-Acetyloctanal
acyl-CoA beta-transaminase ¹⁵	COA- β -AT	KAT_CLOAI	--	3-aminobutyryl-CoA	α -KG
AT domain of a polyketide synthase ¹⁶	PKS-ATd	MYCA_BACIU	--	Glutamine	β -ketothioester
Isomerases					
2-aminohexano-6-lactam racemase	AH6L-R	Q7M181	5.1.1.15	L-2-aminohexano-6-lactam	-
Isoleucine 2-epimerase	ILE-R	AGE45209	--	L-Isoleucine	-
Lyases					
O-phosphoethanolamine phospholyase	PEA-PL	NP_112569	4.2.3.2	O-phosphoethanolamine	-
5-phosphohydroxy-L-lysine phospholyase	PHK-PL	Q8IUZ5	4.2.3.134	5-phosphohydroxy-L-lysine	-

¹ Abbreviation used in this review to indicate to the specific enzyme.

² Accession number in UniProtKB of a representative enzyme with validated activity.

³ Two phylogenetically distinct groups of GABA-AT enzymes exist, one bacterial [26] and one eukaryotic [27], thus one representative sequence per group is given.

⁴ Two phylogenetically distinct groups of LAT enzymes have been described, one from Gram+ [28] and the other from Gram- bacteria [29]; one representative sequence per group is given.

⁵ The listed PUAT enzyme (from *Escherichia coli*) can transaminate efficiently both putrescine and cadaverine [30], and can be legitimately assigned to two different EC numbers.

⁶ 3-ADHC =3-amino 4,5-dihydroxy cyclohex-1-ene-1-carboxylate. The enzyme ABS physiologically catalyzes the transamination between L-glutamate (amino group donor) and 3-dehydroshikimate (amino group acceptor), yielding α -KG and 3-ADHC [31]. The latter product rapidly and irreversibly undergoes the elimination of two water molecules, becoming converted to 3-aminobenzoate. It is not known whether the double dehydration step is catalyzed by the same enzyme or occurs spontaneously [31].

⁷ Despite being formally classified as an isomerase, GSA catalyzes an internal transamination between carbons 1 and 2 of L-glutamate-1-semialdehyde. The reactive form of the enzyme contains PMP at the active site, and in the first step of the reaction mechanism glutamate semialdehyde acts as the amino group acceptor, receiving the amino group from PMP and forming 4,5-diaminovalerate [32, 33]. This product is not released from the active site, however, and functions as the amino group donor in the second part of the reaction, to yield the final product 5-aminolevulinate.

⁸ Mammalian AGXT2 is a promiscuous mitochondrial transaminase that acts on a variety of substrates – in addition to D-3-aminoisobutyrate, these substrates

include L-alanine, 5-aminolevulinate, β -alanine [34, 35]. Accordingly, the enzyme can be assigned to different E.C. numbers.

⁹ Dialkylglycine decarboxylase is listed among the transaminases because its catalytic mechanism encompasses an amino transfer [36, 37]. DGD cannot directly transaminate its substrate (a 2,2-dialkylglycine, which lacks an α -proton), but proceeds to decarboxylate it and then catalyzes a transamination with the decarboxylation product (a dialkylamine, such as isopropylamine), to yield the corresponding ketone [36, 37].

¹⁰ ADO-MeOB = S-Adenosyl-4-methylthio-2-oxobutanoate. The enzyme DAPA-AT is involved in the biosynthesis of biotin, whereby it catalyzes the transamination between S-adenosyl-L-methionine (amino group donor) and 7-keto-8-aminopelargonate (amino group acceptor), to yield 7,8-diaminopelargonate and ADO-MeOB [38].

¹¹ ω -P AT are enzymes studied and used for their biotechnological potentials. Their physiological functions are not known. They can react with various substrates and ketoacids. Even if they transaminate an amine (e.g. (S)- α -methylbenzylamine) they are not able to catalyze the same reaction with β -alanine. Similarly also the β -AT enzymes have been studied only for their biotechnological applications [21].

¹² [39, 40]. ¹³ [41, 42]. ¹⁴ [43, 44]. ¹⁵ [45].

¹⁶ This enzyme represent a aminotransferase domain of multi-domain polyketide synthase[46].

2- Chemical peculiarities of the reactions catalyzed by AT-II enzymes

2.1- Equilibria in ω -amine transaminase reactions

Aminotransferase reactions involving standard amino acids (as donors of their α -amino group) and α -keto acids are generally reversible and their equilibrium constant is often not far from unity [47]. AT-II enzymes are quite peculiar not just because one of the substrates is an amine, but also because one of the two amino group acceptors involved

in the equilibrium is not an α -keto acid but an aldehyde. Given the high reactivity of aldehydes, one might expect the reaction in Eq. 1 to proceed more favorably in the direction of the amine, but under physiological conditions this is not the case.

In fact, while most of the transaminase reactions catalyzed by the AT-II enzymes are reversible *in vitro*, in cells they are nearly always driven towards consumption of the amine. The factors contributing to this behavior do not seem attributable to the transaminases themselves, but rather to the occurrence of spontaneous or tightly coupled enzymatic reactions that follow formation of the aldehyde and determine an almost unidirectional metabolic flux.

For example, the products of lysine AT (α -aminoadipate- γ -semialdehyde) and of putrescine AT (4-aminobutanal), spontaneously convert to cyclic compounds (Δ 1-piperidine-6-carboxylate and 1-pyrroline, respectively) through formation of an intramolecular Schiff base [28], and this is expected to drive the reaction in Eq. 1 to the right. *In vivo*, the reactions catalyzed by these enzymes are strongly biased in favor of amino substrate degradation [29, 48].

Likewise, the reaction of taurine-pyruvate aminotransferase is reversible *in vitro* but in bacteria it only proceeds towards the consumption of taurine and the production of sulfoacetaldehyde [49]. In this case the phenomenon can be attributed to the presence of an acetyltransferase, which metabolizes sulfoacetaldehyde to acetyl phosphate and sulfite [50, 51].

An analogous discrepancy between the *in vitro* and *in vivo* situation is observed also in the case of the reaction catalyzed by mammalian GABA-AT. The equilibrium of this reaction apparently favors the formation of GABA *in vitro* [52], but *in vivo* GABA-AT serves primarily to the

degradation of the amine (e.g., [53]), presumably because the product of GABA transamination, the reactive succinic semialdehyde, is detoxified by succinic semialdehyde dehydrogenase in a tightly coupled reaction [54].

In plants, GABA-PAT transaminates GABA using pyruvate or glyoxylate instead of α -KG as an amino group acceptor. The reaction seems to proceed unidirectionally towards GABA degradation [55]. In addition to the presence of succinic semialdehyde dehydrogenase in plants [56], this is probably due to the fact that the reaction catalyzed by GABA-PAT with glyoxylate is completely irreversible [55]. An analogous near-irreversibility is observed also in other PLP-dependent transaminations where glyoxylate serves as the amino group acceptor [57-61] as well as in the transamination between free pyridoxamine and glyoxylate [62]. Such a strong bias presumably reflects the high reactivity and relative thermodynamic instability of glyoxylate, which not only is an aldehyde, but is also subject to the electron-withdrawing effect of the nearby carboxylic group.

A rare case of ω -AT reaction that appears to be effectively reversible both *in vitro* and *in vivo* is represented by the ornithine aminotransferases (OAT) reaction. In this instance the spontaneous and reversible cyclization of the product glutamate- γ -semialdehyde, to Δ^1 -pyrroline-5-carboxylate, does not seem to prevent the reverse process, at least in mammals [63, 64]. In plants, however, OAT appears to play only a catabolic role [65].

The striking predominance of metabolic reactions in which the amine is consumed and the aldehyde is formed may have a biological, as well as chemical, significance. Due to their substantial reactivity, it is important that aldehydes do not accumulate during metabolism [66].

Aminotransferase reactions, on the other hand, are intrinsically rather slow processes, owing to their complex ping-pong mechanism. Accordingly it may be speculated that, if the main task of ω -ATs was to consume (rather than to produce) aldehydes, buildup of these compounds might be relatively facile and represent a liability for the organism.

In any instance, understanding the factors that modulate the equilibria and fluxes of ω -AT reactions has a very concrete and practical interest, as these transaminases are being used as bioorganic tools for the enantiopure synthesis of chiral amines. In such syntheses, the amines are produced from the corresponding ketones, exploiting the reaction of eq. 1 in the reverse direction. The enantiopure synthesis of chiral amines is highly desirable for the preparation of many compounds of pharmaceutical interest [15, 22, 67].

In the asymmetric synthesis of chiral amino compounds, in order to obtain a good yield of the desired product, it is necessary to define and, often, to change the chemical equilibrium of the reaction. As noted above, the amino acceptor in this case is not an aldehyde but a ketone and it is commonly accepted that transaminations of ketones are thermodynamically unfavourable [68-72]. Ketones have in fact a relatively low electrophilicity of the carbonyl carbon, as compared with α -keto acids and aldehydes, and are more stable than the corresponding amines. To overcome these problems, in the bioorganic applications of ω -ATs, the equilibrium is usually shifted from the side of substrate ketone to the desired product amine by removing the co-product through chemical or enzymatic means. In particular, if the co-product is pyruvate, it can be reduced to lactate by lactate dehydrogenase. To ensure a continuous regeneration of NADH to work, in these systems, a NADH recycling en-

zyme is added to the solution, usually glucose dehydrogenase. Nevertheless it is difficult to obtain the best activity and stability for all the three elements of this enzymatic system. At the moment however only few alternative approaches are reported in literature, e.g. it is possible to use isopropylamine as the amino-donor [73, 74] or an alternative coupled reaction with pyruvate decarboxylase, which does not need NADH [69]).

2.2 - Specificity and dual-specificity issues.

PLP-dependent enzymes acting on α -amino acids can bind their substrates by interacting with two parts of the substrate molecule, in addition to the amino group -namely the α -carboxylate and the side chain. As a first approximation, since all amino acids contain an α -carboxylic group, interactions with this group will only contribute to binding affinity, while interactions with the side chain will confer specificity. In contrast, enzymes acting on terminal amines must seek both binding affinity and specificity *via* interactions with the side chain of the substrate.

The implementation of specificity is particularly delicate in aminotransferases, whose reactions typically require two different substrates to bind in succession to the same cofactor in the same active site. Accordingly, these enzymes must be able to accommodate both substrates while discriminating against all others [4, 75]. Consider for example the case of aromatic amino acid aminotransferase (AroAT) , which uses α -KG as the amino group acceptor: for this enzymes, the problem of dual specificity entails accommodating the negatively charged γ -carboxylate of α -ketoglutarate in a site that must also accept the large hydrophobic side chain of an aromatic amino acid [4].

The problems associated to dual specificity are more pronounced for transaminases where the donor substrate is a terminal amine, since

their substrates, besides differing in their 'side chain' properties, also differ due to the presence/absence of an α -carboxylate. For example, the active site of putrescine AT (PUAT, Table 1) must accommodate both α -KG (which possesses a negatively charged side chain and an α -carboxylate) and putrescine (positively charged side chain, no α -carboxylate) while discriminating against L-ornithine (positively charged side chain plus an α -carboxylate). Despite the complexity of this exercise, the enzyme from *E. coli* fares relatively well, reacting with putrescine some 50-fold better than with L-ornithine [30]

3- Structural peculiarities of AT-II enzymes

3.1 - AT-II vs. AT-I enzymes. Comparing the overall structures

To try to assess what features help AT-II enzymes achieving their peculiar functional specialization, it seems useful to compare the structure of the most studied AT-II transaminases with that of the prototypical aminotransferase, the aspartate aminotransferase (AspAT, assigned by Mehta and Christen to the structural subgroup AT-I). Both AT-I and AT-II enzymes are generally homodimers or homotetramers; a first inspection of the subunit architecture reveals however some important differences between the two types of proteins (Figure 1 A-B).

It is possible to subdivide a fold-type I subunit into two domains: a larger one, whose central feature is a seven-stranded mixed β sheet, and a smaller discontinuous domain. This small domain is formed by the C-terminus of the protein chain, which contributes an antiparallel β -sheet (e.g., four strands in GABA-AT) plus some α -helices that lean against it, and by the N-terminus, contributing a few α -helices (usually one or two) and some antiparallel β strands (three or four).

Analyzing Figure 1A-B, it is evident that the N-terminal part is not conserved between AT-II and AT-I, as confirmed by the literature [6, 10], where this is described as the major determinant of diversity between the subgroups of the fold type I [8, 76].

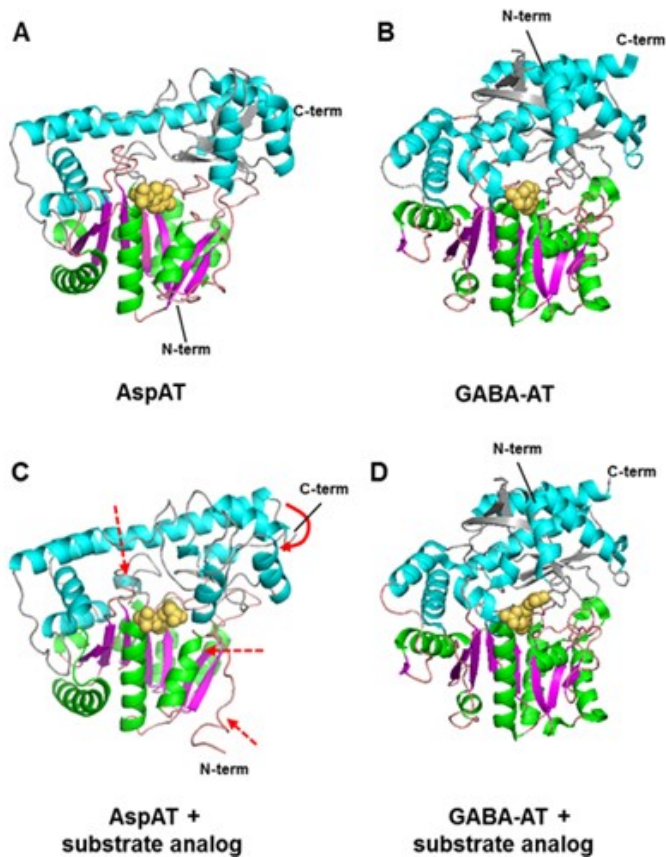


Figure 1: Comparison of the structure of a prototypical AT-I enzyme (mitochondrial AspaAT from *Gallus gallus*) with a prototypical AT-II enzyme (GABA-AT from *Escherichia coli*). (A) Structure of holo-AspAT (PDB ID: 7AAT), the small domain is shown in light blue and gray, the large domain is in green and magenta. PLP is shown in yellow. (B) Structure of holo-GABA-AT (PDB ID: 1SF2). GABA-AT and AspAT share similar large domains, while the small domain, and in particular the N-terminal part, is not conserved. (C) Structure of

AspAT in closed conformation, bound to the inhibitor aminooxyacetate (PDB ID: 1OXP) [77]. The transition between the open and closed conformation is determined by some structural rearrangements: one involves the movement of three α -helices and few β -strands, indicated by a continuous curved arrow. Other minor rearrangements are indicated by with dotted arrows. (D) Structure of GABA-AT complexed with aminooxyacetate (PDB ID: 1SFF) [26]. In this case, no large structural rearrangements are observed upon ligand binding.

For example in AspAT and AroAT (both AT-I) the N-terminal part starts on the surface of the second subunit and then crosses over the active site cleft before joining the small domain. Moreover an α -helix of the N-terminus is part of the active site entrance and interacts with the β -sheet in the C-terminal part of the small domain. These elements are not conserved in AT-II enzymes, where the N-terminal β -sheet and an α -helix simply form a meander in the active site, wedged between the large and the small domains [76].

The C-terminal part of the small domain and the large domain are instead quite conserved between AT-I and AT-II. The large domain has some structural elements that are retained in all the enzymes of fold type I [8]. It is constituted by an helix-loop-helix segment followed by a central seven-stranded β -sheet with complex topology: six parallel and one antiparallel β -strands. The β -strands are surrounded by various α -helices (e.g., 10 in GABA-AT [78]) in a typical α/β fold [79].

3.2 - AT-II vs. AT-I. Comparing the PLP-binding sites

The description above points to some macroscopic structural differences between AT-I and AT-II enzymes, but does not indicate whether such differences are important to explain the peculiar specialization of

AT-II enzymes towards terminal amines. Much clearer insights can be gained by an analysis of active site structures.

The active site of these enzymes can be schematically divided in two parts, one that interacts with the substrate and another one with the cofactor. This latter part is relatively conserved and in the case of AT-II enzymes it is located in the large domain at the interface with the small domain. The phosphate group of PLP is nestled in a specific subsite, sometimes called 'phosphate binding cup', forming a network of several hydrogen bonds to side chains, backbone amide groups and water molecules. All these interactions recur similarly in the structure of AT-II enzymes as well as in that of AspAT [80, 81]. Also, in both the AT-I and AT-II enzymes, the PLP ring is held in place by a hydrogen bond between the pyridine nitrogen and the side chain carboxylate of an Asp residue. This is probably the most conserved residue among the entire fold type I and the mechanistic importance of its interaction with the pyridine ring has been analyzed in several works [5, 76, 82] (Figure 2).

In contrast to the above, other features of the active site and of the interactions between the enzyme and the cofactor are quite distinctive of AT-II enzymes as compared to AT-I [8, 76]:

First of all, the catalytic Lys residue, that covalently binds to PLP and that plays a crucial role in all the PLP-dependent reactions, is not always in the same position in the two subfamilies of enzymes [8, 76]. Even if it is always placed in the loop that connects the last two strands of the large domain, the Lys residue is located earlier in the polypeptide chain of AT-II enzymes (Fig. 3) [8].

This fact is in all likelihood due to a deletion occurred during the evolution of AT-II.

Figure 2: Schematic active site model of AT-II based on structural comparison of enzymes belonging to this subgroup. Some key residues (or group of residues) are indicated by numbers from (1) to (4): (1) Residues involved in the interaction with the α -carboxylic group of the substrate (in pyruvate-specific ATs it may also interact with β or γ carboxylic groups) (2) Residues interacting with the phosphate of PLP (3) Residue interacting with the pyridine nitrogen of the PLP ring (4) Residue interacting with the 5' hydroxyl group of PLP (e.g. Asn). Residues in (1) and (3) are conserved among all the ATs in AT-II. The tabular part of the figure resumes the actual amino acids identities in some known 3D structures of AT-II enzymes, These residues often are not aligned (Figure 3) and they can have different positions inside the structure (Arg residues, column 1) but they have the same role in contacting substrate or cofactor. The symbol * indicates residues that, despite not being alignable with the Gln found in the majority of the enzymes, appear to play the same role in the three-dimensional structure. The symbol - Indicates that a residues in the active site is not directly interacting with the PLP O3' group, but through hydrogen bond with a molecule of water.

Furthermore, a residue providing a hydrogen bond to the phenolic oxygen of the cofactor is present in all the AT-II enzymes except DAPA-AT and few other enzymes (e.g. [83]), where the hydrogen bond is water-mediated. This interaction, that is important for the stability of the internal aldimine [8, 76], is not conserved in fold type I. It determines the pK_a of the internal aldimine (the Schiff base of the PLP with the catalytic lysine), while different networks of residues are involved in electron distribution within the PLP in other classes of PLP-dependent enzymes, like AT-I [84]. Finally, in both AT-I and AT-II enzymes there is an aromatic residue stacking on the PLP pyridine ring. This residue is part of a loop that faces in the active site and it has an important role in

OAT_HUMAN	409	GD	IRFAPPLVDEEEDRESI	ELTNTTILGF		
OAT_VIGAC	400	GD	IRFATTHRRGTDRMCQ	YTKYKH		
OAT_PLAFD	380	DK	IVRLTFPLCIKEDIDECT	ELIVKTVKFFDDNL		
OAT_ARATH	416	NT	IVRLTFPLLSIDSDIDDS	ELIVKTVKFFDDNL		
ACCOAT_ECOLI	372	PD	IVRFAPPLVDEEADIDEGM	QRFPAHAKVYVGA		
SOAT_ECOLI	370	GN	IVRFAPALNVSEEDTGL	DRFPAACEHFVSGSS		
ACCOAT_YEAST	381	KG	IVRFAPALTIEDIDIEHDM	DAPFKAIEAVVA		
FUAT_ECOLI	392	AK	IVRIEPLFLTIEQCELVI	KAKRKAIAAMRVSEEA		
GABA_ATm_HUMAN	469	DK	IRFRPPLVFRDRHAIHFL	NIPSDIADDF		
GABA_ATm_YEAST	441	VH	IRFRPPLTFRERHIDPTI	TIHAKG		
LATOP_MYCTU	358	AD	IVRFPRPLTFTABIDAAI	AAVRSALPVVT		
LATOP_NOLA	419	TR	GRFRPPLTFTVSEEDIDGL	EALJASIASRS		
DABA_AT_HALEL	389	GV	IVKLCLEPLTIDEDLVGGL	DILEQGVKVEYFGA		
DABA_AT_PSEABD	384	GE	IVKLMPLTPTDIDEDGL	RAPFESVAAALGE		
DABA_AT_PSEAB	436	GV	IVRFPLTIDEGQIEEVA	RKFAHIAAALAG		
GABA_ATa_ECOLI	394	YN	IVRIIVLPLTIDEAQIRGL	ELISQDCEARQ		
D_PGAT_PSEBT	406	GR	GVFLSAGHREHREHVLVTTFDRVLRADENL	LSWGGTILSGNS		
DBRAT_STICE	370		
HEAT_STFR	365	AR	ICERLAPVAGGEVGGDAAR	YRVAMNMDGLRQAPDREETTGLARLLDD		
LATOP_XANM	459	EN	IRFPFAMDEEIDLLVG	LIDAKIKGPRVQAREAA		
DAT_MG_LIK	414	MA	LEIADAGDAFA	EALAQVIGQALIM		
DAT_POL_J8666	412	LV	LELFFDAGADEFT	AALDAMVTARHALLPVAG		
GSA_ECOLI	388	FE	AGPVSANM	RTIDANRVFKLI		
GSA_SYNEL	409	FE	AGTSLAHE	ADIE		
GSA_PROFR	401	FE	AWFCSTALDD	DDLEVIDAGLRKAAQAAAGLESLEVR		
GSA_SILSO	397	YE	ITTAANKD	IVIA		
FUMAT_SPHM	378	MF	IAAHTVDVDTTEATD	RAPSAVURDFASLQPHFILMLQAGA		
DAPA_AT_ECOLI	395	KI	ITLMPFYILPQIQRLT	AAVHRAVDTEFFCQ		
DAPA_AT_MYCTU	404	NI	VAMPFYICTFAEITQIT	FAMVVRVRLVSEF		
TAU_PAT_RHCOF	420	AT	MIISPLVADDEHSEL	HGISMLTIDKAIQF		
TAU_PAT_PANDE_PD1222	427	NI	TEISALITADNERTIT	DALDIAITKVA		
IA_PAT_ECHDE	410	D	ILVSPFLVDENQIQIF	EQIGKRVKEVA		
wPAT_PSEAE	418	D	TQFPFNAREEDRIF	DVGEALUNGIA		
wPAT_VIEFL	419	Q	IVLCPFLTEAQNEMF	DKLEKADVFAVA		
wPAT_RHCOF	429	D	TALCPFLTEADVARIL	ERMGRARTADWARAELV		
GABA_PAT_ARATH	462	D	GLMSPLIISPEIDELI	STVGRAKATEKVKELKAGHK		
wPAT_CHELY	420	D	IVSAPFLVTRAEIDEL	AVAEKIEEFTQLEAGLA		
FU_PAT_PSEAE	421	D	IVISPLVIDPSQIDELI	TIARCKLDQTAAVIA		
AGRTZ_HUMAN	478	S	TRFAPSMIKFPEFAV	EVFRDAITGMERRAR		
DGDA_BURCE	402	G	FRFAPPLVSEEDIDGL	DALDIAITKVA		
ANGLR_ACHOB	392	GN	IVFTPLTITETDHRKAL	DILDRAPSELS	AVSNEEIAQFAG	
ILR_K_LACRU	404	GN	IVFPPLVIREQDQAL	QVLDGATAVENGVEYTIKPTGSEGV		
PEA_P_HUMAN	406	RN	IVKIFPMCFEEDAKFMV	DQLDRIITVLEEAMTKTESVTSSENTPCKTRMLKEAHIELLRDSTTDSKENSFRKNGMCTDTHSLSKRLKT		
PHK_P_HUMAN	406	RN	IVKIFPMCFEEDAKFMV	AKIDALITDMEKVS	CETLRQF
AspAT_HUMAN	376	EK	IVLIFGSEIVSGLTFR	LDVAVSISREAVFTQI		
AspAT_YAEST	377	TA	IVLVAGRSIAGLNGCN	VEVAKAIDDEVVRYTIEAKL		
AspAT_ARATH	395	YH	IVTRNGRISAGVTGN	VDTJANAIEVTKSS		
AspAT_ECOLI	364	RF	QVAGGVVAQTDFDN	NALFLQIVAVI		

Figure 3: Alignment of the 48 ATII sequences indicated in Table 3. Black stars indicate residues of OAT (the first up in the list) involved in the interaction with the cofactor (Gly 142, Val 143, Asp 263, Gln 266, Thr 322), the red triangles indicate instead residues interacting with the substrate, the catalytic lysine (Lys 292), the gateway system (Glu 235, Arg 413) and arginine interacting with the ω -carboxylate (Arg 180).

3.3 – The substrate binding site: a gateway system in α -KG-specific AT-II transaminases

The part of the active site of AT-II transaminases that interacts with the substrate also shows some important differences, when compared to AT-I.

The first one regards the changes in molecular conformation that accompany substrate binding. In AspAT and AroAT (both AT-I), the small domain rotates towards the large domain to close the active site upon binding of ligands (Figure 1C). In contrast, if we compare the ligand-bound with the unligated forms of GABA-AT, OAT or AcOAT (aAT-II) they exhibit no large-scale changes in the overall conformation (Fig-

ure 1-D), suggesting that that these enzymes do not generally undergo closure of the active site as the AT-I enzymes do [75, 85].

One notable exception to this observation is found in glutamate 1-semialdehyde aminomutase (GSA). In this enzyme there is an active site gating loop, which is open when the enzyme contains bound PMP and closed when it contains PLP [33, 86]. These variations in accessibility of the active site most likely mirror the fact that the natural substrate of GSA must initially bind to the PMP, and not PLP, form of the cofactor (see the legend of Table 1)¹ [87].

A second difference between AT-II and AT-I transaminases is closely related to the dual-specificity issue described above. The AT-II enzymes must be able to bind a terminal amine and to position their substrates in a way that permits to the ω -amino group to be transferred, while preventing transamination of α -amino acids. To accomplish this, AT-II enzymes that use α -KG as the amino acceptor and amines with long side chain as main donor (GABA, ornithine, lysine...), have evolved a so-called gateway system (Figure 4) [4]. The key elements of this gateway are two juxtaposed residues, an Arg and a Glu (Arg398 and Glu211 in *E. coli* GABA-AT; Arg413 and Glu235 in human OAT). Of these, only the Arg residue is conserved in AspAT (Arg374 in the *E. coli* enzyme), where it serves to bind and position the α -carboxylate of the aspartate substrate, making the transamination of the α -amino group

¹ Another potential (but difficult to interpret) exception is represented by an ω -AT studied by Rausch et al. 15. Rausch, C., Lerchner, A., Schiefner, A. & Skerra, A. (2012) Crystal structure of the ω -aminotransferase from *Paracoccus denitrificans* and its phylogenetic relationship with other class III aminotransferases that have biotechnological potential, *Proteins*. In the crystal structure of this enzyme, the two subunits of the same dimer showed significantly different conformations: the active site of one of the two monomers (containing a potential ligand) was in an open conformation, whereas in the other monomer, apparently unliganded, the small domain was moved towards the large one, determining a closure of the active site.

possible. The Glu residue instead is missing in AspAT and it is conserved only in α -KG specific ATII transaminases (Figure 4).

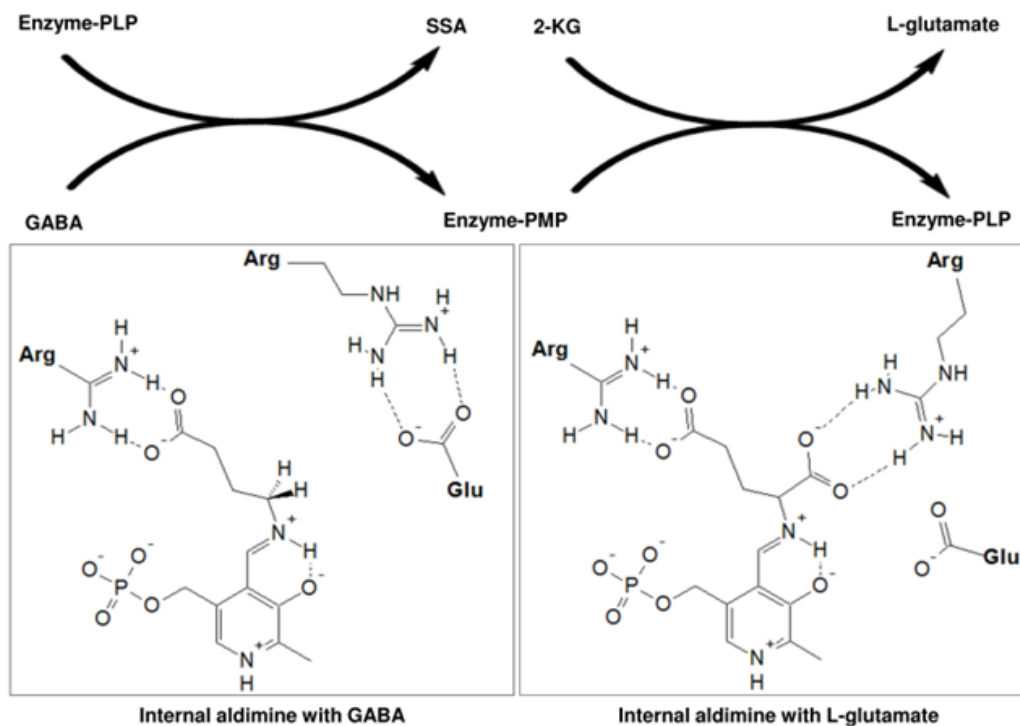


Figure 4: Scheme of the gateway system in GABA aminotransferase (residues numbering refers to the *E. coli* enzyme; [26]). At the beginning of the physiological reaction, the enzyme forms a Schiff base with GABA and during this process the crucial Arg398 residue remains salt-bridged with Glu211. The first half of the reaction ends with release of succinic semialdehyde and conversion of PLP to PMP. In the second half of the transamination, α -KG reacts with PMP to yield the external aldimine of glutamate, which will be released as a second product. Triggered by the formation of PMP, the Arg398 switches its position and becomes available for interacting with the α -carboxylic group of α -KG (or glutamate). A second Arg residue (Arg141) interacts instead with the γ -carboxylic group of both GABA and α -KG and serves for productive binding and correct positioning of the substrates. This residue is conserved also in other α -KG specific AT-II transaminases [4, 26, 78, 85].

Through site-directed mutagenesis experiment with both OAT and GABA-AT, it was concluded that this conserved Glu residue forms a salt bridge with the Arg residue during the first half of the transamination reaction, when the ω -amino substrate enters the active site. The presence of this salt bridge helps restrict the binding and reaction of undesired α -amino acids (e.g., glutamate) or α -keto acids, that are required only for the second half-reaction [26, 85, 88].

On the other hand, in the presence of PMP during the second half-reaction, the salt bridge opens up to allow α -KG to interact with the Arg residue. In other words, in the transition between the first and second half-reactions of these α -KG specific AT-II transaminases, the Glu residue acts as functional switch, triggered by the formation of PMP [88]. Such a switch allows these enzymes to be specific for amino-group donors lacking an α -carboxylate while retaining the ability to bind the α -ketoacid acceptor².

The active sites of α -KG-specific AT-II transaminases also contain typically a second Arg residue (Arg141 in GABA-AT; Figure 4) that forms a salt bridge with the γ -carboxylic group of α -KG [26, 89]. This interaction is a crucial determinant of the selectivity for α -KG as the specific acceptor ketoacid. Furthermore, the same residue also helps recognizing and properly positioning the amino group donor. In fact the α -KG -specific ATs often bind substrates (L-ornithine, GABA, L-lysine...) that contain a carboxylate at the opposite end with respect to the ω -amino group; this carboxylate seems able to interact with the Arg residue as efficiently as the γ -carboxylate of α -KG (Figure 4) [88].

² In contrast AspAT (like other transaminases of subfamily AT-I) lacks the gateway system and retains only the Arg residue, rather rigidly positioned within the active site; this biases the enzyme towards binding both donors and acceptors containing an α -carboxylate.

What about the putrescine aminotransferase discussed in section 2? In contrast to L-ornithine, GABA and the like, putrescine does not contain any carboxylate, but just two amino groups, located at the opposite ends of an aliphatic (linear) chain of carbon atoms. A very recent structural study shows that, in the active site of PUAT from *E. coli*, a Lys residue (Lys183) replaces the Arg, which in OAT and GABA-AT salt-bridges with the carboxylate of the amino-group donor [90]. Compared to Arg, the Lys side chain is smaller and less basic (meaning that it can more easily exist in neutral form), and these differences may help explain the low activity of PUAT towards ornithine and other amino donors containing an α -carboxylate. Another difference noted by the authors of the structural paper relates to the active site entrance, which appears narrower and more restricted in PUAT, possibly favoring access of the 'leaner' polyamines (putrescine and cadaverine) with respect to the bulkier amino acids [90].

3.4 – The substrate binding site: P and O pockets in pyruvate-specific AT-II transaminases

The gateway system, as described in section 3.3, is not operational in AT-II transaminases that employ pyruvate as the preferred amino group acceptor: in fact, while the Arg residue of the gateway is conserved in these enzymes the Glu residue is not (Figure 3). The Arg residue is still involved in recognition of the α -carboxylate of substrates, as indicated among other data by the available structures of pyruvate-specific aminotransferases (a list of the three-dimensional structures of AT-II enzymes currently deposited in the Protein Data Bank is provided in Table 2). However one is left to wonder why in these enzymes, the Arg does not need to form a strong interaction during the first part of the

reaction, to mask its positive charge when the ω -amine binds. More generally, one may wonder why the substrate specificity of several pyruvate-specific ATIs tends to be relatively relaxed.

Name	Sequence	Organism	PDB ID	N° of Subunit
Dialkylglycine Decarboxylase	DGDA_BURCE	Burkholderia cepacia	1D7V, 1D6R, 1D7S, 1DTU, 1DGD, 1DGE, 1DKA, 1M0N, 1M0O, 1M0P, 1M0Q, 1Z3Z, 1ZC9, 1ZOB, 1ZOD, 1DKB	4
GABA AT (bacterial)	GABT_ECOLI	Escherichia coli	1SFF, 1SF2, 1SZK, 1SZS, 1SZU	4
GABA AT (bacterial)	A0QQ04_MYCS2 A0QWJ0_MYCS2 B1MIQ9_MYCA9 B2HN70_MYCMM F9VN77_SULTO	Mycobacterium smegmatis Mycobacterium ab- scessus Mycobacterium mari- num Sulfolobus toko- daii	3Q8N 3OKS 4FFC 3R4T 2EO5	2 4 2 4
GABA AT (eukaryotes)	GABT_PIG	Sus scrofa	1OHV, 1OHW, 1OHY	2
Ornithine AT	OAT_HUMAN OAT_PSEPU OAT_BACAN OAT_PLAF7 OAT_PLAFD OAT_PLAYO	Homo sapiens Pseudomonas putida Bacillus anthracis Plasmodium falcipa- rum Plasmodium yoelii	2OAT, 1OAT, 1GBN, 2BYL, 2BYJ, 2CAN 3A8U 3RUY 3NTJ 3LG0	4 4 2 2 2 2

		yoelii	1Z7D	
Putrescine aminotransferase	PAT_ECOLI	Escherichia coli	4UOX	4
Glu semialdehyde aminomutase	GSA_SYNP6	Synechococcus PCC 6301	2GSA, 2HOY, 2HOZ, 2HP1, 2HP2, 3FQ7, 3FQ8, 3FQA, 3GSB, 4GSA	2
	GSA1_BACAN	Bacillus anthracis	3L44	2
	GSA2_BCAN	Bacillus anthracis	3K28	2
	GSA_AERPE	Aeropyrum pernix	2EPJ, 2ZSL, 2ZSM	2
	GSA_BACSU	Bacillus subtilis	3BS8	2
	GSA_THEEB	Thermosynechococcus elongates	2CFB	2
	GSA_THET8	Thermus thermophiles	2E7U	2
	GSA_YERPE	Yersinia pestis	4E77	2
Acetylornithine AT	ARGD_THET2	Thermus thermophilus	1WKG, 1WKH, 1VEF	2
	ARGD_AQUAE	Aquifex aeolicus	2EH6	2
	ARGD_CAMJE	Campylobacter jejuni	3NX3	2
	ARGD_SALTY	Salmonella typhimurium	2PB0, 2PB2	2
	ARGD_THEMA	Thermotoga maritima	2E54, 2ORD	2
7,8-diaminopelargonate AT	BIOA_ECOLI	Escherichia coli	1QJ3, 1DTY, 1MGV, 1MLY, 1MLZ, 1S06, 1S07, 1S08, 1S09, 1SOA, 3DOD, 3DRD, 3DU4, 3BV0, 3LV2, 3TFT, 3TFU	2
	BIOA_MYCTU	Mycobacterium tuberculosis		2

	BIODA_ARATH	Arabidopsis thaliana	4A0F, 4A0H, 4AOF, 4A0G, 4A0H, 4A0R, 4A0G,	2
L-lysine Aminotransferase	LAT_MYCTU	Mycobacterium tuberculosis	2CJD, 2CJN, 2CJG, 2CJH, 2JJE, 2JJF, 2JG, 2JJH	2
D-phenylglycine aminotransferase	2CY8	Pseudomonas strutzeri ST-201	2CY8	2
Succinyl- ornithine AT	4ADE	Escherichia coli	4ADE	2
Amine:Pyruvate Aminotransferase	OAPT_PSEPU	Pseudomonas putida	3A8U	4
	Q9I700	Pseudomonas aeruginosa	4B98, 4B9B	4
	F2XB9_VIBFL	Vibrio fluvialis	3NUI, 4E3Q, 4E3R	2
	Q7NWG4_CHRVO	Chromobacterium violaceum	4A6T, 4A6R, 4A6U, 4A72, 4AH3	2
	Q3IWE9_RHOS4	Rhodobacter sphaeroides	3I5T, 3HMU	2
2-aminohexano- 6-lactam race- mase	Q7M181	Achromobacter obae	3DXV, 3DXW, 2ZUC	2
Beta- transaminase	A3EYF7_9RHIZ	Mesorhizobium sp. LUK	2YKU, 2YKV, 2YKX, 2YKY, 4AO4	2
3-Acetyloctanal transaminase	L7ZI44_SERMA	Serratia sp. FS14	4PPM	2
Enzymes with unknown function			3N5M, 3I4J	

Table 2: Known 3D structures of ATII with their PDB ID and the numbers of monomers identified in the structure.

To address this sort of questions, as well as to interpret the stereoselectivity of amine:pyruvate transaminases (ω -PATs), Shin and Kim put forward a schematic model of the active site, based on both structure and reactivity analysis [91]. This scheme has been adopted in somewhat modified forms by other researchers in the field [22, 92, 93]. In essence the model is based on a bipartite substrate binding site, consisting of two subsites or 'pockets'. One of the subsites, which accommodates the α -carboxylate of the keto acid, is generally located in the vicinity of the O3' atom of PLP, and it can be indicated as the O-pocket. The other pocket is near the phosphate moiety of PLP and hence is called P-pocket [93]. The two pockets occur both in AT-I and AT-II transaminases, although their relative sizes are different (Figure 5). In the ω -PAT from *Vibrio fluvialis* studied by Shin and Kim, the O pocket could accept both a carboxylate group and hydrophobic substituents. A similar situation can be proposed also for other AT-II transaminases reacting with pyruvate, where the O-pocket appears to be large and the presence of aromatic residues provides a hydrophobic environment and π - π interactions to stabilize aromatic and alkyl amino substrates [15, 92]. In sum, the O-pocket of ω -PATs seems able to bind both the α -carboxylate of the amino group acceptor and the hydrophobic side chains of the amino group donor substrates (Figure 5B).

This dual specificity can presumably be achieved without substantial structural rearrangement. Since in a large O-pocket the internal arginine can move relatively freely, it does not need to mask its positive charge, as it happens in the gateway system, to avoid clashes with the hydrophobic side chain of the amino substrate. Recently Steffen-Munsberg et al., based on the analysis of some ω -ATs, contrasted the mobility of the Arg residue in AT-I and AT-II enzymes [94].

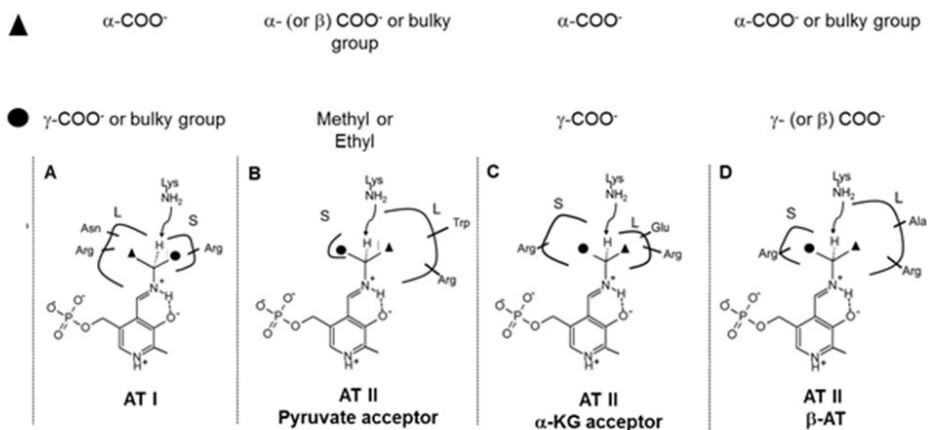


Figure 5: Schematic features of the O and P pockets in different types of ATs. The circle and the triangle indicate the different chemical groups that can be found on the substrates. (A) Model referring to AroAT and other AT-I transaminases [92]. (B) Model for AT-II transaminases that use pyruvate as the amino group acceptor. Based on the work of Shin and Kim on an ω -PAT [91, 94]. (C) Model referring to α -KG-specific ATs, based on the work of Steffen-Munsberg et al. [94] and Hirotsu et al. [95]. (D) Scheme of the atypical active site of a β -AT described by Wybenga and collaborators [96].

According to this analysis, in AT-I the conserved Arg residue is quite packed within the active site, and it can only contact the α -carboxylic group of the substrate, while in AT-II enzymes the Arg is very flexible. Its position in fact is rather variable in the structures of similar enzymes and also in different monomers of the same structure (see also [97]).

The flexibility of this Arg residue allows the enzyme to bind both pyruvate and much larger aldehydes and even a bulky or aromatic substrate. In this last case the Arg side chain is oriented away from the active site, leaving a large cavity behind. The wide size of the O-pocket

may also explain the substantial substrate promiscuity not just of ω -PATs [22] but also of other pyruvate-specific transaminases such as AGXT2 [35].

What about the P pocket? In the study by Shin and Kim, this subsite was small and unable to accommodate substituents larger than an ethyl group. It also showed a strong aversion towards carboxylate groups [22, 91]. Therefore, this site contributes by steric constraints and electrostatic repulsion to impart the enzyme specificity for pyruvate *versus* α -KG as the amino group acceptor (Figure 5B). The P-pocket is the only part of the enzyme that can distinguish between the two keto acids.

The O-pocket of α -KG-specific transaminases is smaller and more constrained than that of pyruvate-specific enzymes [94] (Figure 5C). This fact, together with the occurrence of the gateway system and the presence, for most of these enzymes, of an Arg residue in the P-pocket, as discussed in section 3.3 appears to implement a tendency of α -KG specific ATs to show lower substrate promiscuity. Exceptions exist however, e.g. *Pseudomonas aeruginosa* GABA-AT also accepts diamino acids (ornithine) and diamines (putrescine) [98].

3.5 – An overview of substrate specificity in AT-II transaminases

To summarize very schematically the data discussed in sections 3.3 and 3.4, α -KG and pyruvate specific ATs appear to have adopted two very distinct strategies to select donors bearing an ω -amino group while still permitting binding of the α -ketoacid acceptors. In pyruvate-specific enzymes, binding of an α -carboxylate and binding of a (large) side chain are mutually exclusive because they both should occur in the same pocket (the O pocket). Thus, these enzymes can only accommodate substrates containing no α -carboxylate (ω -amines) or containing an α -carboxylate and a very minimal side chain (pyruvate, glyoxylate). In α -KG specific ATs, dual specificity is achieved through a more sophisticated and more rigid mechanism – namely, when the active site contains PLP, the O-pocket is not accessible to α -carboxylate groups because the Arg-Glu gateway is operational. However, upon formation of PMP the Arg residue in the O-pocket is released and can interact with α -carboxylate groups, whereas another positively charged residue in the P-pocket interacts with the γ -carboxylate of α -KG, imparting specificity for the ketoacid.

There are however exceptions and intermediate situations. One interesting example is a bacterial β -AT, called MesAT, whose physiological function is unknown. The enzyme was selected for applicative purposes (the preparation of enantiopure β -phenylalanine) and shown to react with a broad range of substrates, using α -KG as the amino acceptor [96]. The structure of MesAT however shows elements in common with both those observed in pyruvate-specific and in α -KG-specific AT-II transaminases, as well as in AT-I enzymes.

The P-pocket for γ - and β - carboxylate is relatively small and resembles the O-pocket of AspAT. On the other hand the O-pocket is quite large, it can accept both α -carboxylate and bulky hydrophobic groups and it is hence similar to the O-pocket of AT-II enzymes that use pyruvate as the acceptor (Figure 5D). Furthermore, even if interacting with α -KG, this enzyme does not possess a gateway system but an arginine switch (a switch in position of the Arg-412 side chain is the determinant of O-pocket dual specificity, a similar mechanism is present also in other PLP-dependent enzymes and it was well explained by Eliot and Kirsch [4]. When a β -amino acid binds, the Arg-412 side chain is oriented away from the active site, producing an hydrogen bond with Ala-225. This re-orientation enlarges the O-pocket permitting the accommodation for the hydrophobic side chain of substrates. Subsequently, when α -KG binds the enzymes, Arg-412 relocates inside the O-pocket forming a salt bridge interaction with the α -carboxylate of α -KG. Arg-412 plays thus a key role in active site versatility towards different substrates: α -amino/ α -keto acids and aliphatic or aromatic β -amino/ β -keto acid). This arrangement is different from (and somewhat hybrid between) the models previously presented for the active sites of the other pyruvate and α -KG acceptors, as shown in Figure 5D.

4 – AT-II enzymes that are not aminotransferases

Despite the fact that the initial classification of Metha and collaborators dealt only with ATs, some enzymes belonging to the subgroup II show other activities. Not considering DGDA (which catalyzes both decarboxylation and transamination reactions) and GSA (whose reaction is in effect an internal transamination between two positions of the same substrate; see Table 1), AT-II has been shown to encompass enzymes

with *bona fide* racemase and lyase functions (Table 1 and Figure 6). The first AT-II enzyme reported in the literature to catalyze a reaction different from transamination, was 2-aminoheptano-6-lactam racemase (AH6L-R, table 1). In fact, AH6L-R was characterized before the classification work of Christen, Metha and co-workers [99, 100] and its three dimensional structure is currently known [101].

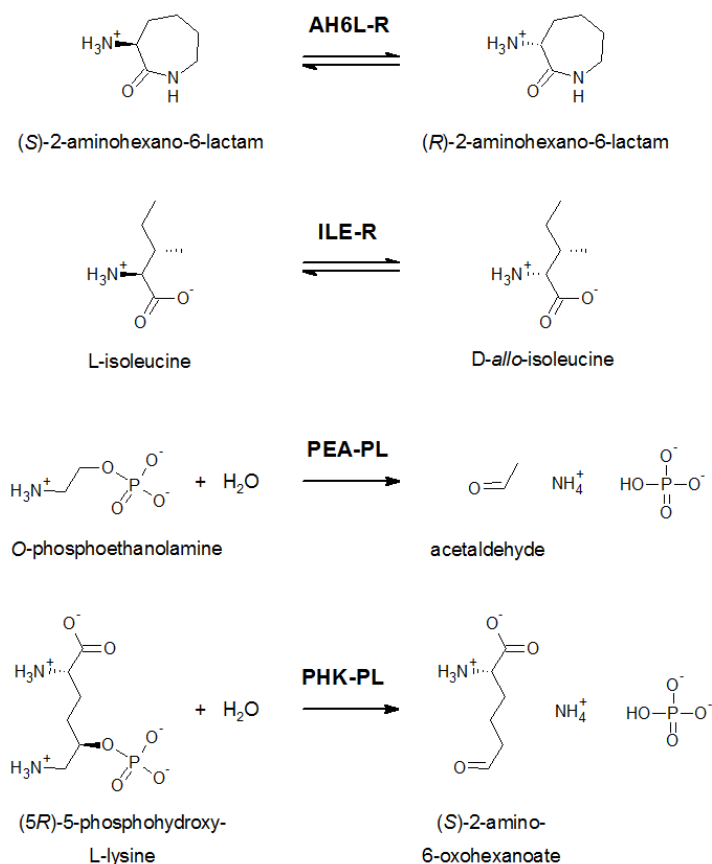


Figure 6: Reactions catalyzed by the currently-known AT-II enzymes that are not ATs. Despite the apparently drastic differences, these reactions share among them (and with the transaminase reactions) some mechanistic foundations. In fact, PLP-dependent transaminases, racemases and lyases are all expected to begin their reaction by forming a Schiff base between PLP and the substrate amino group, followed by deprotonation of the amino carbon. Only at that point mechanisms diverge, to yield specific reactions and products [1, 5]

A comparison of the structure of this enzyme with those of GABA-AT (29% identity with AH6L-R) and DGDA (30% identity) confirmed that both the overall architecture and the active site structure surrounding the cofactor are comparable to those of the other AT-II [101]. AH6L-R however, unique among fold-type I enzymes, possesses an additional C-terminal 'tail' (about 12 residues, forming an α -helix) that is essential for function. Some of the residues in this C-terminal part contribute to shaping the active site cavity, determine substrate specificity, recognize the nitrogen of an amide of lactam in the substrate and control the access to the active site [101].

On the other hand, the racemase lacks an Arg residue to interact with the carboxylic group of the substrate. AH5L-R does not need to bind a substrate bearing an α carboxylate, thus the absence of the Arg residue prevents the interaction of the enzyme with α -keto acids and ultimately the undesired occurrence of transamination. This last feature and the presence of a Tyr residue (Tyr137) involved in acid/base catalysis seem to be the key determinants of the racemase activity (Figure 3). Tyr137 is in fact not conserved among all AT-II enzymes, and in those where it is conserved it was not known to be involved in any acid/base catalysis [102]. Such a role was probably acquired by the racemase during evolution.

Recently, a second racemase belonging to AT-II was identified, namely isoleucine 2-epimerase [103]. This enzyme is quite peculiar not only because it is a racemase, but also because it operates on a standard α -amino acid substrate (together with D-FGAT and DGDA, it is one of the few AT-II enzymes whose preferred substrate is an α -amino acid rather than an ω -amine).

There is no three-dimensional structure available for ILE-R, but inspection of the the sequence alignments shows that the Arg residue involved in the interaction with the α -carboxylate is conserved, whereas the Glu that in α -KG-specific AT-IIIs is involved in the gateway system, although not conserved, is replaced by the chemically similar Asp (Figure 3). It is possible that the same residue that confers the dual specificity to some transaminases of the AT-II subgroup in this case is involved in the catalysis of the racemization with isoleucine. Further biochemical and structural data are necessary to better define the interaction of this enzyme with its substrate and the catalytic mechanism.

The only other known AT-II enzymes not catalyzing transaminations are two closely related lyases, ethanolamine phospho-lyase (PEA-PL) and 5-phosphohydroxy-lysine phospho-lyase (PHK-PL), which were shown to catalyze the elimination of phosphate from phosphoethanolamine and 5-phosphohydroxy-lysine, respectively [104].

The structures of these two phospho-lyases are not known, but some hypotheses can be made about the structural changes that, during evolution, led to their conversion from aminotransferases to lyases [105].

Several similarities can be observed with the sequence of the DGDA (30% identity). For example, as observed in DGDA, the Arg that in most ATs interacts with the substrate α -carboxylic group is not conserved. This is in accordance with the low affinity of PEA-PL towards α -amino acids and with its ineffectiveness as a transaminase (for this enzyme, β -elimination is at least 500-fold more efficient than transamination) [105]. Again similar to DGD, the lyases also lack the Arg residues that in α -KG-specific ATs interacts with the γ -carboxylate of the substrate (see Figures 3 and 4C). This residue is replaced by Met in DGD and by His in PEA-PL. This histidine could perhaps perform acid/base

catalysis, permitting the elimination of the phosphate leaving group (Figure 3).

5 - Inferences on the evolution of AT-II enzymes

It is believed that fold type I enzymes evolved divergently for 1500 millions years and, despite their diversification and specialization to cover a wide range different catalytic functions, they have maintained their structure conserved during evolution. The presence of the cofactor and some conserved hydrophobic residues are probably the driving forces that have kept the original structure conserved during evolution [106]. Analyzing sequences, structures and function of this class of PLP-dependent enzyme is useful for better understanding what are the evolutionary steps that have driven the acquisition of new enzymatic functions or substrate specificities [2, 11].

Figure 7 shows a phylogenetic tree illustrating the relationships between AT-II enzymes. The tree was constructed starting from a set 89 sequences that included all AT-II proteins with a validated physiological function, obtained from the B6 Database [9] (Table 3). Among the sequences in the set, only a few were ω -PATs and β -ATs (for comparison, see [15]). AspATs were used for adding an out-group, belonging to the AT-I. An inspection of the tree, combined with the information provided in the previous sections, allow drawing some inferences and putting forward some hypotheses about evolution of AT-IIs.

The long branch that connects AT-I, here represented by the AspATs, and AT-II is indicative of the evolutionary differences among these groups of enzymes. As described in section 3, there are many parts of the protein sequence that are not conserved between the two subfamilies, and that justify the branch length. In particular, divergence

of AT-II from AT-I seems to have been marked by changes in the structure of the small domain and by some significant rearrangements of the active site, in particular a repositioning, along the sequence, of the catalytic Lys and changes in the organization of the substrate-binding pockets.

Tree ID	UniProt ID
ACOAT_YEAST	ARGD_YEAST
ACOAT_ECOLI	ARGD_ECOLI
SOAT_ECOLI	ASTC_ECOLI
OAT_ARATH	NP_199430
OAT_HUMAN	OAT_HUMAN
OAT_PLAFD	OAT_PLAFD
OAT_VIGAC	OAT_VIGAC
GABA_ATeu_HUMAN	GABT_HUMAN
GABA_ATeu_YEAST	GATA_YEAST
GABA_ATba_ECOLI	GABT_ECOLI
GABA_PAT_ARATH	AAK52899
DAPA_AT_ECOLI	BIOA_ECOLI
DAPA_AT_MYCTU	BIOA_MYCTU
LATgp_MYCTU	LAT_MYCTU
LATgp_NOCLA	LAT_NOCLA
LATgn_XANAX	AAM41659
PUAT_ECOLI	NP_417544
DABA_AT_HALEL	ECB1_HALEL
DABA_AT_PSEAE	C83345
DABA_AT_PSEAEb	AAK01505
AH6LR_ACHOB	Q7M181
AGXT2_HUMAN	AGT2_HUMAN
DGDA_BURCE	DGDA_BURCE
D_FGAT_PSEST	2CY8
wPAT_VIBFL	AEA39183
wPAT_CHRVI	NP_901695
wPAT_RHOSP	YP_001169469
wPAT_PSEAE	4B9B
PU_PAT_PSEAE	AAG03688
bAT_MES_LUK	ABL74379
bAT_POL_JS666	YP_548313
bA_PAT_ACHDE	AAP92672
PEA_PL_HUMAN	NP_112569
PHK_PL_HUMAN	Q8IUZ5

ILE_R_LACBU	AGE45209
GSA_SULSO	AAK40528
GSA_ECOLI	GSA_ECOLI
GSA_SYNEL	GSA_SYNEL
GSA_PROFR	GSA_PROFR
TAU_PAT_RHOOP	AAT40120
TAU_PAT_PARDE_PD1222	ABL72337
NEAT_STRFR	Q53U08
DHENAT_STRTE	CAE22475
FUMAT_SPHMA	ACS27061
AspAT_ARATH	AAT1_ARATH
AspAT_HUMAN	AATC_HUMAN
AspAT_YAEST	AATC_YEAST
AspAT_ECOLI	AAT_ECOLI

Table 3: Sequences of ATII with a known function, reported in B6db and used for the phylogenetic tree. The two columns indicate the name used for the tree and the UniProt ID for each sequence. It is possible to find 48 sequences out of 89 initially identified, since many of them have been removed, as they are similar to other sequences. Aspect of the tree was thus improved without affecting its contents.

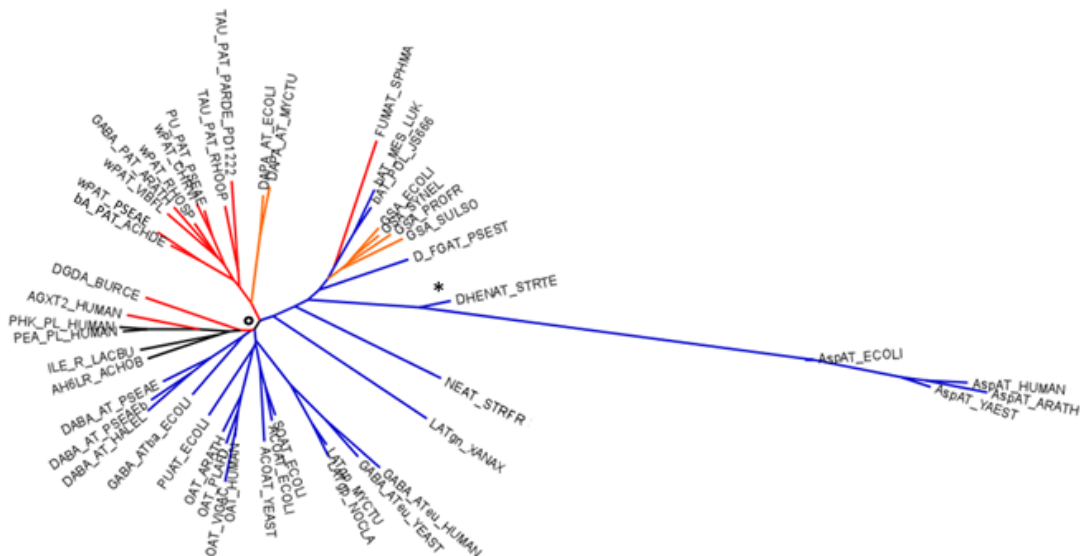
It seems reasonable to speculate that the ancestral AT-II enzyme was an aminotransferase, or at least that its main catalytic function was to carry out transaminase reactions. This hypothesis is in agreement with the current overabundance of AT enzymes within the subfamily (as well as within subgroup AT-I) and with the observation that non-AT enzymes are found far from the tree root. The hypothetical ancestral enzyme might also have had some preference towards the amino group acceptor; in fact, in Fig. 7 the branches of the tree most close to the root represent α -KG specific ATs (DHNEAT, NEAT, LAT and D-FGAT: for the last enzyme, a three dimensional structure has been reported, but not characterized in great detail [107]).

In any case, a neat divide separates the majority of extant α -KG

specific ATs from the pyruvate-specific ATs, even though a unique branchpoint leading to this separation is difficult to individuate. Ultimately, the loss of the Glu residue of the gateway system and other rearrangements of the two pockets of the active site seem the major determinants of difference among the two AT groups. However, specialization for pyruvate may have been acquired progressively and/or separately in different lineages. For example DABA-AT, which occupies a position close to the emergence of pyruvate-specific ATs, is able to catalyze its reaction also with pyruvate, but the K_M is severalfold higher than that with α -KG [108]. Over time, the different groups of enzymes may have optimized their specificity towards one or the other amino group acceptor, owing to the availability and role of a given keto acid in one organism or to specific physiological contexts.

Whatever the evolutionary mechanisms that led to the current situation, there are hints that the absence of a gateway system (as found in pyruvate-specific ATs) correlates with a greater enzyme versatility and/or promiscuity. For example DAPA-AT enzymes, that display a very peculiar substrate specificity, shows a relatedness with pyruvate-specific ATs. Non-AT enzymes (lyases, racemases) cluster together and seem most closely related to some pyruvate-specific ATs showing relaxed substrate specificity (DGDA, AGXT2). Eliot and Kirsch argued that one preferential route towards the evolution of a new PLP-dependent catalytic activity is the acquisition of an altered substrate specificity [4]. Elimination for example can be a very facile reaction if an enzyme binds a substrate with a good leaving group. The presence of the phospho-lyase and DGDA in the same tree branch, the fact that phosphate is a good leaving group and that they possess some active site residues in common is in accordance with the hypothesis described.

β -ATs, like the one shown to have an intermediate active site organization between α -KG and pyruvate-specific ATs [96], forms a separate cluster together with two other peculiar ATs: FUMAT and GSA. Not only all three enzymes lack the Glu residue of the gateway system: in FUMAT and GSA it is also absent the Arg (strongly conserved among AT-II ATs) interacting with the α -carboxylate of the amino group acceptor. In the case of GSA this residue is substituted by a Glu, which interacts with the amino group of the diaminovalerate (produced during the catalysis) and excludes glutamate or other α -amino acids from the active site, since this is the only AT-II transaminase not interacting with any α -carboxylate [109]. The absence of the Arg residue in FUMAT is more difficult to rationalize, but it might be due to the long and bulky side chain of the substrate. In the absence of structural information, it can be hypothesized that the enzyme has evolved a different system to bind this substrate and consequently also the amino group acceptor (FUMAT was reported to use pyruvate [110], despite being located outside the main cluster of pyruvate-specific ATs).



0.7

Figure 7: A phylogenetic tree of the functionally validated AT-II enzymes. The sequences of enzymes whose function had been experimentally validated were taken from the B6 database (<http://bioinformatics.unipr.it/cgi-bin/bioinformatics/B6db/home.pl>) and grouped using the neighbor joining method. A multiple sequence alignment was performed using ClustalX2 (<http://www.clustal.org/>); the number of sequences was subsequently reduced from 89 to 48, in order to facilitate reading of the alignment (see Table 3 and Fig. 3) and of the resulting tree. The radial tree was obtained using aspartate aminotransferases from AT-I as an out-group and displayed through the phylogenetic tree generator FigTree (<http://tree.bio.ed.ac.uk/software/figtree/>). Branches are colored in: blue for α -KG-specific ATs and for AspATs, red for pyruvate-specific ATs, orange for DAPA-AT and GSA, black for lyases and racemases. Symbols are used to indicate, respectively, the change in the position of the catalytic lysine and reorganization of the small domain (\star) and the loss/acquisition of the Glu involved in the gateway system (O).

6 - Conclusions

Over twenty years after the first clear definition of AT-II as a structural subfamily [10], we have provided an up-to-date overview of these enzymes, based on the most recent biochemical and structural literature, illustrating how their properties are distinctive and how they compare with those of the other fold-type I enzymes, as well as sketching a picture of their evolution. As more enzyme functions and protein structures emerge within this structural subgroup, there will be possibilities for elucidating in greater detail their specific properties and for incorporating this knowledge into the current picture. As mentioned in section 2, the practical interest in AT-II enzymes has increased over time, due to their use for the enantiopure synthesis or resolution of chiral amines, as reviewed in detail in a number of recent publications [15, 22, 67]. Hence, new structural and enzymological studies on AT-II enzymes are expected to not only benefit our general knowledge but to also improve our ability of selecting and tailoring these catalysts for applicative purposes.

REFERENCES

1. John, R. A. (1995) Pyridoxal phosphate-dependent enzymes, *Biochim Biophys Acta*. **1248**, 81-96.
2. Mehta, P. K. & Christen, P. (2000) The molecular evolution of pyridoxal-5'-phosphate-dependent enzymes, *Adv Enzymol*. **74**, 129-184.
3. Percudani, R. & Peracchi, A. (2003) A genomic overview of pyridoxal-phosphate-dependent enzymes, *EMBO Rep*. **4**, 850-854.
4. Eliot, A. C. & Kirsch, J. F. (2004) Pyridoxal phosphate enzymes: mechanistic, structural, and evolutionary considerations, *Annu Rev Biochem*. **73**, 383-415.
5. Toney, M. D. (2011) Controlling reaction specificity in pyridoxal phosphate enzymes, *Biochim Biophys Acta*. **1814**, 1407-18.
6. Grishin, N. V., Phillips, M. A. & Goldsmith, E. J. (1995) Modeling of the spatial structure of eukaryotic ornithine decarboxylases, *Protein Sci*. **4**, 1291-304.

7. Jansonius, J. N. (1998) Structure, evolution and action of vitamin B6-dependent enzymes, *Curr Opin Struct Biol.* **8**, 759-69.
8. Schneider, G., Kack, H. & Lindqvist, Y. (2000) The manifold of vitamin B6 dependent enzymes, *Structure Fold Des.* **8**, R1-6.
9. Percudani, R. & Peracchi, A. (2009) The B6 database: a tool for the description and classification of vitamin B6-dependent enzymatic activities and of the corresponding protein families, *BMC Bioinformatics.* **10**, 273.
10. Mehta, P. K., Hale, T. I. & Christen, P. (1993) Aminotransferases: demonstration of homology and division into evolutionary subgroups, *Eur J Biochem.* **214**, 549-61.
11. Christen, P. & Mehta, P. K. (2001) From cofactor to enzymes. The molecular evolution of pyridoxal-5'-phosphate-dependent enzymes, *Chem Rec.* **1**, 436-447.
12. Jensen, R. A. & Gu, W. (1996) Evolutionary recruitment of biochemically specialized subdivisions of Family I within the protein superfamily of aminotransferases, *Journal of bacteriology.* **178**, 2161-71.
13. Kim, K. H. (1964) Purification and properties of a diamine α -ketoglutarate transaminase from *Escherichia coli*, *J Biol Chem.* **239**, 783-6.
14. Albrecht, A. M. & Vogel, H. J. (1964) Acetylornithine δ -transaminase. partial purification and repression behavior, *J Biol Chem.* **239**, 1872-6.
15. Rausch, C., Lerchner, A., Schiefner, A. & Skerra, A. (2012) Crystal structure of the ω -aminotransferase from *Paracoccus denitrificans* and its phylogenetic relationship with other class III aminotransferases that have biotechnological potential, *Proteins.*
16. Sigrist, C. J., de Castro, E., Cerutti, L., Cuche, B. A., Hulo, N., Bridge, A., Bougueleret, L. & Xenarios, I. (2013) New and continuing developments at PROSITE, *Nucleic Acids Res.* **41**, D344-7.
17. Finn, R. D., Bateman, A., Clements, J., Coggill, P., Eberhardt, R. Y., Eddy, S. R., Heger, A., Hetherington, K., Holm, L., Mistry, J., Sonnhammer, E. L., Tate, J. & Punta, M. (2014) Pfam: the protein families database, *Nucleic Acids Res.* **42**, D222-30.
18. Berglund, P., Humble, M. S. & Branneby, C. (2012) 7.18 C–X Bond Formation: Transaminases as Chiral Catalysts: Mechanism, Engineering, and Applications in *Comprehensive Chirality* (Carreira, E. M. & Yamamoto, H., eds) pp. 390-401, Elsevier, Amsterdam.
19. Christen, P. & Metzler, D. E. (1985) *Transaminases*, John Wiley-Interscience, New York.
20. Valmaseda, E. M., Campoy, S., Naranjo, L., Casqueiro, J. & Martin, J. F. (2005) Lysine is catabolized to 2-aminoadipic acid in *Penicillium chrysogenum* by an ω -aminotransferase and to saccharopine by a lysine

2-ketoglutarate reductase. Characterization of the ω -aminotransferase, *Mol Genet Genomics*. **274**, 272-82.

21. Rudat, J., Brucher, B. R. & Syltatk, C. (2012) Transaminases for the synthesis of enantiopure beta-amino acids, *AMB Express*. **2**, 11.

22. Malik, M. S., Park, E. S. & Shin, J. S. (2012) Features and technical applications of ω -transaminases, *Appl Microbiol Biotechnol*. **94**, 1163-71.

23. Kohls, H., Steffen-Munsberg, F. & Höhne, M. (2014) Recent achievements in developing the biocatalytic toolbox for chiral amine synthesis, *Current opinion in chemical biology*. **19**, 180-192.

24. Chen, C. C., Zhang, H., Kim, A. D., Howard, A., Sheldrick, G. M., Mariano-Dunaway, D. & Herzberg, O. (2002) Degradation pathway of the phosphonate ciliatine: crystal structure of 2-aminoethylphosphonate transaminase, *Biochemistry*. **41**, 13162-9.

25. Sayer, C., Martinez-Torres, R. J., Richter, N., Isupov, M. N., Hailes, H. C., Littlechild, J. A. & Ward, J. M. (2014) The substrate specificity, enantioselectivity and structure of the (*R*)-selective amine : pyruvate transaminase from *Nectria haematococca*, *FEBS J*. **281**, 2240-53.

26. Liu, W., Peterson, P. E., Carter, R. J., Zhou, X., Langston, J. A., Fisher, A. J. & Toney, M. D. (2004) Crystal structures of unbound and aminoxyacetate-bound *Escherichia coli* γ -aminobutyrate aminotransferase, *Biochemistry*. **43**, 10896-905.

27. Storici, P., Capitani, G., De Biase, D., Moser, M., John, R. A., Jansonius, J. N. & Schirmer, T. (1999) Crystal structure of GABA-aminotransferase, a target for antiepileptic drug therapy, *Biochemistry*. **38**, 8628-34.

28. Mani Tripathi, S. & Ramachandran, R. (2006) Direct evidence for a glutamate switch necessary for substrate recognition: crystal structures of lysine ϵ -aminotransferase (Rv3290c) from *Mycobacterium tuberculosis* H37Rv, *J Mol Biol*. **362**, 877-86.

29. Fujii, T., Narita, T., Agematu, H., Agata, N. & Isshiki, K. (2000) Characterization of L-lysine 6-aminotransferase and its structural gene from *Flavobacterium lutescens* IFO3084, *J Biochem*. **128**, 391-7.

30. Samsonova, N. N., Smirnov, S. V., Altman, I. B. & Ptitsyn, L. R. (2003) Molecular cloning and characterization of *Escherichia coli* K12 yjgG gene, *BMC Microbiol*. **3**, 2.

31. Hirayama, A., Eguchi, T. & Kudo, F. (2013) A single PLP-dependent enzyme PctV catalyzes the transformation of 3-dehydroshikimate into 3-aminobenzoate in the biosynthesis of pactamycin, *ChemBiochem : a European journal of chemical biology*. **14**, 1198-203.

32. Pugh, C. E., Harwood, J. L. & John, R. A. (1992) Mechanism of glutamate semialdehyde aminotransferase. Roles of diamino- and dioxo-intermediates in the synthesis of aminolevulinate, *J Biol Chem*. **267**,

1584-8.

33. Contestabile, R., Angelaccio, S., Maytum, R., Bossa, F. & John, R. A. (2000) The contribution of a conformationally mobile, active site loop to the reaction catalyzed by glutamate semialdehyde aminomutase, *J Biol Chem.* **275**, 3879-86.
34. Kontani, Y., Kaneko, M., Kikugawa, M., Fujimoto, S. & Tamaki, N. (1993) Identity of D-3-aminoisobutyrate-pyruvate aminotransferase with alanine-glyoxylate aminotransferase 2, *Biochim Biophys Acta.* **1156**, 161-6.
35. Rodionov, R. N., Jarzebska, N., Weiss, N. & Lentz, S. R. (2014) AGXT2: a promiscuous aminotransferase, *Trends Pharm Sci.* **35**, 575–582.
36. Bailey, G. & Dempsey, W. (1967) Purification and properties of an α -dialkyl amino acid transaminase, *Biochemistry.* **6**, 1526–1533.
37. Sun, S., Zabinski, R. F. & Toney, M. D. (1998) Reactions of Alternate Substrates Demonstrate Stereoelectronic Control of Reactivity in Dialkylglycine Decarboxylase, *Biochemistry.* **37**, 3865-3875.
38. Stoner, G. L. & Eisenberg, M. A. (1975) Purification and properties of 7, 8-diaminopelargonic acid aminotransferase, *J Biol Chem.* **250**, 4029-36.
39. Hartinger, D., Schwartz, H., Hametner, C., Schatzmayr, G., Haltrich, D. & Moll, W.-D. (2011) Enzyme characteristics of aminotransferase FumI of *Sphingopyxis* sp. MTA144 for deamination of hydrolyzed fumonisin B1, *Applied microbiology and biotechnology.* **91**, 757-768.
40. Leslie, H., Paul, W. D. & Lishan, Z. (2004) Transaminases, deaminases and aminomutases and compositions and methods for enzymatic detoxification in, Google Patents,
41. Van Arsdell, S. W., Perkins, J. B., Yocum, R. R., Luan, L., Howitt, C. L., Prasad Chatterjee, N. & Pero, J. G. (2005) Removing a bottleneck in the *Bacillus subtilis* biotin pathway: BioA utilizes lysine rather than S - adenosylmethionine as the amino donor in the KAPA - to - DAPA reaction, *Biotechnology and bioengineering.* **91**, 75-83.
42. Dey, S., Lane, J. M., Lee, R. E., Rubin, E. J. & Sacchettini, J. C. (2010) Structural characterization of the *Mycobacterium tuberculosis* biotin biosynthesis enzymes 7, 8-diaminopelargonic acid synthase and dethiobiotin synthetase, *Biochemistry.* **49**, 6746-6760.
43. Williamson, N. R., Simonsen, H. T., Ahmed, R. A., Goldet, G., Slater, H., Woodley, L., Leeper, F. J. & Salmond, G. P. (2005) Biosynthesis of the red antibiotic, prodigiosin, in *Serratia*: identification of a novel 2 - methyl - 3 - n - amyl - pyrrole (MAP) assembly pathway, definition of the terminal condensing enzyme, and implications for undecylprodigiosin biosynthesis in *Streptomyces*, *Molecular microbiology.* **56**, 971-989.

44. Lou, X., Ran, T., Han, N., Gao, Y., He, J., Tang, L., Xu, D. & Wang, W. (2014) Crystal structure of the catalytic domain of PigE: A transaminase involved in the biosynthesis of 2-methyl-3-*n*-amylpyrrole (MAP) from *Serratia* sp. FS14, *Biochemical and biophysical research communications*. **447**, 178-183.
45. Perret, A., Lechaplais, C., Tricot, S., Perchat, N., Vergne, C., Pellé, C., Bastard, K., Kreimeyer, A., Vallenet, D. & Zapparucha, A. (2011) A Novel Acyl-CoA Beta-Transaminase Characterized from a Metagenome, *PloS one*. **6**, e22918.
46. Aron, Z. D., Dorrestein, P. C., Blackhall, J. R., Kelleher, N. L. & Walsh, C. T. (2005) Characterization of a New Tailoring Domain in Polyketide Biogenesis: The Amine Transferase Domain of MycA in the Mycosubtilin Gene Cluster, *Journal of the American Chemical Society*. **127**, 14986-14987.
47. Tewari, Y. B., Kishore, N., Goldberg, R. N. & Luong, T. N. (1998) An equilibrium and calorimetric study of some transamination reactions, *J Chem Thermodyn*. **30**, 777-793.
48. Large, P. J. (1992) Enzymes and pathways of polyamine breakdown in microorganisms, *FEMS Microbiol Rev*. **8**, 249-62.
49. Laue, H. & Cook, A. M. (2000) Biochemical and molecular characterization of taurine:pyruvate aminotransferase from the anaerobe *Bilophila wadsworthia*, *Eur J Biochem*. **267**, 6841-8.
50. Ruff, J., Denger, K. & Cook, A. M. (2003) Sulphoacetaldehyde acetyltransferase yields acetyl phosphate: purification from *Alcaligenes defragrans* and gene clusters in taurine degradation, *Biochem J*. **369**, 275-85.
51. Shimamoto, G. & Berk, R. S. (1980) Taurine catabolism. II. biochemical and genetic evidence for sulfoacetaldehyde sulfo-lyase involvement, *Biochim Biophys Acta*. **632**, 121-30.
52. van Bemmelen, F. J., Schouten, M. J., Fekkes, D. & Bruinvels, J. (1985) Succinic semialdehyde as a substrate for the formation of γ -aminobutyric acid, *J Neurochem*. **45**, 1471-4.
53. Behar, K. L. & Boehm, D. (1994) Measurement of GABA following GABA-transaminase inhibition by gabaculine: a ^1H and ^{31}P NMR spectroscopic study of rat brain *in vivo*, *Magn Reson Med*. **31**, 660-7.
54. Hearl, W. G. & Churchich, J. E. (1985) A mitochondrial NADP⁺-dependent reductase related to the 4-aminobutyrate shunt. Purification, characterization, and mechanism, *J Biol Chem*. **260**, 16361-6.
55. Clark, S. M., Di Leo, R., Dhanoa, P. K., Van Cauwenberghe, O. R., Mullen, R. T. & Shelp, B. J. (2009) Biochemical characterization, mitochondrial localization, expression, and potential functions for an *Arabidopsis* γ -aminobutyrate transaminase that utilizes both pyruvate

- and glyoxylate, *J Exp Bot.* **60**, 1743-57.
56. Busch, K. B. & Fromm, H. (1999) Plant succinic semialdehyde dehydrogenase. Cloning, purification, localization in mitochondria, and regulation by adenine nucleotides, *Plant Physiol.* **121**, 589-97.
57. Liepman, A. H. & Olsen, L. J. (2003) Alanine aminotransferase homologs catalyze the glutamate:glyoxylate aminotransferase reaction in peroxisomes of *Arabidopsis*, *Plant Physiol.* **131**, 215-27.
58. Nakamura, Y. & Tolbert, N. E. (1983) Serine: glyoxylate, alanine:glyoxylate, and glutamate:glyoxylate aminotransferase reactions in peroxisomes from spinach leaves, *J Biol Chem.* **258**, 7631-8.
59. Kendziorek, M. & Paszkowski, A. (2008) Properties of serine:glyoxylate aminotransferase purified from *Arabidopsis thaliana* leaves, *Acta Biochim Biophys Sin (Shanghai)*. **40**, 102-10.
60. Cellini, B., Bertoldi, M., Montioli, R., Paiardini, A. & Borri Voltattorni, C. (2007) Human wild-type alanine:glyoxylate aminotransferase and its naturally occurring G82E variant: functional properties and physiological implications, *Biochem J.* **408**, 39-50.
61. Donini, S., Ferrari, M., Fedeli, C., Faini, M., Lamberto, I., Marletta, A. S., Mellini, L., Panini, M., Percudani, R., Pollegioni, L., Caldinelli, L., Petrucco, S. & Peracchi, A. (2009) Recombinant production of eight human cytosolic aminotransferases and assessment of their potential involvement in glyoxylate metabolism, *Biochem J.* **422**, 265-272.
62. Metzler, D. E., Olivard, J. & Snell, E. E. (1954) Transamination of pyridoxamine and amino acids with glyoxylic acid, *J Am Chem Soc.* **76**, 644-648.
63. Smith, A. D., Benziman, M. & Strecker, H. J. (1967) The formation of ornithine from proline in animal tissues, *Biochem J.* **104**, 557-63.
64. Wu, G., Bazer, F. W., Hu, J., Johnson, G. A. & Spencer, T. E. (2005) Polyamine synthesis from proline in the developing porcine placenta, *Biol Reprod.* **72**, 842-50.
65. Funck, D., Stadelhofer, B. & Koch, W. (2008) Ornithine- δ -aminotransferase is essential for arginine catabolism but not for proline biosynthesis, *BMC Plant Biol.* **8**, 40.
66. O'Brien, P. J., Siraki, A. G. & Shangari, N. (2005) Aldehyde sources, metabolism, molecular toxicity mechanisms, and possible effects on human health, *Critical reviews in toxicology.* **35**, 609-62.
67. Koszelewski, D., Tauber, K., Faber, K. & Kroutil, W. (2010) ω -Transaminases for the synthesis of non-racemic α -chiral primary amines, *Trends Biotechnol.* **28**, 324-32.
68. Tufvesson, P., Jensen, J. S., Kroutil, W. & Woodley, J. M. (2012) Experimental determination of thermodynamic equilibrium in biocatalytic transamination, *Biotechnol Bioeng.* **109**, 2159-62.

69. Hohne, M., Kuhl, S., Robins, K. & Bornscheuer, U. T. (2008) Efficient asymmetric synthesis of chiral amines by combining transaminase and pyruvate decarboxylase, *ChemBiochem : a European journal of chemical biology*. **9**, 363-5.
70. Shin, J.-S. & Kim, B.-G. (1999) Asymmetric synthesis of chiral amines with ω -transaminase, *Biotechnology and bioengineering*. **65**, 206-211.
71. Seo, J. H., Kyung, D., Joo, K., Lee, J. & Kim, B. G. (2011) Necessary and sufficient conditions for the asymmetric synthesis of chiral amines using ω -aminotransferases, *Biotechnol Bioeng*. **108**, 253-63.
72. Shin, J.-S. & Kim, B.-G. (1998) Kinetic modeling of ω -transamination for enzymatic kinetic resolution of α -methylbenzylamine, *Biotechnol Bioeng*. **60**, 534-540.
73. Savile, C. K., Janey, J. M., Mundorff, E. C., Moore, J. C., Tam, S., Jarvis, W. R., Colbeck, J. C., Krebber, A., Fleitz, F. J., Brands, J., Devine, P. N., Huisman, G. W. & Hughes, G. J. (2010) Biocatalytic Asymmetric Synthesis of Chiral Amines from Ketones Applied to Sitagliptin Manufacture, *Science (New York, NY)*. **329**, 305-309.
74. Mallin, H., Höhne, M. & Bornscheuer, U. T. (2014) Immobilization of (R)- and (S)-amine transaminases on chitosan support and their application for amine synthesis using isopropylamine as donor, *Journal of Biotechnology*. **191**, 32-37.
75. Hirotsu, K., Goto, M., Okamoto, A. & Miyahara, I. (2005) Dual substrate recognition of aminotransferases, *Chem Rec*. **5**, 160-172.
76. Kack, H., Sandmark, J., Gibson, K., Schneider, G. & Lindqvist, Y. (1999) Crystal structure of diaminopelargonic acid synthase: evolutionary relationships between pyridoxal-5'-phosphate-dependent enzymes, *J Mol Biol*. **291**, 857-76.
77. Marković-Housley, Z., Schirmer, T., Hohenester, E., Khomutov, A. R., Khomutov, R. M., Karpeisky, M. Y., Sandmeier, E., Christen, P. & Jansonius, J. N. (1996) Crystal structures and solution studies of oxime adducts of mitochondrial aspartate aminotransferase, *Eur J Biochem*. **236**, 1025-1032.
78. Storici, P., De Biase, D., Bossa, F., Bruno, S., Mozzarelli, A., Peneff, C., Silverman, R. B. & Schirmer, T. (2004) Structures of γ -aminobutyric acid (GABA) aminotransferase, a pyridoxal 5'-phosphate, and [2Fe-2S] cluster-containing enzyme, complexed with γ -ethynyl-GABA and with the antiepilepsy drug vigabatrin, *J Biol Chem*. **279**, 363-73.
79. Alexander, F. W., Sandmeier, E., Mehta, P. K. & Christen, P. (1994) Evolutionary relationships among pyridoxal-5' -phosphate-dependent enzymes, *Eur J Biochem*. **219**, 953-960.

80. Denesyuk, A. I., Denessiouk, K. A., Korpela, T. & Johnson, M. S. (2002) Functional attributes of the phosphate group binding cup of pyridoxal phosphate-dependent enzymes, *J Mol Biol.* **316**, 155-72.
81. Denesyuk, A. I., Denessiouk, K. A., Korpela, T. & Johnson, M. S. (2003) Phosphate group binding "cup" of PLP-dependent and non-PLP-dependent enzymes: leitmotif and variations, *Biochim Biophys Acta.* **1647**, 234-8.
82. Yano, T., Kuramitsu, S., Tanase, S., Morino, Y. & Kagamiyama, H. (1992) Role of Asp222 in the catalytic mechanism of Escherichia coli aspartate aminotransferase: the amino acid residue which enhances the function of the enzyme-bound coenzyme pyridoxal 5'-phosphate, *Biochemistry.* **31**, 5878-5887.
83. Midelfort, K. S., Kumar, R., Han, S., Karmilowicz, M. J., McConnell, K., Gehlhaar, D. K., Mistry, A., Chang, J. S., Anderson, M., Villalobos, A., Minshull, J., Govindarajan, S. & Wong, J. W. (2013) Redesigning and characterizing the substrate specificity and activity of Vibrio fluvialis aminotransferase for the synthesis of imagabalin, *Protein engineering, design & selection : PEDS.* **26**, 25-33.
84. Yano, T., Mizuno, T. & Kagamiyama, H. (1993) A hydrogen-bonding network modulating enzyme function: asparagine-194 and tyrosine-225 of Escherichia coli aspartate aminotransferase, *Biochemistry.* **32**, 1810-1815.
85. Lee, H., Juncosa, J. I. & Silverman, R. B. (2014) Ornithine aminotransferase versus GABA aminotransferase: Implications for the design of new anticancer drugs, *Med Res Rev.*
86. Stetefeld, J., Jenny, M. & Burkhard, P. (2006) Intersubunit signaling in glutamate-1-semialdehyde-aminomutase, *Proc Natl Acad Sci USA.* **103**, 13688-93.
87. Stetefeld, J., Jenny, M. & Burkhard, P. (2006) Intersubunit signaling in glutamate-1-semialdehyde-aminomutase, *Proceedings of the National Academy of Sciences of the United States of America.* **103**, 13688-93.
88. Markova, M., Peneff, C., Hewlins, M. J., Schirmer, T. & John, R. A. (2005) Determinants of substrate specificity in ω -aminotransferases, *J Biol Chem.* **280**, 36409-16.
89. Storici, P., Capitani, G., Muller, R., Schirmer, T. & Jansonius, J. N. (1999) Crystal structure of human ornithine aminotransferase complexed with the highly specific and potent inhibitor 5-fluoromethylornithine, *J Mol Biol.* **285**, 297-309.
90. Cha, H. J., Jeong, J. H., Rojviriya, C. & Kim, Y. G. (2014) Structure of putrescine aminotransferase from *Escherichia coli* provides Insights into the substrate specificity among class-III aminotransferases, *PLoS one.* **9**, e113212.

91. Shin, J. S. & Kim, B. G. (2002) Exploring the active site of amine:pyruvate aminotransferase on the basis of the substrate structure-reactivity relationship: how the enzyme controls substrate specificity and stereoselectivity, *J Org Chem.* **67**, 2848-53.
92. Hwang, B.-Y., Cho, B.-K., Yun, H., Koteshwar, K. & Kim, B.-G. (2005) Revisit of aminotransferase in the genomic era and its application to biocatalysis, *J Mol Catal B: Enzym.* **37**, 47-55.
93. Lyskowski, A., Gruber, C., Steinkellner, G., Schurmann, M., Schwab, H., Gruber, K. & Steiner, K. (2014) Crystal structure of an (*R*)-selective ω -transaminase from *Aspergillus terreus*, *PLoS one.* **9**, e87350.
94. Steffen-Munsberg, F., Vickers, C., Thontowi, A., Schätzle, S., Meinhardt, T., Svedendahl Humble, M., Land, H., Berglund, P., Bornscheuer, U. T. & Höhne, M. (2013) Revealing the Structural Basis of Promiscuous Amine Transaminase Activity, *ChemCatChem.* **5**, 154-157.
95. Hirotsu, K., Goto, M., Okamoto, A. & Miyahara, I. (2005) Dual substrate recognition of aminotransferases, *The Chemical Record.* **5**, 160-172.
96. Wybenga, G. G., Crismaru, C. G., Janssen, D. B. & Dijkstra, B. W. (2012) Structural determinants of the β -selectivity of a bacterial aminotransferase, *J Biol Chem.* **287**, 28495-502.
97. Sayer, C., Isupov, M. N., Westlake, A. & Littlechild, J. A. (2013) Structural studies of *Pseudomonas* and *Chromobacterium* omega-aminotransferases provide insights into their differing substrate specificity, *Acta crystallographica Section D, Biological crystallography.* **69**, 564-76.
98. Voelgly, R. & Leisinger, T. (1976) Role of 4-aminobutyrate aminotransferase in the arginine metabolism of *Pseudomonas aeruginosa*, *Journal of bacteriology.* **128**, 722-729.
99. Ahmed, S. A., Esaki, N., Tanaka, H. & Soda, K. (1984) L- α -amino- β -thio- ϵ -caprolactam, a new sulfur-containing substrate for α -amino- ϵ -caprolactam racemase, *FEBS Lett.* **174**, 76-79.
100. Ahmed, S. A., Esaki, N., Tanaka, H. & Soda, K. (1986) Mechanism of α -amino- ϵ -caprolactam racemase reaction, *Biochemistry.* **25**, 385-388.
101. Okazaki, S., Suzuki, A., Mizushima, T., Kawano, T., Komeda, H., Asano, Y. & Yamane, T. (2009) The novel structure of a pyridoxal 5'-phosphate-dependent fold-type I racemase, α -amino- ϵ -caprolactam racemase from *Achromobacter obae*, *Biochemistry.* **48**, 941-50.
102. Okazaki, S., Suzuki, A., Mizushima, T., Kawano, T., Komeda, H., Asano, Y. & Yamane, T. (2009) The novel structure of a pyridoxal 5'-phosphate-dependent fold-type I racemase, alpha-amino-epsilon-caprolactam racemase from *Achromobacter obae*, *Biochemistry.* **48**,

941-50.

103. Mutaguchi, Y., Ohmori, T., Wakamatsu, T., Doi, K. & Ohshima, T. (2013) Identification, purification, and characterization of a novel amino acid racemase, isoleucine 2-epimerase, from *Lactobacillus* species, *Journal of bacteriology*. **195**, 5207-15.
104. Veiga-da-Cunha, M., Hadi, F., Balligand, T., Stroobant, V. & Van Schaftingen, E. (2012) Molecular identification of hydroxylysine kinase and of ammoniophospholyases acting on 5-phosphohydroxy-L-lysine and phosphoethanolamine, *J Biol Chem*. **287**, 7246-55.
105. Schirolli, D., Cirrincione, S., Donini, S. & Peracchi, A. (2013) Strict reaction and substrate specificity of AGXT2L1, the human O-phosphoethanolamine phospho-lyase, *IUBMB life*. **65**, 645-50.
106. Paiardini, A., Bossa, F. & Pascarella, S. (2004) Evolutionarily conserved regions and hydrophobic contacts at the superfamily level: The case of the fold-type I, pyridoxal-5'-phosphate-dependent enzymes, *Protein Sci*. **13**, 2992-3005.
107. Kongsaree, P., Samanchart, C., Laowanapiban, P., Wiyakrutta, S. & Meevootisom, V. (2003) Crystallization and preliminary X-ray crystallographic analysis of D-phenylglycine aminotransferase from *Pseudomonas stutzeri* ST201, *Acta Crystallogr D Biol Crystallogr*. **59**, 953-4.
108. Vandenende, C. S., Vlasschaert, M. & Seah, S. Y. (2004) Functional characterization of an aminotransferase required for pyoverdine siderophore biosynthesis in *Pseudomonas aeruginosa* PAO1, *Journal of bacteriology*. **186**, 5596-602.
109. Hennig, M., Grimm, B., Contestabile, R., John, R. A. & Jansonius, J. N. (1997) Crystal structure of glutamate-1-semialdehyde aminomutase: an α_2 -dimeric vitamin B6-dependent enzyme with asymmetry in structure and active site reactivity, *Proc Natl Acad Sci USA*. **94**, 4866-71.
110. Heintl, S., Hartinger, D., Thamhesl, M., Schatzmayr, G., Moll, W. D. & Grabherr, R. (2010) An aminotransferase from bacterium ATCC 55552 deaminates hydrolyzed fumonisin B(1), *Biodegradation*. **22**, 25-30.

Purpose of research

The initial section of the present thesis has offered a broad perspective on a structural subgroup of PLP-dependent enzymes (termed here AT-II), specialized in transforming terminal amines (rather than standard amino acids). We have tried to outline some of the factors that contribute to such a peculiar specificity, particularly in aminotransferases, which represent the vast majority of these enzymes.

The main purpose of the experimental work presented in the following sections was to explore the properties, and in particular the specificity, of one of the few AT-II enzymes that is not a transaminase, namely O-phosphoethanolamine phospho-lyase (PEA-PL). This enzyme is quite peculiar for several reasons. First, it is the only known AT-II enzyme (together with its closely related paralog, O-phospho-5-hydroxy-L-lysine phospho-lyase) whose primary function is to catalyze an elimination reaction. Second, because its substrate is, quite unusually, an amine containing a phosphate group. Third, because the enzyme, despite being phylogenetically very close to pyruvate-dependent AT-II transaminases (in particular, to the promiscuous AGXT2) was reported to lack any transaminase activity.

The first issue that we addressed was defining the boundaries of substrate specificity by PEA-PL. To this end, we carried out an extensive screening of potential substrates and ligands of the enzyme, trying to assess whether PEA-PL is able to recognize only amines or also amino acids and how the phosphate group is important in dictating substrate specificity. A further question that we tackled related to the ability of the enzyme to act as an aminotransferase – we quantitated the ability of PEA-PL to carry out transaminases reaction, providing a measure of it

reaction specificity. The results of this first part of the work allowed us to conclude that both the substrate- and reaction specificity of PEA-PL are remarkably strict for a PLP-dependent enzyme.

To rationalize these findings, and to better understand their mechanistic basis, we then undertook a wide kinetic study encompassing (i) the relative ability of various anionic compounds in inhibiting the PEA-PL reaction; (ii) the pH dependence of the enzyme's steady-state catalytic parameters and of the inhibitors effectiveness; (iii) a spectroscopic study of the interaction of the enzyme with substrates and inhibitors and (iv) a pre-steady state analysis of the PEA-PL reaction, to gain more information on the formation of catalytic intermediates and generally on the reaction mechanism of the enzyme. Interpretation of all these data was guided by the pre-existing literature on PLP-dependent enzymes, that allowed to draw some conclusions about the mechanistic and structural basis of PEA-PL specificity and catalytic efficiency.

Having established the high substrate specificity of PEA-PL, we also decided to explore its practical usefulness, by developing an enzymatic assay for the selective detection of PEA in liquid samples. This assay would be most useful for the clinical laboratory: as PEA levels are increased in in some biological fluids in the course of metabolic, genetic and psychiatric diseases, a method for the rapid and quantitative detection of this analyte would be of relevance to the diagnosis and monitoring of such diseases. The fluorometric assay we developed could satisfactorily quantitate micromolar amounts of PEA in a buffer-water system, but did not work in plasma, presumably due to interference by other components of the biological matrix.

Strict reaction and substrate specificity of AGXT2L1, the human O-phosphoethanolamine phospho-lyase

Davide Schioli^a, Simona Cirrincione^a, Stefano Donini^b, and Alessio Peracchi^{a,c}

^a Department of Biosciences, University of Parma, 43124 Parma, Italy.

^b Department of Pharmaceutical Sciences, University of Piemonte Orientale Amedeo Avogadro, 28100 Novara, Italy.

^c Corresponding author. Phone: +39 0521905137 Fax: +39 0521905151.
Email: alessio.peracchi@unipr.it.

Keywords: pyridoxal-phosphate; class-II aminotransferases; catalytic promiscuity; schizophrenia; bipolar disorder; phospholipid metabolism.

Abbreviations: PLP, pyridoxal-5' phosphate; PMP, pyridoxamine-5' phosphate; AGXT2, alanine-glyoxylate transaminase 2; AGXT2L1, alanine-glyoxylate transaminase 2-like 1; 5-ALA, 5-aminolevulinate; PEA, O-phosphoethanolamine; SEA, O-sulfoethanolamine; 3-APP, 3-aminopropylphosphonate; GABA-AT, γ -aminobutyrate aminotransferase;

This chapter was published in *IUBMB Life*: Schioli, D., Cirrincione, S., Donini, S. & Peracchi, A. (2013) Strict reaction and substrate specificity of AGXT2L1, the human O-phosphoethanolamine phospho-lyase, *IUBMB Life*. 65, 645-50.

ABSTRACT

Dysregulated expression of the *AGXT2L1* gene has been associated to neuropsychiatric disorders. Recently the gene product was shown to possess *O*-phosphoethanolamine phospho-lyase activity. We here analyze the specificity of *AGXT2L1* in terms of both reaction and substrate. We show that the enzyme, despite having evolved from a transaminase ancestor, is at least 500-fold more active as a lyase than as an aminotransferase. Furthermore, the lyase reaction is very selective for *O*-phosphoethanolamine, strongly discriminating against closely related compounds, and we dissect the factors that contribute to such narrow substrate specificity. Overall, *AGXT2L1* function appears to be rigidly confined to phospholipid metabolism, which is altered in neuropsychiatric disturbances.

INTRODUCTION

Although enzymes are often described as exquisitely specific, both in terms of catalyzed reaction and recognized substrates, this is not the rule. Today it is well appreciated that a substantial fraction of metabolic enzymes are promiscuous, meaning that they can catalyze reactions of different types and with different substrates [2, 3]. In particular, enzymes dependent on the cofactor pyridoxal 5'-phosphate (PLP) are considered prototypical promiscuous catalysts, due to the intrinsic versatility of PLP [4, 5]. One pertinent example is alanine-glyoxylate aminotransferase 2 (AGXT2), a mitochondrial PLP-dependent enzyme that transaminates a variety of substrates – such as L-alanine, 5-aminolevulinate (5-ALA), β -alanine and D-3-aminoisobutyrate [6] - and also acts as a lyase on L-cysteine conjugates [7] – a secondary activity possessed by several aminotransferases [8].

AGXT2L1 is a brain enzyme, so-named after its similarity to AGXT2 (36% sequence identity), that may be involved in the pathogenesis of severe neuropsychiatric disturbances. For example, in a study designed to pinpoint common gene expression profiles between schizophrenia and bipolar disorder, the *AGXT2L1* gene was the most consistently upregulated in the brains of deceased patients with either condition, as compared to control subjects [9]. Such an increased expression might contribute to the diseases or represent a compensatory response to some prior neurochemical imbalance. Potentially consistent with this latter possibility was the finding that, in mouse brain, *AGXT2L1* was the most upregulated gene following treatment with the mood-stabilizer lithium carbonate [10]. All these findings elicited a considerable interest on *AGXT2L1*, but for a long time the function of the encoded protein remained obscure.

Recently, Veiga-da-Cunha and coworkers [11] demonstrated in an elegant study that AGXT2L1 is a lyase acting on O-phosphoethanolamine (PEA). In other words, they showed that the enzyme irreversibly degrades PEA to acetaldehyde, phosphate and ammonia (Figure 1A; [1, 11-13], also providing a limited characterization of this activity. While this result was remarkable, it left several questions unanswered.

First, the reported catalytic efficiency of the PEA phospho-lyase reaction was modest, raising doubts that perhaps other metabolites could be better substrates of AGXT2L1. Furthermore, it remained unclear whether the enzyme showed reaction promiscuity (like its relative AGXT2) and could for example act as a transaminase towards some substrate, contributing to different metabolic pathways. More generally, it was not known whether AGXT2L1 would bind other common amino compounds, which might function as modulators, as reported for other brain-specific PLP-dependent enzymes [14]. Addressing these and similar questions seemed important to better understand AGXT2L1 as a catalyst and to shed more light on its actual biological role.

Herein, we explore the reaction and substrate selectivity of AGXT2L1, showing that the enzyme is strikingly specific and non-promiscuous. We discuss the implications of these findings for the evolution, mechanism and metabolic function of AGXT2L1.

MATERIALS AND METHODS

Materials

Recombinant AGXT2L1 was prepared as described [15]. Yeast alcohol dehydrogenase (ADH) and *Bacillus subtilis* L-alanine dehydrogenase were from Sigma, rabbit muscle lactate dehydrogenase (LDH) was from Fluka. Ciliatine was from Wako Chemicals.

Glycerophosphoethanolamine was a kind gift from Euticals (Lodi, Italy). O-phospho-L-homoserine was prepared enzymatically [16]. All other reagents were from Fluka or Sigma-Aldrich.

Enzymatic assays

Solutions for the PEA phospho-lyase assay (200 μ l final volume) contained 25 mM buffer (triethanolamine or MES) at the desired pH value, 100 mM KCl, 0.8 mM EGTA, 5 μ M PLP, 0.5 mg/ml bovine serum albumin (BSA), 0.2 mM NADH, 50 units/ml ADH, in addition to AGXT2L1 (typically 0,5 μ M) and PEA. Reactions were conducted at 30°C, and the rate of acetaldehyde formation was measured by monitoring spectrophotometrically the coupled disappearance of NADH at 340 nm. Nonlinear least-squares fittings of the data were performed using Sigma Plot (SPSS Inc.).

Tests for 1,2-elimination reactions involving PEA analogs such as O-sulfoethanolamine (SEA) were conducted as above, except that the analogs were used in place of PEA.

To test the possible phospho-lyase activity of AGXT2L1 towards O-phospho-L-serine, O-phospho-L-threonine or O-phospho-L-homoserine, we assessed formation of the predicted carbonyl products (pyruvate or α -ketobutyrate) by a coupled assay with LDH [16]. The reaction mixture

contained 25 mM triethanolamine (pH 8, 30°C), 100 mM KCl, 5 μ M PLP, 0.5 mg/ml BSA, 0.2 mM NADH, 50 units/ml LDH, in addition to AGXT2L1 (3 μ M) and the phosphorylated amino acid.

The amine-pyruvate transaminase reactions, leading to the formation of alanine, were tested by a discontinuous assay based on the use of L-alanine dehydrogenase [17]. AGXT2L1 (16 μ M) was incubated with the amino-donor compound (e.g., hypotaurine 20 mM) and pyruvate (20 mM) in 50 mM triethanolamine buffer, pH 8, 30°C. Total initial volume was 200 μ l. Aliquots (50 μ l each) were collected at appropriate intervals over a six-hour period. Further reaction in each aliquot was stopped by mixing with 2.5 μ l of a hydrazine (10 M)/EDTA (14 mM) solution; samples were also heated at 95 °C for 5 min to completely inactivate the enzyme. Each aliquot was subsequently mixed with 50 μ l of a solution containing 100 mM sodium carbonate (pH 10), L-alanine dehydrogenase (1.26 unit), and NAD⁺ (0.25 mM) and incubated at 25 °C for 30 min, until an end-point was reached. Finally, absorption spectra in the 340 nm region were taken to quantitate the extent of NADH formation and hence the concentration of L-alanine in the initial aliquot.

Spectrophotometric measurements

To monitor the interaction of AGXT2L1 with amino compounds (potential substrates or inhibitors), solutions containing the enzyme (9 μ M) in 25 mM bis-tris propane (BTP) buffer, pH 8, 20 °C, were supplemented with the compound under examination (typically, 5 mM). Changes in the PLP absorption were monitored using a Cary 400 spectrophotometer (Varian).

The setup for measuring the kinetics of half-transamination reactions was as above, except that triethanolamine buffer (pH 8) was used and

the temperature was 30 °C. Spectra were collected at regular intervals after mixing the enzyme with the ligand.

RESULTS

Efficiency and specificity of the lyase reaction catalyzed by AGXT2L1

We characterized the activity of recombinant AGXT2L1 towards PEA. At the optimal pH 8.0, the observed kinetic parameters were: $K_M^{PEA}=0.9$ mM, $k_{cat}^{PEA}=2.3$ s⁻¹ and $(k_{cat}/K_M)^{PEA}=2600$ M⁻¹s⁻¹ (Fig. 1B). These values are close to those reported by Veiga-da-Cunha et al [11], who performed their experiments at pH 7.4. The K_M^{PEA} value was also very similar to that reported over 40 years ago by Fleshood and Pitot for a partially purified PEA phospho-lyase from rabbit [13].

Tests on a dozen commercially available PEA analogs showed that the lyase activity of AGXT2L1 is extremely substrate-specific (Table 1). When the phosphate moiety of PEA was replaced by other good leaving groups, such as bromine or a thiol, the elimination reaction was virtually undetectable. A carboxylate adjacent to the amino carbon (as in *O*-phosphoserine) or a glycerol moiety attached to the phosphate (as in glycerophosphoethanolamine) also drastically prevented activity.

We studied in detail the reaction of AGXT2L1 with *O*-sulfoethanolamine (SEA), a PEA analog containing a sulfate (rather than phosphate) leaving group. Despite its close structural similarity to PEA, SEA reacted very poorly. Its specificity constant, $(k_{cat}/K_M)^{SEA}$, was ~1.4 M⁻¹ s⁻¹, or 1800-fold lower than $(k_{cat}/K_M)^{PEA}$. While the SEA elimination rate did not reach saturation even at 300 mM substrate (Fig. 1B), preventing determination of accurate individual values for k_{cat}^{SEA} and K_M^{SEA} , most of the discrimination against SEA clearly mirrored a very high K_M for this compound. The k_{cat}/K_M gap between PEA and SEA did not change much in the pH 6-9 range (Fig. 2).

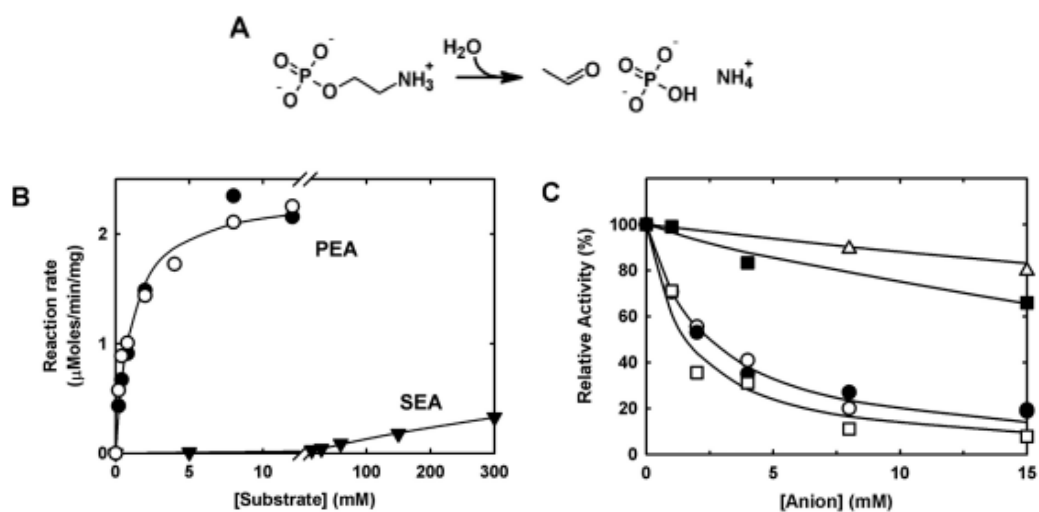
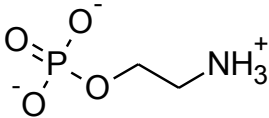
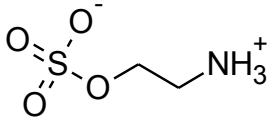
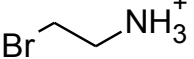
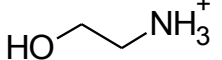
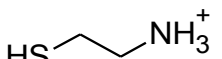
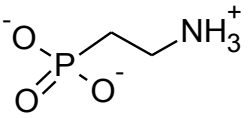
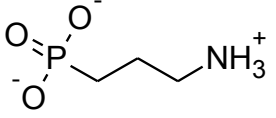
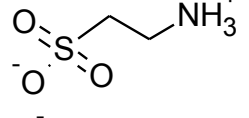
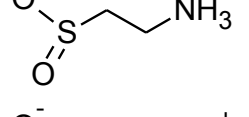
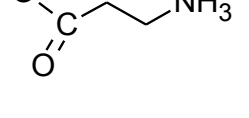
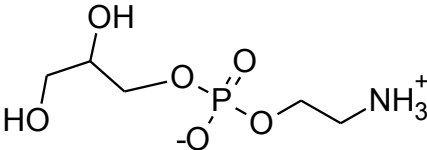
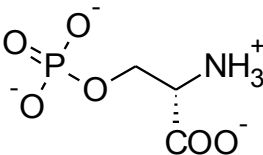
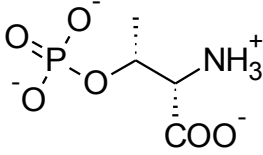
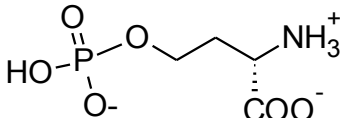


Figure 1 - (A) The PEA phospho-lyase reaction [12, 13] catalyzed by recombinant AGXT2L1 [1, 11]. (B) Rate of the elimination reaction as a function of the concentration of PEA (○, ●) or SEA (▼) at 30°C, pH 8.0. Fitting of the PEA data points to the Michaelis-Menten equation yielded $K_M^{PEA} = 0.9 \pm 0.2$ mM and $V_{max} = 2.4 \pm 0.2$ μMoles/min per mg of protein (corresponding to $k_{cat}^{PEA} = 2.3$ s⁻¹). Since the SEA elimination rate did not reach saturation even at the highest substrate concentration tested, reliable values of k_{cat}^{SEA} and K_M^{SEA} could not be determined by data fitting. However, $(k_{cat}/K_M)^{SEA}$, representing the initial slope of the Michaelis-Menten hyperbola, was 1.4 ± 0.3 M⁻¹ s⁻¹. (C) Inhibitory effect of various anions on the rate of the PEA elimination reaction, pH 8. PEA concentration was 1 mM. The data points refer to phosphate (○), sulfate (●), glyoxylate (□), methyl sulfate (■) and SEA (Δ). Calculated K_i values are given in Table 2.

Table 1Absolute and relative specificity of AGXT2L1 for various PEA analogs

Compound		k_{cat}/K_M ($M^{-1} s^{-1}$)	$\frac{(k_{cat}/K_M)^{analog}}{(k_{cat}/K_M)^{PEA}}$ (1)
O-phosphoethanolamine (PEA)		2600	
O-sulfoethanolamine (SEA)		1.4	5.4×10^{-4}
2-bromoethylamine		0.12 ^a	4.6×10^{-5}
Ethanolamine		<0.015 _b	< 5.8×10^{-6}
Cysteamine		^c <1	< 3.8×10^{-4}
Ciliatine		<0.015 _b	< 5.8×10^{-6}
3-aminopropyl phosphonate (3-APP)		<0.5 ^d	< 1.9×10^{-4}
Taurine		<0.015 _b	< 5.8×10^{-6}
Hypotaurine		<0.2 ^d	< 7.6×10^{-5}
β -alanine		<0.015 _b	< 5.8×10^{-6}

Glycerophospho Ethanolamine		0.27 ^e	10 ⁻⁴
O-phospho-L-serine		<0.015 _b	<5.8×10 ⁻⁶
O-phospho-L-threonine		<0.015 _b	<5.8×10 ⁻⁶
O-phospho-L-homoserine		<0.015 _b	<5.8×10 ⁻⁶

^a The very slow elimination reaction with 2-bromoethylamine ended after a few turnovers, due presumably to irreversible inactivation of the enzyme.

^b These analogs did not undergo any detectable elimination when reacted at a 30 mM concentration with 3 μM enzyme (< 2 μM product formed in 20 min).

^c No elimination detected. A limit was estimated considering that, within a few minutes, cysteamine formed an unreactive thiazolidine adduct with PLP.

^d No elimination detected. Limits were estimated considering that, in a few minutes, these analogs completely converted PLP to PMP.

^e Glycerophosphoethanolamine could be contaminated by small amounts of PEA, so this k_{cat}/K_M may also be an upper limit.

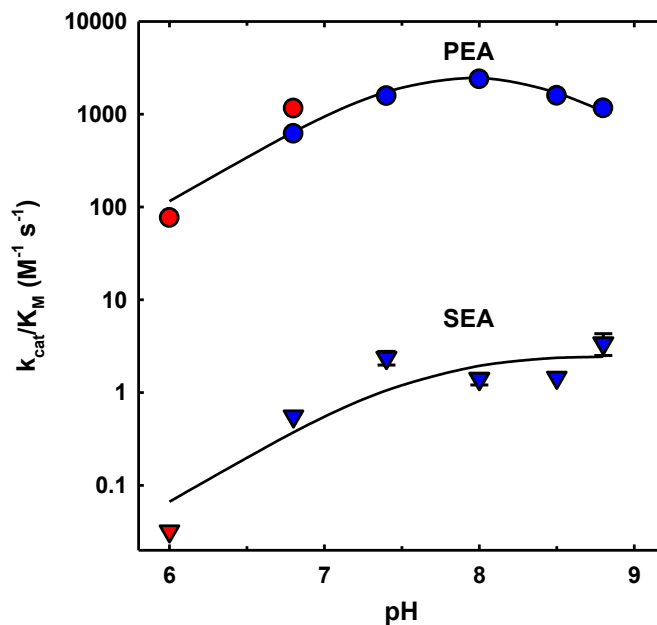


Figure 2 – pH dependence of $(k_{cat}/K_M)^{PEA}$ (circles) and $(k_{cat}/K_M)^{SEA}$ (triangles). Kinetics were measured as described in the Methods, in triethanolamine (blue datapoints) or MES buffer (red datapoints). Note that the pH dependence of $(k_{cat}/K_M)^{PEA}$ was almost entirely dictated by changes in K_M^{PEA} , as k_{cat}^{PEA} changed little in the explored pH range (data not shown). The solid line through the PEA data is a least-squares fitting to an equation that assumes the dependence of $(k_{cat}/K_M)^{PEA}$ on the ionization of two groups [18]: one group with apparent $pK_a=6.9 \pm 0.5$ and another with apparent $pK_a=8.9 \pm 0.4$. Absence of the alkaline limb of the dependence for the SEA data suggests that one of the two groups might be a general acid involved in activation of the substrate leaving group.

Relatively unspecific inhibition of AGXT2L1 by anions

The strict substrate specificity of AGXT2L1 contrasted with its facile inhibition by a variety of anionic compounds. In addition to the reported competitive inhibition of AGXT2L1 by phosphate [11], we observed a very similar inhibition by other inorganic anions such phosphite and sulfate (Fig. 1C and Table 2). Methyl sulfate was one order of magnitude less effective than sulfate, while SEA inhibited very weakly. Glyoxylate and to a lesser extent pyruvate were also inhibitors (Fig. 1C and Table 2).

Spectroscopic screening of AGXT2L1 binding selectivity

In PLP-dependent enzymes, cofactor absorption is often exploited to monitor the binding of ligands and the formation of catalytic intermediates (e.g., [19, 20]. For example in aminotransferases, reaction with an amino-group donor substrate in the absence of amino-group acceptors leads to a half-transamination, i.e., the conversion of PLP ($\lambda_{\max} \approx 410$ nm) to pyridoxamine 5'-phosphate (PMP; $\lambda_{\max} \approx 330$ nm).

The reaction of AGXT2L1 with PEA was accompanied by significant changes in the cofactor spectrum, which we tentatively attributed to the formation of a Schiff base with the amine (Fig. 3). We also screened spectroscopically the interaction of AGXT2L1 with ~70 other amino compounds (Table 2), to identify possible additional ligands. Our test set tried to include the most common amino metabolites (especially amino acids and brain amines) as well as compounds sufficiently diverse in terms of chemical properties (anionic, cationic, aromatic etc.), to gather information on the binding selectivity of AGXT2L1. The results of this screening can be summarized as follows.

Table 2

Inhibition of the PEA phospho-lyase reaction by different anions. Reactions were performed as described in the Methods, at pH 8, 30°C. PEA concentration was 1 mM. Anions were usually added as sodium salts; for each of them, the maximum concentration used was 15 mM. Decreases in activity as a function of the added anion were fit to the equation:

$$\text{Relative activity} = v_i/v_0 = \frac{K_i(K_M^{\text{PEA}} + [\text{PEA}])}{K_i(K_M^{\text{PEA}} + [\text{PEA}]) + K_M^{\text{PEA}}[I]}$$

The equation assumes purely competitive inhibition. v_i is the reaction rate measured in the presence of the inhibitor, while v_0 is the rate in the absence of inhibitor. $[I]$ is the concentration of the anion and K_i is the respective inhibition constant.

Anion	K_i (mM)
Phosphate	1.2 ± 0.2^a
Sulfate	1.2 ± 0.2
Phosphite	1 ± 0.2
Arsenate	3.6 ± 0.9
Pyrophosphate	1.3 ± 0.4
Methyl sulfate	15 ± 3
Oxalate	2.8 ± 0.7
Glyoxylate	0.7 ± 0.2^b
Pyruvate	5.0 ± 1.6
α -ketoglutarate	2.7 ± 0.9
SEA	>25
Ciliatine	7.6 ± 2.0
3-APP	1.8 ± 0.4^c

^a The K_i of phosphate is identical, within error, to the value reported for a partially purified PEA phospho-lyase from rabbit [13].

^b The K_i of glyoxylate was roughly threefold smaller at pH 8.5; at this higher pH, we also compared the glyoxylate inhibition observed in triethanolamine with that observed in borate-Na, obtaining essentially identical K_i values in the two buffer systems.

^c To obtain a K_i for 3-APP, v_i was measured in the first minute of the kinetics. On longer times, a further progressive decrease of the reaction rate was evident, as 3-APP slowly converted the enzyme-bound PLP to PMP (see main text).

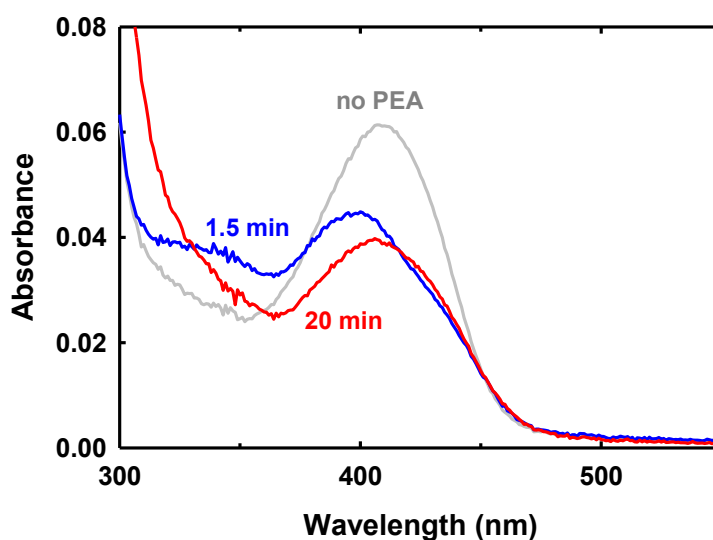


Figure 3 –Changes in the UV-visible spectrum accompanying the reaction of AGXT2L1 (9 μ M) with PEA (50 mM), in 25 mM Bis-Tris propane, pH 8, 20°C. Addition of the substrate to the enzyme caused an immediate shift from ~410 to ~400 nm of the main PLP absorption band, whose intensity also decreased. This could indicate the disappearance of the ‘internal’ Schiff base between PLP and the enzyme, with accumulation of an ‘external’ Schiff base between PLP and PEA. In PLP-dependent enzymes, formation of external Schiff bases usually causes a red-shift of the spectrum, but blue shifts are also occasionally observed (e.g., ref. [21]. Alternatively, the spectral

change may indicate the formation of intermediates further down the reaction pathway, for example an ethyleneamine intermediate formed upon release of the phosphate leaving group. Over time, the λ_{\max} of the main PLP band reverted to ~410 nm, although absorption remained low.

i – The vast majority of compounds caused only negligible spectral changes, implying their inability (at least at the 5 mM concentration used) to bind and react at the AGXT2L1 active site. Most of the compounds that did react were ω -amines, i.e., carried a terminal amino group not adjacent to a carboxylate.

ii - L-cysteine and related aminothiols gave rise to bands at ~340 nm (Fig. 4A), attributable to thiazolidine adducts formed with PLP [14]. Aminothiols in fact behaved as time-dependent inhibitors of AGXT2L1 (not shown), although inhibition was negligible at the concentrations of L-cysteine typically found in the cytosol (≤ 0.1 mM; [22]).

iii – Reaction of AGXT2L1 with 5-ALA, a substrate of AGXT2 [6], produced a sharp band at 507 nm (Fig. 4A). This band strongly resembled the peaks that, in other enzymes, are attributed to stabilized carbanionic intermediates (quinonoids), formed upon cleavage of one of the bonds connecting the amino carbon to its substituents [23]. Quinonoid bands were formed by other compounds that, like 5-ALA, bear a keto function adjacent to the amino group (e.g., 2-aminoacetophenone).

iv - The only evidences for substantial PMP formation, and hence for half-transamination, were obtained upon incubating the enzyme with small, anionic ω -amines such as taurine, hypotaurine and 3-APP. Even in these cases, accumulation of a 330 nm band took minutes to occur

(Fig. 4B). Formation of this species could be partially reversed by the addition of pyruvate, glyoxylate or α -ketoglutarate (not shown).

Aminotransferase activity of AGXT2L1

We studied in more detail the reaction of 3-APP, which differs from PEA only for having the ester oxygen atom replaced by a methylene group. This difference is expected to interfere with the lyase reaction, which in fact was undetectable (table 1), but not necessarily with the transamination. Indeed, 3-APP formed PMP faster than any other amino compound tested.

We monitored the reaction of 3-APP (0.1-10 mM) with AGXT2L1 at 30°C. At each 3-APP concentration, the data fit well to a monoexponential process and the observed pseudo first-order rate constants increased hyperbolically as a function of the amine concentration (Figure 4C). The initial slope of the hyperbola (i.e., the apparent second-order rate constant for the half-transamination) was $5.3 \pm 1.3 \text{ M}^{-1} \text{ s}^{-1}$. This value represents an upper limit of k_{cat}/K_M for a full transamination reaction, which cannot proceed faster than its first half. Stated another way, our data imply that the specificity constant for 3-APP transamination (whatever the amino group acceptor) is going to be ≥ 500 -fold lower than $(k_{cat}/K_M)^{PEA}$ for the lyase reaction.

To buttress this conclusion, we assessed the actual amine-pyruvate aminotransferase activity of AGXT2L1, by monitoring formation of the product L-alanine [17]. Pyruvate was kept constant at 20 mM, while 3-APP was used at concentrations up to 50 mM. In all these assays, the observed rate of 3-APP transamination remained well below the limit expected based on the half-transamination data (Fig. 5).

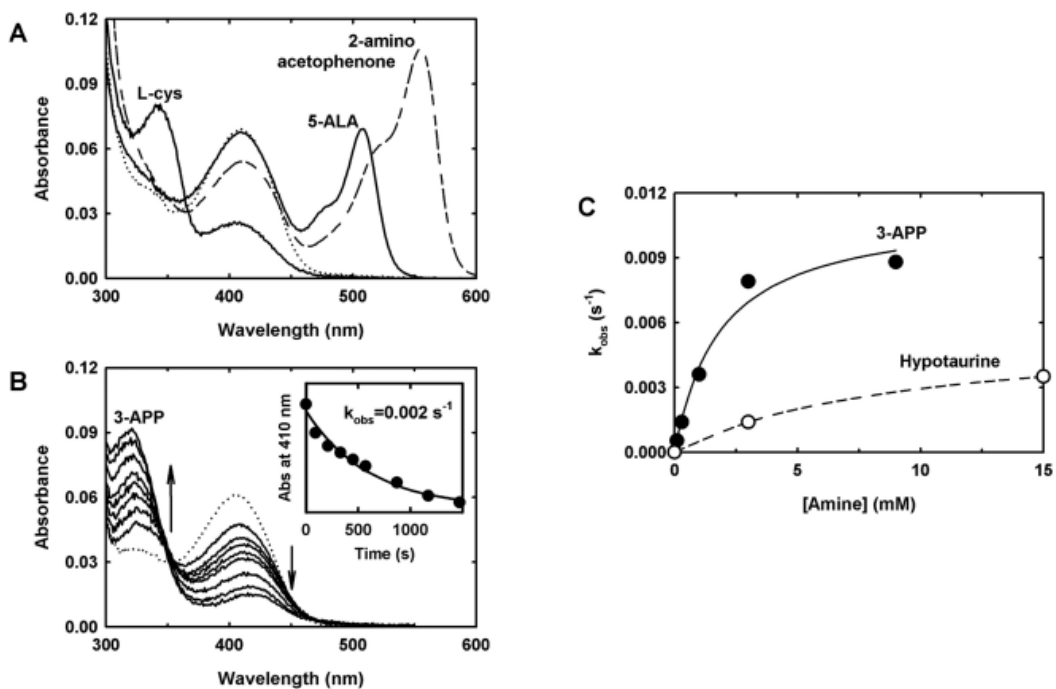


Figure 4 - (A) Absorption spectra of recombinant AGXT2L1 (9 μM) in 25 mM Bis-Tris propane, pH 8, 20°C, were recorded in the absence of ligands (dotted line) and upon reaction with 5 mM L-cysteine, or 5 mM 5-ALA or 0.5 mM 2-aminoacetophenone. (B) Progressive spectral changes observed in the presence of 5 mM 3-APP (pH 8, 20°C). Inset: time-course of the half-transamination. (C) Dependence of k_{obs} for the half-transamination (PMP formation) on the concentration of 3-APP (25 mM triethanolamine buffer, pH 8, 30 °C). The solid line is a fit of the data to a hyperbolic function, yielding $K_{0.5} = 1.9 \text{ mM}$ and an extrapolated maximum k_{obs} of $1.1 \times 10^{-2} \text{ s}^{-1}$. For comparison, the half-transamination rates obtained at two concentrations of hypotaurine are also shown.

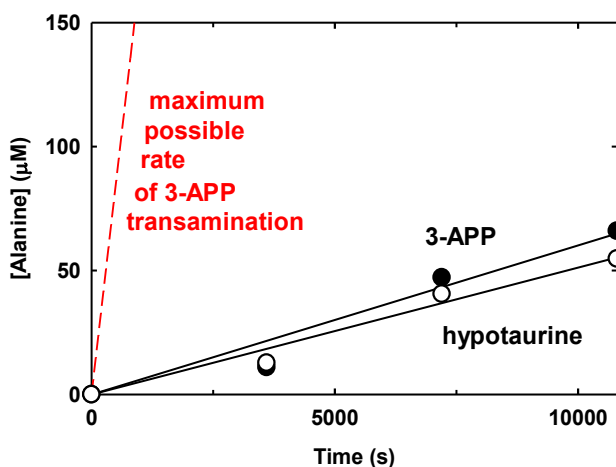


Figure 5 –An assay of the complete amine-pyruvate transamination reaction catalyzed by AGXT2L1. The enzyme (16 μM) was incubated with 20 mM pyruvate and either 50 mM 3-APP (open circles) or 50 mM hypotaurine (filled circles) in 50 mM triethanolamine buffer, pH 8, 30°C. Formation of L-alanine over time was assessed through an assay based on L-alanine dehydrogenase, as described in the Methods [17].

The time-courses of the two reactions in figure were fitted to straight lines with slopes 0.006 $\mu\text{M/s}$ (3-APP) or 0.005 $\mu\text{M/s}$ (hypotaurine). For comparison, a dashed red line (slope 0.17 $\mu\text{M/s}$) represents the maximum rate theoretically achievable with 3-APP under the adopted conditions, assuming that formation of PMP is completely rate-limiting the overall process. The fact that the observed rate is 30-fold lower than this upper boundary and the similar rates observed with 3-APP and hypotaurine may indicate that the regeneration of PLP (i.e., the second half of the transamination reaction) is largely rate-limiting.

DISCUSSION

Evolution of AGXT2L1: of an aminotransferase a phospho-lyase made

AGXT2L1 belongs to a subfamily of proteins termed “class II aminotransferases” [24] that, as the name suggests, is composed almost entirely by transaminases (Fig. 6). This subfamily is not known to include any *bona fide* lyase apart from AGXT2L1 (and the related protein AGXT2L2 [11]), strongly suggesting that the enzyme has evolved from an aminotransferase ancestor. However AGXT2L1 is at least 500-fold more efficient as a phospho-lyase than as an aminotransferase, implying that evolution has led to both a new reaction specificity and to a strongly limited catalytic promiscuity.

What modifications converted an ancestral aminotransferase into a (specific) phospho-lyase? Some insights may be obtained by analyzing conservation at key active site positions between AGXT2L1, AGXT2 and other related transaminases of known structure, such as the bacterial GABA aminotransferase (GABA-AT; Table 3). A striking change involves Ile50, which in GABA-AT provides a roof for the substrate binding site and may help dictate reaction specificity. This aliphatic residue corresponds to Val110 in AGXT2 but has no obvious counterpart in AGXT2L1, suggesting substantial differences in the local structure. Another significant change involves Arg398, which in GABA-AT binds the α -carboxylate of the ketoacid substrate: this residue is conserved in AGXT2, but mutated to a shorter Lys in AGXT2L1.

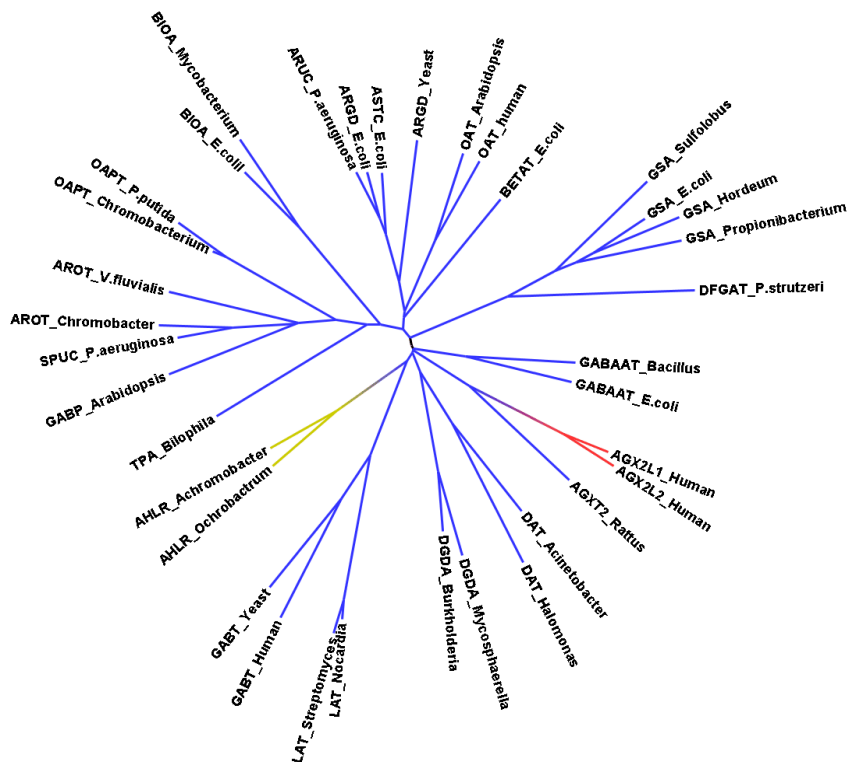


Figure 6 - Phylogenetic relationships of AGXT2L1 with 35 functionally validated enzymes of the same structural subgroup (“class-II aminotransferases”). Sequences taken from the B6 database [25] were aligned with the Clustal Omega software [26]. An unrooted phylogenetic tree was calculated with ClustalW2 [27] using the neighbor-joining algorithm after correction for multiple substitutions and displayed with FigTree (v. 1.4.0; <http://tree.bio.ed.ac.uk/software/figtree/>). Branches leading to enzymes with aminotransferase activity are shown in blue. Dialkylglycine decarboxylases (DGD) and glutamate semi-aldehyde aminomutases (GSA) are included among aminotransferases because their reaction mechanisms comprise the formation of PMP. Branches leading to enzymes with racemase activity (2-aminohexano-6-lactam racemases, AHLR) are shown in yellow. Branches leading to enzymes with lyase activity (including AGXT2L1) are shown in red. The tree does not include some bacterial homologs of AGXT2L1 that almost invariably possess an additional ki-

nase domain [28]. Although the function of these homologs has not been experimentally validated, they are almost certainly phospho-lyases. Indeed, it was precisely thanks to clues offered by the genomic context of these bacterial homologs that Veiga-da-Cunha and collaborators discovered the PEA phospho-lyase activity of AGXT2L1 [11]. Independently, but following an identical line of reasoning, our group had also reached the same functional identification [29].

Table 3

Spectroscopic changes observed upon reacting AGXT2L1 with selected amino compounds. Potential ligands (5 mM) were mixed with the enzyme at pH 8, 20 °C. Spectral changes were measured within 5 min after mixing, looking in particular for the disappearance of the main band of PLP (410 nm) and concomitant appearance of new bands, such as those attributable to PMP (~330 nm), thiazolidine adducts (~340 nm) or quinonoids (>450 nm). The accumulation of new spectroscopic species is indicated semi-quantitatively by a number of + signs ranging from none (negligible) to three (nearly complete).

	PMP	Quinonoid	Thiazolidine	Other ^a
Standard amino acids				
L-Alanine				
L-Arginine				
L-Asparagine				
L-Aspartate				
L-Cysteine			+++	
L-Gluamate				
L-Glutamine				
Glycine				
L-Histidine				
L-Isoleucine				
L-Leucine				
L-Lysine	+			
L-Methionine				
L-Phenylalanine				

L-Proline		
L-Serine		
L-Threonine		
L-Tryptophan		
L-Tyrosine		
L-Valine		
Other α -amino acids		
L-Citrulline		
L-Homocysteine		++
L-Ornithine	+	
L-Allysine		
L-Kynurenine		
3-hydroxy L-kynurenine		
L-Phosphoserine		
S-methyl L-cysteine		
N ^G ,N ^G -dimethyl-L-arginine		
L-Cycloserine		++
D-Cycloserine		+
D-Alanine		
D-Cysteine		++
β -, γ -, or δ -amino acids		
β -alanine	+	
Isoserine		
2-amino isobutyrate		
γ -aminobutyrate (GABA)	+	
5-aminovalerate		
5-aminolevulinate (5-ALA) ^b		++
Anionic amines		
Sulfoethanolamine (SEA)		
Ciliatine	+	
3-aminopropylphosphonate (3-APP)	+++	
3-aminopropylsulfonate	+	
Taurine	++	
Hypotaurine	+++	
Thiataurine	++	
Aromatic amines		
Tyramine		

Octopamine	+		
Dopamine			
Norepinephrine			
Phenylethylamine			
Phenylethanolamine			
Serotonin	+		
Kynurenamine			
Serotonin O-sulfate			
4'-bromo-2-aminoacetophenone ^b		++	
2-aminoacetophenone ^b		++	
<i>Trans</i> -2-phenylcyclopropylamine			
Other amines			
Ethanolamine			
2-bromoethylamine			+
Cysteamine		+++	
Penicillamine		+++	
L-Leucine chloromethyl ketone		+	
Histamine			
Spermidine			
Putrescine			
Sarcosine			
D-Glucosamine			
D-Galactosamine			
D-Mannosamine			
1,4-diamino-2-butanone	++		

^a – L-cycloserine caused a substantial decrease in absorption at 410 nm, with a concomitant broad increase in the region below 350 nm. D-cycloserine caused a shift of the main PLP band to 420 nm. 2-bromoethylamine, over the course of a few minutes, caused a red shift of the main PLP band and a broad increase in the region below 350 nm.

^b – The quite spectacular spectral changes caused by 5-ALA and by other compounds that bear a keto function adjacent to the amino group (see Figure

2A in the main text) reflected the very high extinction coefficients of quinonoids, rather than a high affinity of the ligands, which in fact were only weak inhibitors of the lyase reaction.

Determinants of binding selectivity in AGXT2L1

The specificity of AGXT2L1 for PEA as compared to structural analogs can be mostly explained as binding selectivity. Our data suggest that at least three factors may be enforcing such selectivity. First, the enzyme clearly favors binding ω -amines, suggesting that the active site structure discriminates against amino compounds that contain an α -carboxylate (e.g., O-phospho-L-serine). Second, the size of the ligand is certainly a factor and it is reasonable to assume that binding of bulky PEA analogs such as glycerophosphoethanolamine (Table 1) or O-phospho-5 hydroxy-L-lysine [11] may be hampered due to steric hindrance. Finally, some analogs that are smaller than PEA and potentially very reactive (e.g., 2-bromoethylamine) may nevertheless bind poorly because they lack an anionic function.

Indeed, our data imply the occurrence, in the AGXT2L1 active site, of a subsite responsible for binding anionic groups. By itself this subsite does not seem very selective, as a variety of anions, in addition to phosphate, can act as competitive inhibitors. On the other hand, the requirements for interacting with the subsite may be stricter when it comes to binding anionic amines.

Consider in particular SEA. This compound is nearly isosteric with PEA, while free sulfate shows a K_i nearly identical to phosphate. Nonetheless, $(k_{cat}/K_M)^{SEA}$ is 1800-fold lower than $(k_{cat}/K_M)^{PEA}$ and such a dramatic difference is mostly attributable to weaker binding of SEA (Figure 1B). The sulfate group in SEA bears a single negative

charge (rather than two like the phosphate group in PEA) but this explains only in part this affinity gap; in fact, K_i for monoanionic methylsulfate is just 12-fold higher than K_i for plain sulfate (Table 2). Thus, an exceedingly large discrimination between phosphate and sulfate appears to occur when the two groups are part of an anionic amine. One possibility is that binding of the amine is accompanied by a conformational change that imparts an increased selectivity to the anion subsite.

Support for a conformational change upon substrate binding comes from an analysis of K_M^{PEA} . There are indications that this parameter can be considered an overall dissociation constant of the substrate from AGXT2L1. If this is the case, K_M^{PEA} should depend both on the interactions of PEA with the anion subsite and on the formation of covalent intermediates with PLP. However, the value of K_M^{PEA} is nearly identical to K_i for inorganic phosphate, suggesting that the binding energy gained from covalently linking the amino group to PLP is almost entirely used up to pay for some other unfavorable process, possibly a rearrangement of the active site structure [30].

Considerations on the biological role of AGXT2L1

AGXT2L1 has been apparently shaped by evolution to maximize specificity and limit promiscuity, rather than to optimize absolute catalytic performance (even though its catalytic parameters are comparable to those reported for other mammalian phospho-lyases [11, 16]). A recent study [2] has highlighted three major conditions under which specific enzymes are metabolically preferred to promiscuous ones, namely i) when the catalyzed reaction is essential, ii) when a high metabolic flux is needed, and iii) when the enzyme activity must be tightly regulated. The

need for a strict regulation may be especially relevant for AGXT2L1, whose reaction is irreversible and generates potentially toxic products.

When is AGXT2L1 activity effectively required? PEA is both a product of sphingolipid degradation and a precursor of glycerophospholipid biosynthesis (Fig. 7) and it can accumulate when membrane remodeling or degradation increases. Such an accumulation may be undesirable for several reasons - for example, it has been shown that PEA and the parent compound ethanolamine interfere with mitochondrial function [31] - and under these circumstances AGXT2L1 could act as a 'relief valve', to counteract the rise in PEA concentration. PEA can be also degraded by specific phosphatases, but this reaction generates ethanolamine and is easily reversed by ethanolamine kinase (Fig. 7).

There is a vast literature associating neuropsychiatric disorders to alterations in the brain levels of PEA and related phosphomonoesters and in the membrane phospholipid metabolism [32] and references therein). In keeping with this association, our findings confine the role of AGXT2L1 to phospholipid metabolism. An increased expression of AGXT2L1 during disease [9] might be primarily a compensatory mechanism to alleviate the effects of, e.g., excessive membrane degradation. On the other hand, drawbacks of a prolonged overproduction of AGXT2L1 may include a chronic exposition of the cells to acetaldehyde and ammonia and an altered homeostasis of sphingolipids and glycerophospholipids.

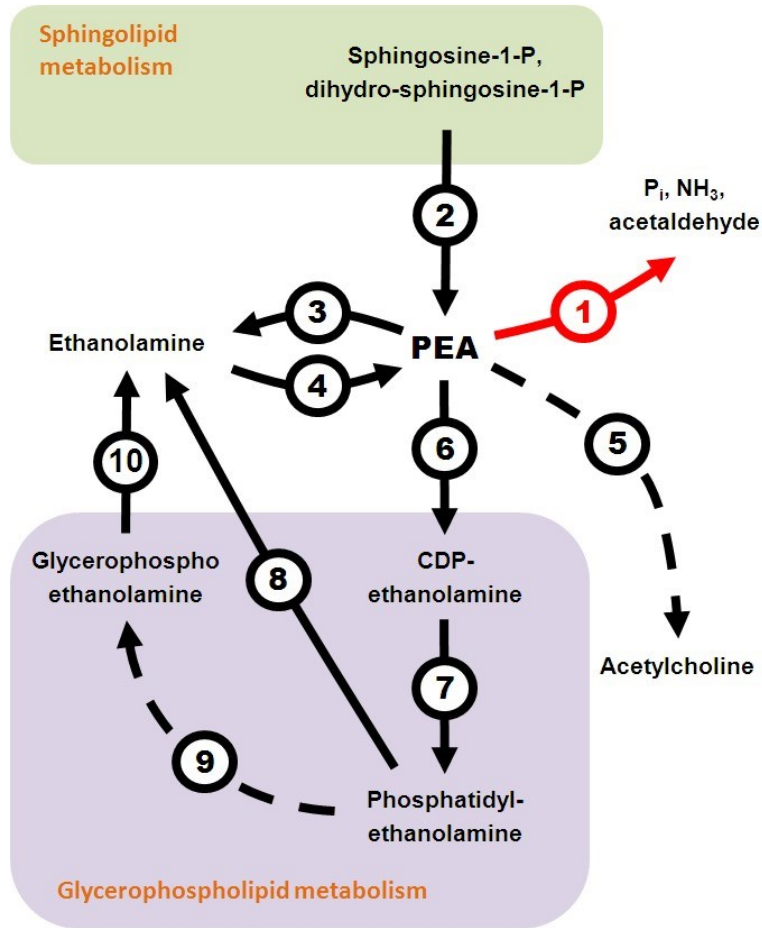


Figure 7 – A schematic view of the metabolism of PEA. The reaction catalyzed by AGXT2L1/PEA phospho-lyase (1) is shown as the red arrow. Other reactions are catalyzed by:

- 2) sphingosine-1-phosphate lyase [33];
- 3) PEA phosphatases [34];
- 4) ethanolamine kinase [35];
- 5) methyl-transferases, phosphatases and O-acetyltransferases leading to the formation of acetylcholine
- 6) ethanolamine-phosphate cytidyltransferase [36];
- 7) CDP-ethanolamine:diacylglycerol ethanolaminephosphotransferase;
- 8) phospholipase D;

- 9) phospholipase A1 and lysophospholipase;
- 10) glycerophosphodiester phosphodiesterase.

ACKNOWLEDGEMENTS

This work was funded in part by the Italian MIUR (COFIN 2007).

REFERENCES

2. Nam, H., Lewis, N. E., Lerman, J., Lee, D. H., Chang, R. L., Kim, D. & Palsson, B. O. (2012) Network context and selection in the evolution to enzyme specificity, *Science (New York, NY)*. **337**, 1101-4.
3. Weng, J. K. & Noel, J. P. (2013) The remarkable pliability and promiscuity of specialized metabolism *Cold Spring Harb Symp Quant Biol*, in press.
4. O'Brien, P. J. & Herschlag, D. (1999) Catalytic promiscuity and the evolution of new enzymatic activities, *Chem Biol*. **6**, R91-R105.
5. Percudani, R. & Peracchi, A. (2003) A genomic overview of pyridoxal-phosphate-dependent enzymes, *EMBO Rep*. **4**, 850-854.
6. Kontani, Y., Kaneko, M., Kikugawa, M., Fujimoto, S. & Tamaki, N. (1993) Identity of D-3-aminoisobutyrate-pyruvate aminotransferase with alanine-glyoxylate aminotransferase 2, *Biochim Biophys Acta*. **1156**, 161-6.
7. Cooper, A. J., Krasnikov, B. F., Okuno, E. & Jeitner, T. M. (2003) L-alanine-glyoxylate aminotransferase II of rat kidney and liver mitochondria possesses cysteine S-conjugate β -lyase activity: a contributing factor to the nephrotoxicity/hepatotoxicity of halogenated alkenes?, *Biochem J*. **376**, 169-178.
8. Cooper, A. J., Krasnikov, B. F., Niatsetskaya, Z. V., Pinto, J. T., Callery, P. S., Villar, M. T., Artigues, A. & Bruschi, S. A. (2011) Cysteine S-conjugate beta-lyases: important roles in the metabolism of naturally occurring sulfur and selenium-containing compounds, xenobiotics and anticancer agents, *Amino acids*. **41**, 7-27.
9. Shao, L. & Vawter, M. P. (2008) Shared gene expression alterations in schizophrenia and bipolar disorder, *Biol Psychiatry*. **64**, 89-97.
10. McQuillin, A., Rizig, M. & Gurling, H. M. (2007) A microarray gene expression study of the molecular pharmacology of lithium carbonate on mouse brain mRNA to understand the neurobiology of mood stabilization and treatment of bipolar affective disorder, *Pharmacogenet Genomics*. **17**, 605-17.
11. Veiga-da-Cunha, M., Hadi, F., Balligand, T., Stroobant, V. & Van Schaftingen, E. (2012) Molecular identification of hydroxylysine kinase and of the ammoniophospholyases acting on 5-phosphohydroxy-L-lysine and phosphoethanolamine, *J Biol Chem*. **287**, 7246-55.
12. Sprinson, D. B. & Weliky, I. (1969) The conversion of ethanolamine to acetate in mammalian tissues, *Biochem Biophys Res Commun*. **36**, 866-70.

13. Fleshood, H. L. & Pitot, H. C. (1970) The metabolism of O-phosphorylethanolamine in animal tissues. I. O-phosphorylethanolamine phospho-lyase: partial purification and characterization, *J Biol Chem.* **245**, 4414-20.
14. Dunlop, D. S. & Neidle, A. (2005) Regulation of serine racemase activity by amino acids, *Brain research.* **133**, 208-14.
15. Donini, S., Ferrari, M., Fedeli, C., Faini, M., Lamberto, I., Marletta, A. S., Mellini, L., Panini, M., Percudani, R., Pollegioni, L., Caldinelli, L., Petrucco, S. & Peracchi, A. (2009) Recombinant production of eight human cytosolic aminotransferases and assessment of their potential involvement in glyoxylate metabolism, *Biochem J.* **422**, 265-272.
16. Donini, S., Percudani, R., Credali, A., Montanini, B., Sartori, A. & Peracchi, A. (2006) A threonine synthase homolog from a mammalian genome, *Biochem Biophys Res Commun.* **350**, 922-8.
17. Laue, H. & Cook, A. M. (2000) Biochemical and molecular characterization of taurine:pyruvate aminotransferase from the anaerobe *Bilophila wadsworthia*, *Eur J Biochem.* **267**, 6841-8.
18. Fersht, A. R. (1999) *Structure and Mechanism in Protein Science - A Guide to Enzyme Catalysis and Protein Folding*, Freeman & Co., New York.
19. Karsten, W. E. & Cook, P. F. (2002) Detection of intermediates in reactions catalyzed by PLP-dependent enzymes: O-acetylserine sulfhydrylase and serine-glyoxalate aminotransferase, *Methods Enzymol.* **354**, 223-237.
20. Rossi, G. L., Mozzarelli, A., Peracchi, A. & Rivetti, C. (1992) Time course of chemical and structural events in protein crystals measured by microspectrophotometry, *Phil Trans Royal Soc Lond.* **340**, 191-207.
21. Cellini, B., Bertoldi, M., Montioli, R., Paiardini, A. & Borri Voltattorni, C. (2007) Human wild-type alanine:glyoxylate aminotransferase and its naturally occurring G82E variant: functional properties and physiological implications, *Biochem J.* **408**, 39-50.
22. Cooper, A. J. (1983) Biochemistry of sulfur-containing amino acids., *Annu Rev Biochem* **52**, 187-222.
23. Toney, M. D. (2005) Reaction specificity in pyridoxal phosphate enzymes, *Arch Biochem Biophys.* **433**, 279-87.
24. Mehta, P. K. & Christen, P. (2000) The molecular evolution of pyridoxal-5'-phosphate-dependent enzymes, *Adv Enzymol.* **74**, 129-184.
25. Percudani, R. & Peracchi, A. (2009) The B6 database: a tool for the description and classification of vitamin B6-dependent enzymatic activities and of the corresponding protein families, *BMC Bioinformatics.* **10**, 273.

26. Sievers, F., Wilm, A., Dineen, D., Gibson, T. J., Karplus, K., Li, W., Lopez, R., McWilliam, H., Remmert, M., Soding, J., Thompson, J. D. & Higgins, D. G. (2010) Fast, scalable generation of high-quality protein multiple sequence alignments using Clustal Omega, *Molecular systems biology*. **7**, 539.
27. Larkin, M. A., Blackshields, G., Brown, N. P., Chenna, R., McGettigan, P. A., McWilliam, H., Valentin, F., Wallace, I. M., Wilm, A., Lopez, R., Thompson, J. D., Gibson, T. J. & Higgins, D. G. (2007) Clustal W and Clustal X version 2.0, *Bioinformatics (Oxford, England)*. **23**, 2947-8.
28. Donini, S. (2008) *Molecular cloning and biochemical characterization of pyridoxal 5'-phosphate dependent enzymes of unknown function*, PhD Thesis, University of Parma.
29. Schioli, D. (2011) *The brain enzyme AGXT2L1 is a phospho-lyase acting on phosphorylated amines (in Italian)*, MS Thesis, University of Parma.
30. Jencks, W. P. (1981) On the attribution and additivity of binding energies, *Proc Natl Acad Sci USA*. **78**, 4046-50.
31. Modica-Napolitano, J. S. & Renshaw, P. F. (2004) Ethanolamine and phosphoethanolamine inhibit mitochondrial function in vitro: implications for mitochondrial dysfunction hypothesis in depression and bipolar disorder, *Biol Psychiatry*. **55**, 273-7.
32. Miller, J., Drost, D., Jensen, E., Manchanda, R., Northcott, S., Neufeld, R. W., Menon, R., Rajakumar, N., Pavlosky, W., Densmore, M., Schaefer, B. & Williamson, P. (2012) Progressive membrane phospholipid changes in first episode schizophrenia with high field magnetic resonance spectroscopy, *Psychiatry Res* **201**, 25-33.
33. Bourquin, F., Capitani, G. & Grütter, M. G. (2011) PLP-dependent enzymes as entry and exit gates of sphingolipid metabolism, *Protein Sci*.
34. Roberts, S. J., Stewart, A. J., Sadler, P. J. & Farquharson, C. (2004) Human PHOSPHO1 exhibits high specific phosphoethanolamine and phosphocholine phosphatase activities, *Biochem J*. **382**, 59-65.
35. Lykidis, A., Wang, J., Karim, M. A. & Jackowski, S. (2001) Overexpression of a mammalian ethanolamine-specific kinase accelerates the CDP-ethanolamine pathway, *J Biol Chem*. **276**, 2174-9.
36. Bakovic, M., Fullerton, M. D. & Michel, V. (2007) Metabolic and molecular aspects of ethanolamine phospholipid biosynthesis: the role of CTP:phosphoethanolamine cytidyltransferase (Pcyt2), *Biochem Cell Biol*. **85**, 283-300.

Kinetic characterization of the human O-phosphoethanolamine phospho-lyase reveals unconventional features of this specialized pyridoxal phosphate-dependent lyase

Davide Schirotti^a, Luca Ronda^b and Alessio Peracchi^{a,c}

^a Department of Life Sciences, Laboratory of Biochemistry, Molecular Biology and Bioinformatics, University of Parma, 43124 Parma, Italy.

^b Department of Neurosciences, University of Parma, 43124 Parma, Italy. ^c Corresponding author. Phone: +39 0521905137 Fax: +39 0521905151. Email: alessio.peracchi@unipr.it.

Keywords: pyridoxal-phosphate; elimination reaction; rapid kinetics; substrate specificity; product inhibition; phospholipid metabolism; neuropsychiatric diseases.

Abbreviations: PLP, pyridoxal-5' phosphate; PMP, pyridoxamine-5' phosphate; PEA, O-phosphoethanolamine; 3-APP, 3-amino-propylphosphonate; MSu, methylsulfonate; ESu, ethylsulfonate; MES, 2-(N-morpholino)ethanesulfonate; Bis-Tris propane, 1,3-bis(tris(hydroxymethyl)methylamino)propane; Tris, tris (hydroxymethyl) aminomethane; EGTA, 2,2'-Ethylenedioxybis(ethylamine)-N,N,N',N'-tetraacetic acid; SVD, singular value decomposition.

This chapter was published in FEBS: Schirotti, D., Ronda, L. & Peracchi, A. (2015) Kinetic characterization of the human O-phosphoethanolamine phospho-lyase reveals unconventional features of this specialized pyridoxal phosphate-dependent lyase, *FEBS Journal*. **282**, 183-199.

ABSTRACT

Human O-phosphoethanolamine (PEA) phospho-lyase is a pyridoxal 5'-phosphate (PLP) dependent enzyme that catalyzes the degradation of PEA to acetaldehyde, phosphate and ammonia. Physiologically, the enzyme is involved in phospholipid metabolism and is found mainly in the brain, where its expression becomes dysregulated in the course of neuropsychiatric diseases. Mechanistically, PEA phospho-lyase shows a remarkable substrate selectivity, strongly discriminating against other amino compounds structurally similar to PEA.

Herein, we studied the enzyme under steady-state and pre-steady-state conditions, analyzing its kinetic features and getting insights into the factors that contribute to its specificity. The pH-dependence of the catalytic parameters and the pattern of inhibition by the product phosphate and by other anionic compounds suggest that the active site of PEA phospho-lyase is optimized to bind dianionic groups and that this is a prime determinant of the enzyme specificity towards PEA. Single- and multiple-wavelength stopped-flow studies show that upon reaction with PEA the main absorption band of PLP ($\lambda_{\text{max}}=412$ nm) rapidly blue-shifts to ~ 400 nm. Further experiments suggest that the newly formed and rather stable 400-nm species most likely represents a Michaelis (non-covalent) complex of PEA with the enzyme. Accumulation of such an early intermediate during turnover is unusual for PLP-dependent enzymes and appears counterproductive for absolute catalytic performance, but it can contribute to optimize substrate specificity. PEA phospho-lyase may hence represent a case of selectivity-efficiency tradeoff. In turn, the strict specificity of the enzyme seems important to prevent inactivation by other amines, structurally resembling PEA, that occur in the brain.

INTRODUCTION

Enzymes that depend on pyridoxal-5'-phosphate (PLP) display a remarkable variety of activities on amino acids and other amines [1-3]. PLP-dependent enzymes base their effectiveness and versatility on covalent catalysis. In fact PLP can covalently link to the amino group of the substrate and then act as an electrophile to stabilize different carbanionic species [1-3]. Depending on the type of stabilized carbanion and on the formation of further covalent intermediates, different PLP-dependent enzymes can function for example as decarboxylases, transaminases, racemases, lyases or aldolases [1-5]. In spite of their functional diversity, all structurally characterized PLP-dependent enzymes belong to just a few distinct structural families, or 'fold-types' [6-8], amongst which the so-called fold-type I is the most populated and functionally multifarious [8].

PLP-dependent enzymes have been studied since the 1940s and their mechanistic, kinetic and spectroscopic properties are relatively well understood. However, much of this knowledge arises from a wealth of in-depth studies on a limited set of 'exemplary' enzymes. For example, aspartate aminotransferase represents the prototypical transaminase [1, 2, 9], alanine racemase is a prototypical PLP-dependent racemase [2, 3, 10, 11], tryptophan indole-lyase can be considered the prototypical lyase [12-14] and so forth.

The present work focuses on a PLP-dependent enzyme that somehow stands apart from the most well-studied models.

O-phosphoethanolamine (PEA) phospho-lyase had been described as an activity over 40 years ago [15, 16], but only recently Veiga-da-Cunha and coworkers achieved the molecular identification of this

enzyme as the product of the human gene *AGXT2L1* - thereafter renamed *ETNPPL* [17].

The enzyme catalyzes the irreversible 1,2 elimination reaction of PEA to yield acetaldehyde, phosphate and ammonia. Other PLP-dependent enzymes catalyze similar eliminations [18, 19], thus by analogy it is possible to outline a mechanism for the reaction carried out by PEA phospho-lyase (Fig. 1).

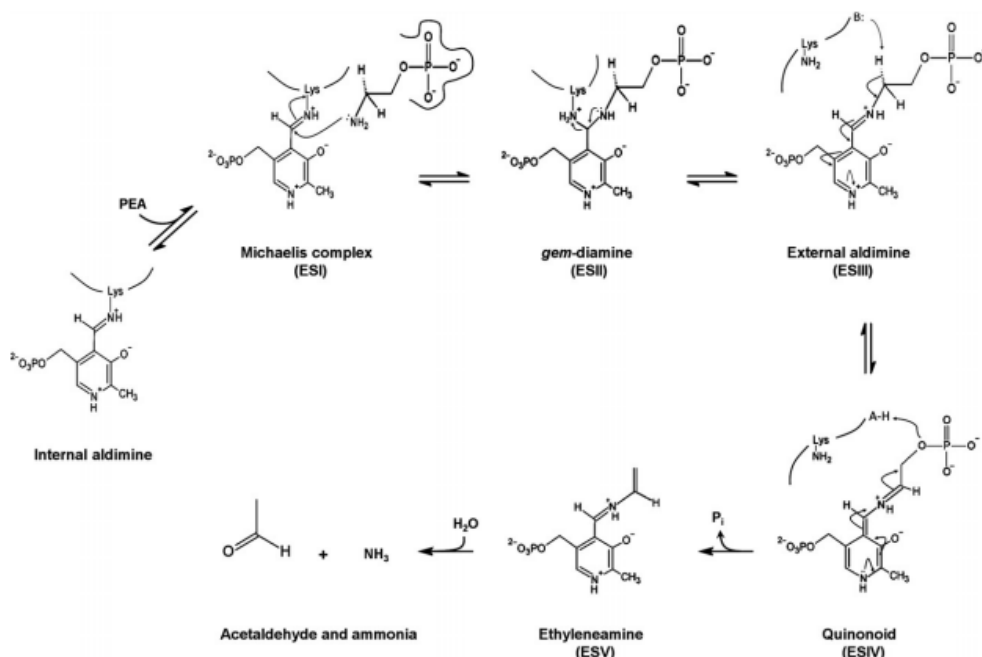


Figure 1 – Proposed mechanism for the 1,2-elimination reaction catalyzed by PEA phospho-lyase, based on the known enzymatic mechanisms of other PLP-dependent lyases [18, 19]. After entering the active site and forming an initial Michaelis complex (ES I), PEA can attack the Schiff base formed by PLP with the active site lysine (internal aldimine) and – passing through a *gem*-diamine intermediate (ES II) - complete the transaldimination step to yield the external aldimine (ES III). Proton abstraction from the amino carbon produces a PLP-stabilized carbanion (ES IV), and the subsequent elimination of phosphate yields the PLP derivative of ethyleneamine (ES V). The eventual hydrolysis of ethyleneamine, to form acetaldehyde and ammonia, presumably

occurs after this compound is released from the active site [18, 19]. Based on the literature on PLP-dependent enzymes, the expected λ_{\max} for at some of the chemical species shown here are: internal aldimine (ketoenamine tautomer, as shown), λ_{\max} =410-425 nm; *gem*-diamine, λ_{\max} =320-340 nm; external aldimine, λ_{\max} =415-440 nm; quinonoid, λ_{\max} =440-530 nm.

Nevertheless PEA phospho-lyase is peculiar because it is the only known PLP-dependent lyase acting on an ω -amine (as opposed to an amino acid). It also belongs to a structural subgroup within fold type I, composed almost exclusively by transaminases, and within this subgroup it is the only lyase described to date [20]. Finally, while many PLP dependent enzymes show a tendency to catalytic promiscuity, PEA phospho-lyase seems to have been shaped by evolution to maximize substrate and reaction specificity, by discriminating against certain other amino substrates, despite their close resemblance to PEA [20].

We report here an investigation of the PEA phospho-lyase kinetics, which also manifest some unusual features. Our study sheds light on the determinants of the enzyme's strict specificity and on the mechanism of its reaction. Since PEA phospho-lyase has a key role in brain phospholipid metabolism and seems involved in the pathophysiology of some psychiatric diseases we also discuss the possible physiological significance of the observed kinetic features.

RESULTS

In a preliminary study of the human PEA phospho-lyase reaction, we determined the following values for the catalytic parameters at pH 8, 30°C: $k_{cat}=2.3 \text{ s}^{-1}$, $K_M=0.9 \text{ mM}$ and $k_{cat}/K_M=2600 \text{ M}^{-1}\text{s}^{-1}$ [20]. Similar values had been reported by Veiga-da-Cunha et al. [17], who performed their experiments at pH 7.4. As in the present work we carried out some kinetic experiments at 20°C, we also re-determined the catalytic parameters at this temperature (pH 8) and found that K_M was essentially unchanged (1 mM) whereas k_{cat} and k_{cat}/K_M were reduced by about twofold ($k_{cat}=1.2 \text{ s}^{-1}$ and $k_{cat}/K_M=1100 \text{ M}^{-1}\text{s}^{-1}$) (data not shown)

pH dependence of k_{cat} and K_M

Figures 2A and 2B show how k_{cat} and K_M of the PEA phospho-lyase reaction varied with pH in the range 6-8.8 (30°C). In this interval, k_{cat} showed only limited changes, varying from 2.3 s^{-1} at pH 8 to 0.9 s^{-1} at pH 6 (Fig. 2A). Since k_{cat} reflects the slowest step(s) of the reaction occurring after substrate binding [21], these data imply that such rate-limiting step(s) are only modestly pH-dependent.

As for K_M , this parameter remained fairly constant between pH 7 and 8.8, but increased by about one order of magnitude when the pH was lowered from 7 to 6 (Fig. 2B). This suggests that binding of PEA to the enzyme is hampered by the protonation of at least one ionizable group. By fitting the data in Fig. 2B to Eq. 3 (solid line) we obtained an apparent pK_a of 6.7 for this group [21]. One reasonable possibility is that K_M may depend on the protonation of the PEA phosphate moiety (which is dianionic at neutral pH but would become monoanionic at acidic pH). Since the calculated apparent pK_a is higher than the pK_{a2} of the phosphoryl group of free PEA (~6; [22]), contributions from ionizable groups on the

enzyme are also possible. Alternatively or additionally, the discrepancy may in principle have a kinetic origin, as K_M is a combination of kinetic constants which may be differently affected by pH.

pH dependence of the inhibition by selected anions

We also studied in detail the pH dependence of inhibition of the PEA phospho-lyase reaction by some anions (Fig. 2C–D): phosphate, sulfate, methylsulfonate (MSu), ethylsulfonate (ESu) and 3-aminopropylphosphonate (3-APP)

At physiological pH values (between pH 6.8 and 8) both phosphate and sulfate behaved as competitive inhibitors, implying that the phospho-lyase was completely inhibited by saturating concentrations of these anions [20]. Phosphate and sulfate showed consistently superimposable K_i s, which also varied very little within the above-mentioned interval (Fig. 2C).

Below pH 6.8, however, the K_i of phosphate increased substantially, reaching ~8 mM at pH 6, while the K_i of sulfate remained quite constant (Fig. 2C). This divergent behavior can be attributed to protonation of the phosphate ion at low pH. At pH 6, in fact, sulfate remains completely dianionic, while free phosphate is more than 80% protonated (due to an 'effective' pK_{a2} of 6.8 under physiological conditions [23]) and hence is mainly monoanionic. Surprisingly, at pH >8.0 the K_i values for both phosphate and sulfate abruptly increased (Fig. 2C), while the inhibition patterns switched from purely competitive to partial (mixed hyperbolic) type (Fig. 3). These results suggest that at alkaline pH values the binding mode of phosphate and sulfate may change significantly, allowing formation of ternary enzyme-PEA-inhibitor complexes which still retain considerable catalytic activity. The increase of K_i at alkaline pH is too

sharp to be explained by a change in the protonation state of a single group, either on the inhibitors or on the enzyme; rather, the observed behavior might result from the deprotonation of multiple residues that titrate cooperatively [24, 25], possibly associated to a conformational change of the enzyme.

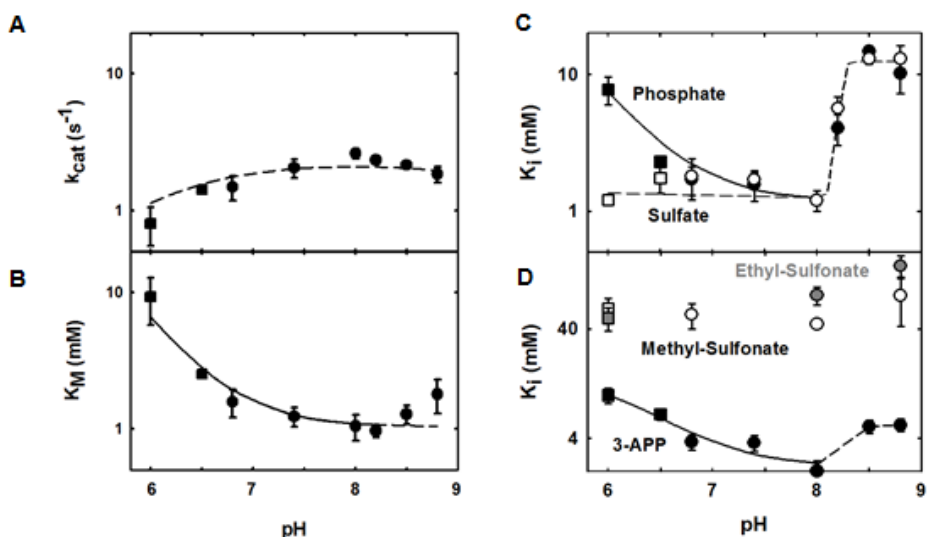


Figure 2 – pH dependence of the PEA phospho-lyase catalytic parameters and of the inhibition constants by different anionic compounds, in the pH range 6.0-8.8. Kinetic measurements were carried out as described in the Methods, in triethanolamine (circles) or MES buffer (squares). (A) pH dependence of k_{cat} . (B) pH dependence of K_M . The solid line through the data points is a least-squares fitting to Eq. 3, that assumes that K_M varies depending on the ionization of a single group with $pK_a=6.7 \pm 0.3$ in the free enzyme or free substrate. (C) pH dependence of K_i for phosphate and for sulfate. The solid line is a least-squares fitting of the phosphate data (in the pH 6-8 range) to Eq. 3 (that assumes modulation of K_i by a single ionizable group) yielding a $pK_a=6.7 \pm 0.2$. The dashed line is drawn to indicate the trend of the sulfate data and does not represent a fit to a theoretical equation. (D) pH dependence of K_i for 3-APP, MSu and ESu. The solid line is a least-squares fitting of the 3-APP data (in the pH 6-8 range) to Eq. 3, yielding a $pK_a=7.0 \pm 0.3$.

Fig. 2D shows the pH dependence of inhibition by three other anionic compounds, namely methylsulfonate (MSu), ethylsulfonate (ESu) and 3-APP. MSu is nearly isosteric with sulfate, but contrary to sulfate it bears only one negative charge. MSu and its bulkier relative ESu were on average ~40 times less effective than sulfate as inhibitors, in keeping with the idea that the enzyme active site strongly favors the binding of dianions with respect to monoanions. Furthermore, the K_i values for MSu and ESu changed relatively little across the whole pH range explored, even though at pH 8.8 the inhibition by these two compounds, too, was no longer purely competitive.

As for the phosphonate analogue of PEA, 3-aminopropylphosphonate (3-APP) the K_i s for this compound were consistently 2 to 3 fold higher than K_M for PEA in the pH range 6.8-8. The increase in K_i with decreasing pH was less pronounced than for, e.g., phosphate, but it seemed to follow a higher pK_a (it should be noted that the pK_{a2} of 3-APP is close to 7.1) [26].

Steady-state spectrophotometric and fluorometric analysis of the interaction of PEA phospho-lyase with PEA, phosphate and 3-APP

In PLP-dependent enzymes, monitoring substrate binding and the formation of catalytic intermediates is facilitated because these processes are usually accompanied by changes in the optical properties of the cofactor – either absorption (e.g., [27-31]) or fluorescence (e.g. [32-36]). In particular, formation of a Schiff base between the substrate and the cofactor (the so-called external aldimine; ESIII in Fig. 1) is commonly associated to a red shift of the main PLP absorption band [12, 27, 37-40]. Similarly, external aldimines show fluorescence emission bands that

are typically 10-20 nm red shifted and often more intense with respect to the emission of the native enzymes.

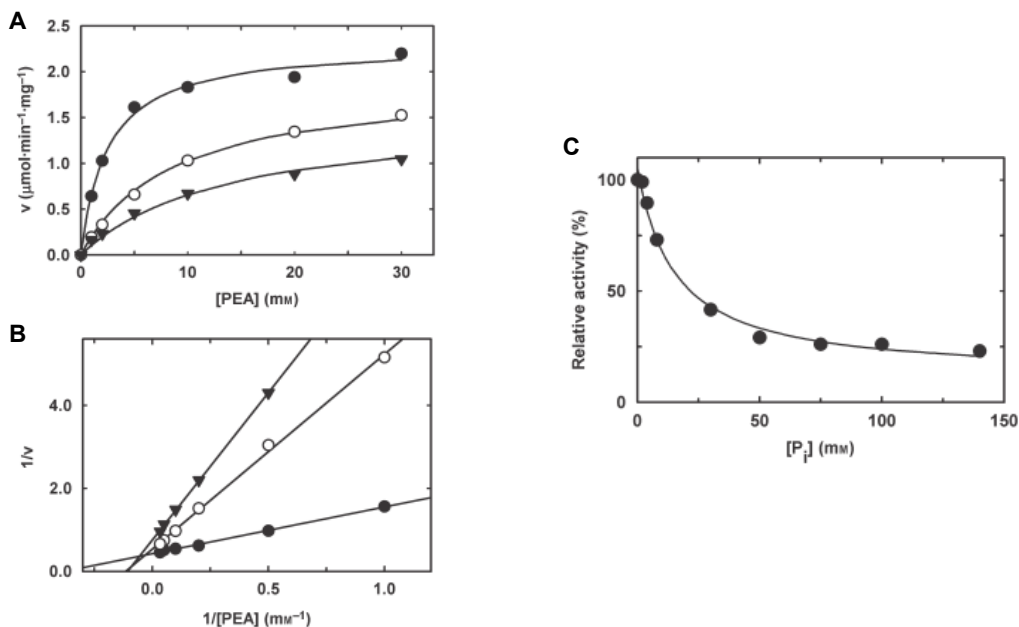


Figure 3 – Mixed-type, partial inhibition of PEA phospho-lyase by phosphate at pH 8.8. Experiments were carried out in triethanolamine buffer, 30°C. (A) Michaelis-Menten curves were collected at 0 (black circles), 30 (white circles) and 100 mM phosphate (black triangles). Fitting of the data to Eq. 2 in the Methods yielded $K_i = 8 \pm 2$ mM, $\alpha = 8.5 \pm 2$ and $\beta = 0.48 \pm 0.1$. (B) Double-reciprocal plot of the same data. (C) Titration with phosphate in the presence of 1 mM PEA.

The spectroscopic study of the PEA phospho-lyase reaction revealed some peculiar features. Upon reaction with PEA, the absorbance of the enzyme-bound cofactor increased around 350 nm and decreased at 412 nm, leading to a steady-state spectrum in which a main band with a maximum at 400 nm was predominant (Fig. 4A). This species was stable for minutes, although over time the band slowly shifted back to-

wards 412 nm [20]. Fluorescence spectra showed that the newly formed species was less fluorescent than the native enzyme and also emitted at a shorter wavelength (470 nm vs. 480 nm) (Fig. 4B). In PLP-dependent enzymes the attribution of a blue-shifted spectrum to an external aldimine is unusual, although it has been proposed in few cases [41-43]. An alternative possibility is that the 400 nm-species we observed belongs to a different intermediate, either preceding or following the formation of ESIII. As for the augmented absorbance at 340 nm, upon excitation at this wavelength the measured emission at 390-400 nm increased only slightly (<5%; data not shown) providing no indications of a substantial accumulation of *gem*-diamine intermediate (ESII).

We also studied the spectral changes ensuing upon reaction of the enzyme with 10 mM phosphate. In this case, too, we observed a blue shift of the main PLP band, even if only by a few nanometers (from 412 to 408 nm) (Fig. 4C). Phosphate also reduced the fluorescence emission of PLP and shifted its maximum towards shorter wavelengths (Fig. 4D). As phosphate cannot form covalent adducts with PLP, these findings imply that binding of phosphate at or near the active site affects the environment around the cofactor, either directly or by inducing a conformational rearrangement. A large structural change seems unlikely, however, since the excitation of the enzyme tryptophans at 280 nm did not reveal any appreciable change in their direct emission upon phosphate binding (data not shown).

The apparent K_d of phosphate, obtained by monitoring the induced changes in fluorescence, was 1.8 mM (Fig. 4D, inset), similar to the K_i measured under the same conditions (1.2 mM). Titrations of the enzyme with phosphate (up to 70 mM) were also carried out at pH 8.8, and the changes in the PLP emission allowed us to determine a K_d of 10 mM,

again very similar to the K_i determined independently at the same pH (Fig. 3).

We also studied fluorometrically the interaction of PEA phospho-lyase with 3-APP. Spectra collected within 1-2 min after reacting the enzyme with this substrate analog showed a blue shift of PLP emission similar to the shifts brought about by PEA and phosphate (Fig. 4E). Upon longer incubation with 3-APP, the emission peak of the cofactor gradually disappeared (Fig. 4E), due to a slow half-transamination reaction that leads to the formation of pyridoxamine-5' phosphate (PMP) [20].

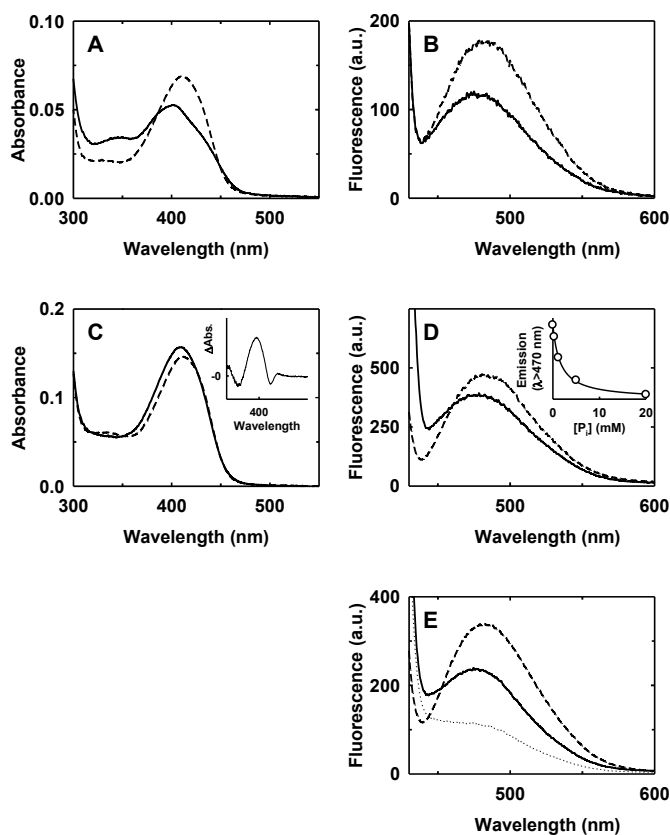


Figure 4 – Absorbance and fluorescence changes observed upon reacting PEA phospho-lyase with PEA, phosphate and 3-APP. Spectra were collected

as described in the Methods. (A) Changes in the UV-visible spectrum accompanying the reaction of PEA phospho-lyase (11 μM) with PEA (20 mM), in 25 mM triethanolamine, pH 8, 30°C. Addition of the substrate to the enzyme caused a shift of the main band of the native spectrum (dashed line) from 412 to 400 nm (solid line; spectrum collected 1.5 min after PEA addition). Over longer times, the main band slowly moved back towards 412 nm. (B) Emission spectra upon excitation at 410 nm of a solution containing 0.75 μM PEA phospho-lyase, Bis-Tris propane buffer (pH 8), at 20°C in the absence (dashed line) and in the presence (solid line) of 10 mM PEA. This latter spectrum was collected 2 minutes after adding the substrate. (C) Changes in the UV-visible spectrum accompanying the reaction of PEA phospho-lyase (30 μM) with inorganic phosphate (10 mM), in 25 mM Triethanolamine, pH 8, 30°C. Addition of the ligand to the enzyme caused a shift of the main PLP absorption band from 412 nm in the native enzyme (dashed line) to 408 nm (solid line). Inset: the difference in absorption between the enzyme-phosphate complex and the native enzyme. (D) Emission spectrum upon excitation at 410 nm of a solution containing 2 μM PEA phospho-lyase, 25 mM Bis-Tris propane, pH 8, at 20°C in the absence (dashed line) and presence of 20 mM phosphate (solid line). Inset: decrease in fluorescence emission at $\lambda > 470$ nm upon increasing phosphate concentration. The solid line represents the best fitting of the data to a hyperbolic function, yielding an apparent K_d of 1.8 mM. (E) Emission spectrum ($\lambda_{\text{ex}} = 410$ nm) of a solution containing 1.5 μM PEA phospho-lyase, Bis-Tris propane, pH 8, at 20°C in the absence (dashed line) and presence of 20 mM 3-APP after 1 minute (solid line) and after 25 minutes (dotted line). This last spectrum corresponds to the complete conversion of PLP to PMP [20].

Multi- and single-wavelength pre-steady-state kinetics

Multi-wavelength rapid-scanning experiments were carried out to detect the formation of transient species under pre-steady state conditions upon mixing PEA phospho-lyase with 10 mM PEA.

The spectral changes detected in the first tens of milliseconds after mixing consisted of a blue shift of the main PLP band from ~412 nm to ~400 nm and a concomitant increase of absorbance around 340 nm (Fig. 5A). In other words, we observed what appeared to be the conversion of the internal aldimine to a mixture of reaction intermediates most similar to that observed at the steady state. The formation of earlier spectral species within the dead time of the instrument seemed unlikely, as the spectrum of the native enzyme almost overlapped with the first spectrum collected upon mixing with PEA. A plot of the absorbance at 425 nm (where a maximum Δ absorbance is observed) versus time could be satisfactorily fit by Eq. 4, with an apparent rate constant (k_{obs}) of 53 s^{-1} (Fig. 6-A). To further assess the absence of 'hidden' processes in the observed kinetics, we analyzed the spectral evolution by singular value decomposition (SVD) [44, 45] (Fig. 6-B and 7). Fitting of the first spectral component (Fig. 7-D) using a single exponential function gave a k_{obs} of 68 s^{-1} , close to the value obtained above.

To better understand the fast process under examination, single-wavelength stopped-flow experiments were carried out at 340 and 425 nm, where multi-wavelength kinetics had shown the maximum positive and negative changes in absorbance, respectively. Fitting of the time courses to Eq. 4 gave similar k_{obs} values at both wavelengths (data not shown).

k_{obs} values for the spectral transition at 425 nm were then determined using increasing concentrations of PEA (Fig. 5B). The observed rate constant increased with [PEA], from 80 s^{-1} (at 8 mM PEA) to 421 s^{-1} (at 75 mM PEA). The extrapolated offset for all these kinetics was identical, within standard error, to the initial absorbance of the unreacted enzyme, and the amplitude of the transition was, again, identical for all the

three curves (Fig. 5B). k_{obs} values were plotted as a function of the PEA concentration and tentatively fit to a hyperbolic function (Fig. 5C) yielding a $K_{0.5}$ of ≈ 100 mM and a limiting k_{obs} value of ≈ 1000 s⁻¹. The apparent second order kinetic constant, estimated from the linear phase of the hyperbola was hence about 10000 M⁻¹s⁻¹ (Fig. 5C), one order of magnitude higher with respect to the k_{cat}/K_M for PEA at 20°C.

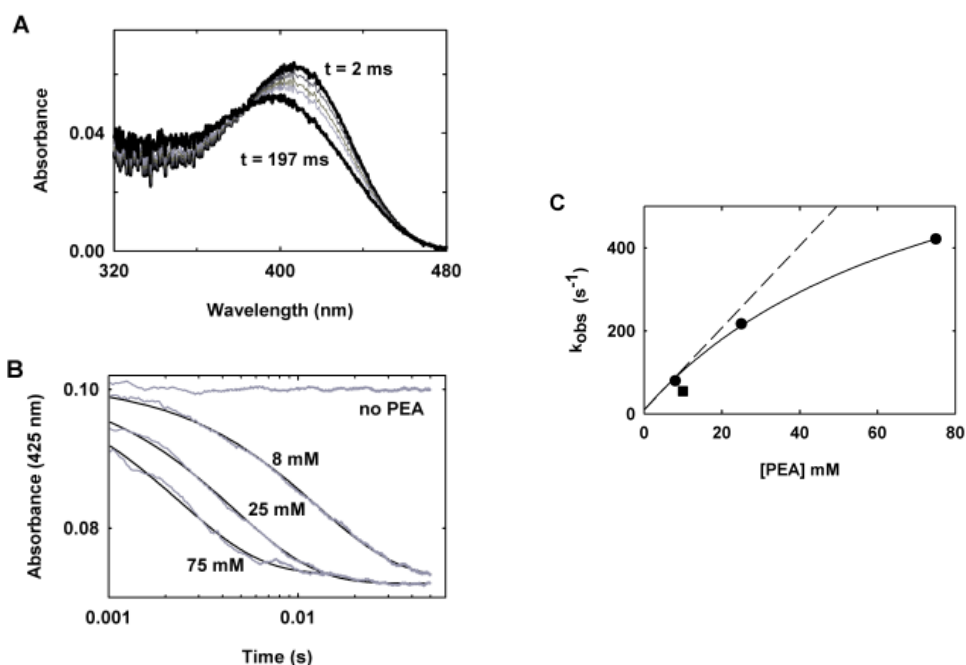


Figure 5 – Multi- and single-wavelength pre-steady-state kinetics of the reaction of PEA phospho-lyase with its substrate. Kinetics were measured in triethanolamine buffer pH 8, 20°C. (A) Rapid scanning stopped-flow spectra recorded upon reaction of PEA phospho-lyase (12 μ M final) with 10 mM PEA. The shown, representative spectra were collected sequentially after 0 ms, 5 ms, 10 ms, 15 ms, 32.5 ms and 195 ms. (B) Single-wavelength stopped-flow kinetics of the reaction of 20 μ M PEA phospho-lyase with various concentrations of PEA, monitored at 425 nm. The experimental traces (gray lines) were fit to a monoexponential function (Eq. 4). Such fittings (represented by the black lines), yielded the following parameters: with 8 mM PEA, $k_{obs} = 80 \pm 1$ s⁻¹,

$A_0=0.101 \pm 0.001$ and $\Delta A=0.028 \pm 0.001$; with 25 mM PEA, $k_{obs}=217 \pm 1 \text{ s}^{-1}$, $A_0=0.101 \pm 0.001$ and $\Delta A=0.029 \pm 0.001$; with 75 mM PEA, $k_{obs}=421 \pm 5 \text{ s}^{-1}$, $A_0=0.102 \pm 0.002$ and $\Delta A=0.028 \pm 0.001$. (C) Dependence on PEA of the observed reaction rate constants (k_{obs}). In addition to the values of k_{obs} above (circles) the plot also includes a datum from the rapid-scanning experiment (square). The solid line is a tentative fitting of the data to a hyperbolic function, yielding a $K_{0.5}$ of $100 \pm 15 \text{ mM}$. The dashed line represents the initial slope of the hyperbola, equaling $10,000 \pm 1000 \text{ M}^{-1}\text{s}^{-1}$.

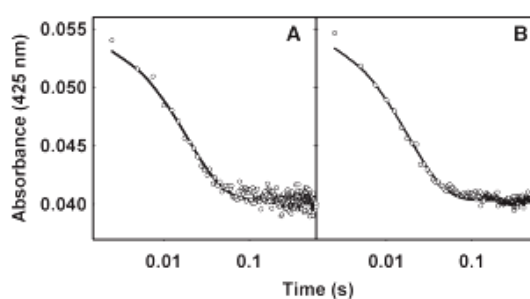


Figure 6 – Time-courses at 425 nm extracted from rapid-scanning stopped-flow data of the reaction between PEA and PEA phospho-lyase (see Fig. 5A). The time-course obtained directly from the raw data (Panel A) is compared to the same time-course after ‘cleaning’ the data through SVD (Panel B). The comparison illustrates the reduction of noise obtained by applying the SVD procedure. Fittings to Eq. 4 in the Methods (solid lines through the data points) yielded $k_{obs}=53 \pm 3 \text{ s}^{-1}$ ($r^2=0.925$) for the original data, and $k_{obs}=55 \pm 1 \text{ s}^{-1}$ ($r^2=0.973$) for the ‘cleaned’ data.

Multi- and single wavelength kinetics were also employed to study the reaction of PEA phospho-lyase with phosphate. With this inhibitor, analysis of the spectral changes was complicated by their very limited magnitude (Fig. 4C). However, preliminary experiments indicated that the kinetics observable with phosphate were substantially slower with respect to those observed with PEA. This allowed us to collect rapid-

scanning spectra every 8 ms, rather than every 2.5 ms, thus compensating for the smaller signal by a higher integration time.

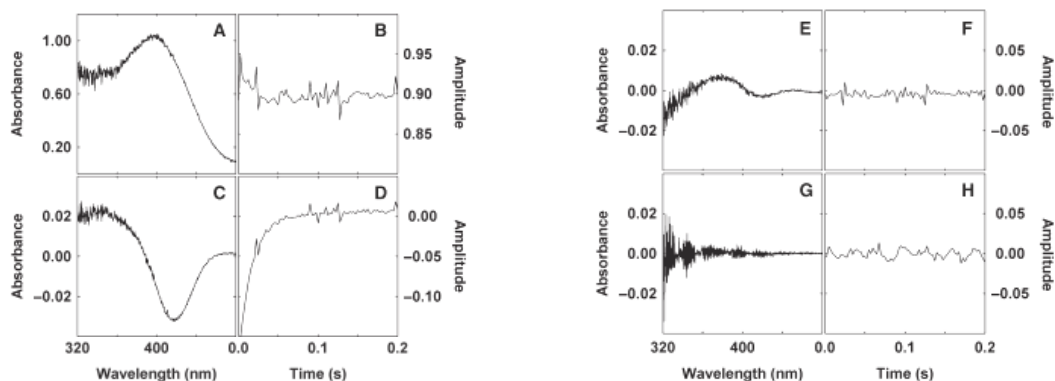


Figure 7 – SVD of the rapid scanning data obtained upon reaction of PEA phospho-lyase with PEA. Panels A, C, E, G show the first four U components extracted from the time-resolved spectra, multiplied by their singular values S. Panels B, D, F, H show the corresponding time evolution (V). The first three SVD components, which gave spectral features significantly different from noise, were used to reconstitute cleaned data matrix.

Rapid scanning experiments showed that the spectral changes associated to binding of phosphate (10 mM) occurred in two well-distinct phases. In a first phase, completed in about 1 s, we observed only a slight increase in absorbance of the 412 nm band of PLP (Fig. 8A); in a second phase, occurring over many seconds, the λ_{\max} of the PLP band shifted towards 408 nm (Fig. 8B).

Single-wavelength kinetics were measured at 390 nm using different concentrations of phosphate (5, 10 and 40 mM). In all instances the observed time-courses were biphasic (Fig. 8C). Furthermore, when the data were fit to the biexponential Eq. 5, the k_{obs} values for both phases were essentially independent of the concentration of phosphate: k_{obs1}

was invariably around 6 s^{-1} , while k_{obs2} was about two orders of magnitude slower. This concentration-independence implies that the observed kinetics do not reflect (nor are tightly coupled to) the initial binding of phosphate, which must occur within the dead time of the instrument, but rather some much later events, possibly slow conformational changes of the active site in the enzyme-phosphate complex.

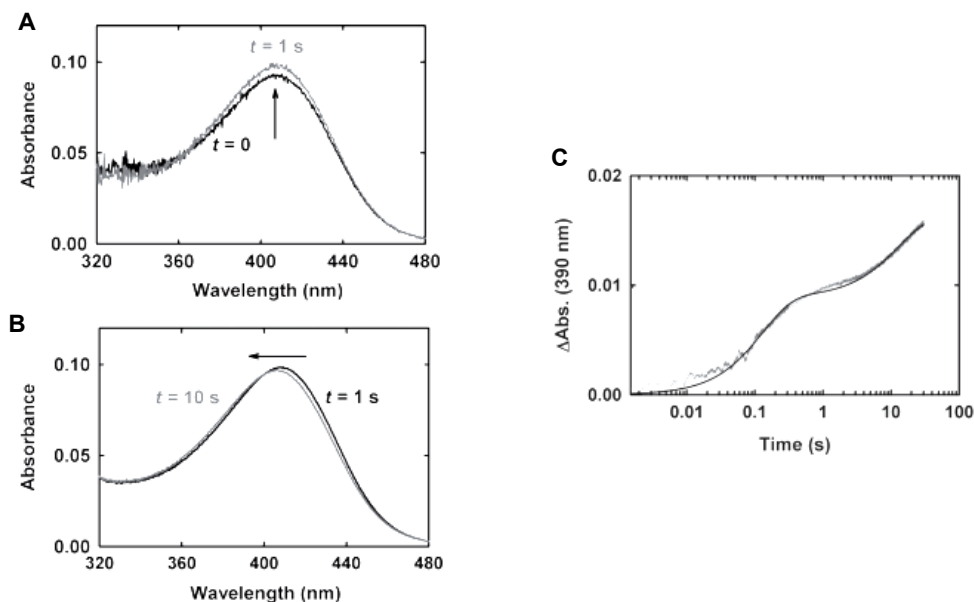


Figure 8 – Multi- and single-wavelength stopped-flow kinetic measurements of the reaction of PEA phospho-lyase with phosphate, in triethanolamine buffer pH 8, 20°C. (A) Rapid scanning stopped-flow spectra recorded in the first 1 s after mixing 30 μM PEA phospho-lyase with 10 mM phosphate. The black line indicates the initial spectrum (native), while the gray line indicates the spectrum collected after 1 s. The time collection for each spectrum was 2.5 ms. (B) Rapid scanning stopped-flow spectral changes occurring between 1 and 10 s upon reaction of 30 μM PEA phospho-lyase with 10 mM phosphate. In this case the time collection for each spectrum was 8 ms. (C) Single-wavelength stopped-flow kinetics of the reaction of 30 μM PEA phospho-lyase, recorded at 390 nm, with 40 mM phosphate. The time-course (in gray) was fit to Eq. 5 (black line),

yielding two k_{obs} of $7.70 \pm 0.02 \text{ s}^{-1}$ and $0.076 \pm 0.001 \text{ s}^{-1}$. Essentially identical results and k_{obs} values were obtained using 10 mM phosphate.

NaBH₄ reduction of different PLP species at the active site of PEA phospho-lyase

To try to assess whether the main spectroscopic species formed during the reaction with PEA was a covalent PLP-substrate intermediate, a NaBH₄ reduction experiment was carried out. PEA phospho-lyase was reacted for a few seconds with 15 mM PEA, to allow formation of the 400 nm spectroscopic species, after which the reaction mixture was treated with an excess of NaBH₄ and finally dialyzed against 6 M urea. In parallel, a sample of native enzyme and another sample of enzyme that had formed PMP (after half-transamination with 3-APP for 20 min) were also reduced and dialyzed as above (Fig. 9).

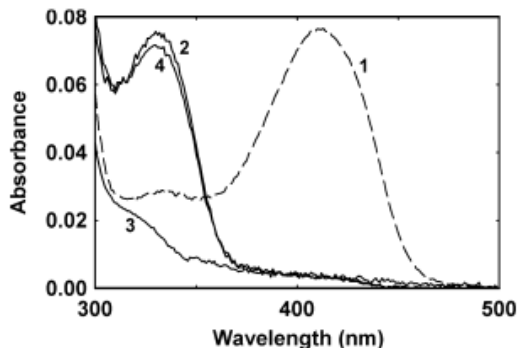


Figure 9 – Sodium borohydride treatment of different forms of PEA phospho-lyase. The native spectrum of PEA phospho-lyase in triethanolamine 25 mM, pH 8, at 30° (Spectrum 1 - dashed line) is compared to spectra of enzyme that had been treated in different conditions before reducing with sodium borohydride and dialyzing against 6 M urea. Spectrum 2: sample treated with sodium borohydride in the absence of ligands, the peak at 325 nm represents the typical peak of a reduced internal aldimine. Spectrum 3: sample pre-treated: with 3-APP, that completely transforms the PLP to PMP [20], Spectrum 4: PEA

phospho-lyase sample treated with sodium borohydride ~5 seconds after mixing the enzyme with 15 mM PEA.

In PLP-dependent enzymes, reduction of the internal aldimine (Fig. 1) typically yields an adduct with a maximum absorbance at ~320 nm. Since it contains a stable covalent bond between the C4' of the cofactor and the ϵ -amino group of lysine, this adduct cannot be released from the protein, even under denaturing conditions. Indeed, upon treating the native enzyme with NaBH₄ we observed formation of a peak at 325 nm, which remained associated to the protein after extensive dialysis against urea.

In contrast, reduction of Schiff bases formed between the cofactor and the substrate (or the product, or other reaction intermediates) would be expected to yield adducts that are not covalently linked to the protein and that can be released upon dialysis. As a proxy for this case, we used a sample of enzyme that had formed PMP upon reaction with 3-APP. After reduction and dialysis, this sample showed no significant absorbance peak above 300 nm, suggesting that the cofactor had been totally removed during dialysis.

In comparison to the two controls above, the enzyme briefly reacted with PEA and then reduced and dialyzed, showed a spectrum with a peak at 325 nm (Fig. 9). In other words, the behavior of this sample was very similar to the behavior of the native enzyme. Taken at face value, these data suggest that PLP, at the steady-state of the PEA phospho-lyase reaction, exists predominantly in the form of internal aldimine, rather than as a covalent adduct with PEA.

Other possibilities ought to be considered however. In the literature concerning PLP-dependent enzymes, it is reported that certain external

Schiff bases of PLP react slowly with NaBH_4 , [46] or do not react at all [11, 47, 48], perhaps reflecting a reduced accessibility of the cofactor upon the binding of ligands at the active site. Yet the possibility that an analogous behavior might be distorting the results of the experiment seems unlikely. In fact, the phospho-lyase reacted with PEA and then treated with NaBH_4 underwent spectral changes consistent with a complete reduction of PLP. Furthermore, such a complete reduction was achieved despite the presence of a PEA concentration ~ 15 -fold higher than K_M , at which the active sites of the enzyme were largely saturated by the substrate.

DISCUSSION

A noncovalent enzyme-substrate complex accumulates at the steady-state of the PEA phospho-lyase reaction

Based on the vast literature on PLP-dependent enzymes, the absorption properties of most of the intermediates shown in Fig. 1 can be predicted with some confidence (see legend of Fig. 1). Upon reaction with saturating substrate, the enzyme is expected to reach a steady-state distribution of these intermediates, all of which should contribute (in different proportions, depending on their relative amounts and extinction coefficients) to the absorption spectrum of the enzyme [49]. However, we were initially puzzled by the identity of the main band of PLP absorption observed upon reaction of PEA phospho-lyase with PEA (Fig. 4A). This band could not be assigned to ESIV, (as quinonoid species show very typical, narrow absorption bands, with $\lambda_{\max} > 440$ nm [12, 20, 49-51]) nor to ESII, which, much like PMP, is characterized by a tetrahedral geometry around cofactor C4' and should show a peak around 325 nm [52, 53].

Furthermore, the hypothesis that this prominent intermediate may correspond to the ethylenamine Schiff base (ES V) seemed in contrast with two observations. First, the rapid-scanning measurements indicated that the 400-nm species forms without the previous appearance of other spectroscopically detectable intermediates. Second, the apparent second-order rate constant for formation of the 400 nm-species (Fig. 5C) is about tenfold higher than the k_{cat}/K_M of the overall reaction at 20°C. As k_{cat}/K_M reflects all the catalytic processes up to the first irreversible step (which arguably in this case is the release of the phosphate leaving

group) [54], the 400-nm species should correspond to an intermediate that precedes formation of the ethyleneamine Schiff base.

This leaves only two candidates, among the intermediates shown in Fig. 1, that could correspond to the 400-nm species – namely the Michaelis complex (ESI) and the external aldimine of PEA (ES III). There are several lines of evidence that, taken together, strongly suggest that the former option is the correct one.

First, the changes in the cofactor spectra (both in absorbance and fluorescence) observed upon reaction with PEA are qualitatively similar to those observed with phosphate (Fig. 4A-D), which cannot form covalent intermediates with PLP. In contrast, the spectroscopic properties of the 400-nm species do not match those of typical external aldimines (which usually display red-shifted and slightly increased absorption spectra, as well as red-shifted and increased emissions [12, 27, 37-40]).

Second, the experiment with sodium borohydride is consistent with the predominant formation of non-covalent intermediate(s) upon reaction of PEA phospho-lyase with its substrate.

Furthermore, the predominant accumulation of a noncovalent complex at the steady-state of the reaction would imply that the transaldimination step (and in particular the formation of ESII) is rate-limiting the overall reaction and that K_M approximates the ‘true’ dissociation constant of PEA for the enzyme (i.e., $K_M \approx K_d^{PEA}$). This scenario is broadly consistent with our steady-state results, in particular with the similarities (both in absolute values and in pH dependencies) between K_M for PEA and the K_i for 3-APP (which cannot form the same covalent intermediates as PEA) and phosphate (which cannot form covalent intermediates at all).

If really the 400 nm-species represents a noncovalent reaction intermediate, it is however likely that it be preceded by other ES species. In fact, the apparent second-order rate constant for formation of the 400 nm-band is many orders of magnitude slower than a diffusion-limited process and also slower than the typical rates of ligand binding by proteins. Also, the rate of formation of this intermediate, measured at the stopped-flow upon increasing PEA concentration, shows an apparent hyperbolic trend which would be consistent with the formation of an earlier (more weakly bound, and spectroscopically undetectable) intermediate. Conversion to the 400 nm-species could then entail a physical translation of PEA within the active site and/or a conformational change of the active site itself. The possibility that initial binding of ligands to the enzyme may be followed by much slower rearrangements of the active site seems also broadly consistent with the results of our rapid kinetic studies with phosphate (Fig. 8).

Neglecting the fleeting species evoked above and based on the arguments put forward previously, a crude kinetic model for the reaction of PEA phospho-lyase can be envisaged. The fundamental feature of this model is that the conversion of ESI to ESII represents the rate-limiting step for catalysis and is much slower than dissociation of the substrate; these features would allow the system to approach a binding pre-equilibrium and would lead, at saturating concentrations of PEA, to the predominant accumulation of ESI. A pictorial version of this model, with a few estimated rate constants, is presented in Fig. 10.

PEA phospho-lyase as an example of selectivity-efficiency tradeoff

It must be noted that the preferential accumulation of a noncovalent complex during turnover is unusual for a PLP-dependent enzyme. To

our knowledge, it has been postulated only in the case of a *Bacillus stearothermophilus* alanine racemase [10, 11]. Intuitively this makes perfect sense: as catalysis by PLP-dependent enzymes relies on the covalent binding of the cofactor to the substrate, accumulating a noncovalent reaction intermediate seems counterproductive for efficiency.

On the other hand, slowing down the transaldimination step may be a straightforward means to implement substrate specificity. In fact, if the rate-limiting step of the process occurs just before the formation of covalent intermediates (more committed to catalysis) the enzyme will have the opportunity to select among competing substrates mainly on the basis of their binding affinities and not necessarily of their reactivities. To appreciate this, one may consider the case of *O*-sulfoethanolamine. This compound is nearly isosteric with PEA and endowed with a better leaving group, so on pure chemical grounds it should react faster. Nevertheless we showed previously that PEA phospho-lyase catalyzes the 1,2-elimination of *O*-sulfoethanolamine with a k_{cat}/K_M 1800-fold lower than that of PEA - a gap in catalysis largely attributable to a much increased K_M (and K_d) for *O*-sulfoethanolamine [20].

Tawfik has recently pointed out that often enzymes requiring a high specificity appear to have evolved this trait at the expenses of pure catalytic performance, and has suggested that this specificity-efficiency tradeoff is an intrinsic feature of biocatalysts [55]. PEA phospho-lyase seems to fit perfectly in the picture, an impression which is reinforced if one compares its behavior with that of a 'prototypical' PLP-dependent lyase, tryptophan indole-lyase. The enzyme from *E.coli* shows a k_{cat}/K_M of $30,000 \text{ M}^{-1} \text{ s}^{-1}$ with the natural substrate, L-tryptophan, and an even

higher activity ($510,000 \text{ M}^{-1} \text{ s}^{-1}$) with a substrate bearing a good leaving group such as S-(2-nitrophenyl)-L-cysteine [56]. This is in stark contrast with PEA phospho-lyase, whose k_{cat}/K_M (under the best conditions we found) is just $2,600 \text{ M}^{-1} \text{ s}^{-1}$, while with O-sulfoethanolamine (despite the good leaving group) k_{cat}/K_M drops to $1.4 \text{ M}^{-1} \text{ s}^{-1}$ [20].

The active site of PEA phospho-lyase is set to bind dianions

If a slow transaldimination allows the enzyme time to select substrates based on their binding affinity, what are the substrate features actually exploited to implement selectivity? Our data provide strong evidence that the active site of PEA phospho-lyase is optimized to bind dianions and that the dianionic nature of PEA is a prime determinant of substrate specificity by this enzyme. While O-sulfoethanolamine is nearly isosteric with PEA, its sulfate group is monoanionic (in contrast to the dianionic phosphate group of PEA) which suggested that the net charge of the group could dictate ligand affinity at the enzyme active site [20]. Here, we have buttressed that early suggestion with other pieces of data.



Figure 10 – A rough kinetic framework for the reaction of PEA phospho-lyase (at 20°C, pH 8 and ~10 mM PEA), based on the data presented in this paper. Intermediates numbering follows Figure 1. Since the Michaelis complex (ESI) appears to accumulate during the steady-state of the reaction, conversion of ESI to ESII and then ESIII must be the major rate-limiting step of the process. The rate constant for this conversion is taken as very close to k_{cat} , whereas all subsequent steps must be faster. The apparent second-order rate constant for

formation of the ESI comes from stopped-flow experiments (Fig. 5C). Finally, an estimate for the kinetic dissociation constant of the substrate from ESI is obtained employing the basic kinetic relationship $k_{off} = k_{on} \times K_d$ and assuming $K_M \approx K_d^{PEA}$. According to this model, the substrate is allowed to approach a binding pre-equilibrium before beginning to form covalent intermediates. In this pre-equilibrium step, potential alternative substrates or quasi-substrates (such as O-sulfoethanolamine, GABA or taurine) would presumably bind with low affinity, due e.g. to the presence of a monoanionic –rather than dianionic – group. Hence, they would be selected against before they become more committed to reaction by forming a covalent linkage to PLP. Note that the low k_{cat}/K_M of O-sulfoethanolamine reflects mainly a very high K_M of PEA phospholyase for this compound [20].

For example, we have shown that the K_M for PEA increases substantially below pH 6.8, an observation attributable at least in part to the protonation of the phosphate group of the substrate under acidic conditions (Fig. 2B). A similar (but somewhat right-shifted) pH dependence was also observed for the K_I of 3-APP, which is an analog of PEA unable to undergo the elimination reaction (Fig. 2D). 3-APP bears a phosphonate group that at pH 8.0 is mostly dianionic, but whose pK_{a2} is substantially higher than the pK_{a2} of PEA [26] Furthermore, as noted in the results, the K_I of phosphate increased at acidic pH with an apparent pK_a of 6.7 (identical within error to the pK_{a2} that governs the equilibrium between the singly- and doubly-charged form of the anion) whereas the K_I of sulfate did not increase at low pH. Finally, MSu (which bears only one negative charge) shows a K_I that at pH 8 is about 40 times higher with respect to sulfate, and that remains roughly constant in the 6-8.8 pH range.

We do not know when, along evolution, PEA phospho-lyase acquired such a strong selectivity for divalent anions, but we can envisage some advantages this preference affords for the physiological function of this enzyme in the brain. Indeed, PEA phospho-lyase seems to have a key role in brain metabolism where it is mainly expressed and where it was found to be dysregulated in schizophrenia and bipolar disorder [57, 58].

In the central nervous system, many biogenic amines are involved in neurotransmission and homeostasis. In particular, the importance in neurotransmission and in neurophysiology of γ -aminobutyrate (GABA) [59] and taurine [60] is well established. Both these compounds are, similarly to PEA, ω -amines carrying an anionic group, but the carboxylate group of GABA and the sulfonate group of taurine bear only one negative charge. It is possible to suppose that the ability of PEA phospho-lyase to discriminate against monoanionic groups is instrumental to avoid interferences from these other amines, that could in principle not just act as competitive inhibitors but also stably cripple the enzyme by converting PLP to PMP.

Considerations on the inhibition of PEA phospho-lyase by phosphate

The high selectivity of the enzyme active site for divalent ions is a double-edged sword as it is also the determinant of competitive inhibition. We showed earlier that the enzyme is inhibited efficiently by small inorganic dianions such as phosphate, sulfate, phosphite and arsenate, with K_i values in the low millimolar range [20]. For most of these compounds, inhibition has a purely academic interest since these ions do not occur in the cell at millimolar concentrations. Phosphate, however, has a key role in the physiology of the cells, where it reaches

cytosolic concentration of 1-2 mM, comparable to the concentration of PEA and sufficient to substantially inhibit PEA phospho-lyase. The question is hence: what is the advantage of having an enzyme that is constitutively inhibited, to a significant extent, by a common component of the cytosolic medium?

In principle, as phosphate is a product of the reaction, its inhibition could have a role of feedback regulation of the enzyme. Additionally or alternatively, it is possible that concentration of free phosphate may not be uniform throughout the cytosol, which might induce a location-dependent (and potentially useful) modulation of PEA phospho-lyase activity.

We however would like to suggest one further speculative possibility, namely that phosphate inhibition may be irrelevant *in vivo*. We have in fact shown that, at pH >8, the K_i of phosphate increases sharply and the inhibition pattern changes from competitive to mixed/partial (Fig. 2A-C; Fig. 3). Such a change in inhibition mode has few antecedents in the literature (e.g., [61, 62]) and its basis are completely elusive. One reviewer of this paper suggested that an accumulation at high pH of ESV, with which phosphate could preferentially interact, would produce a non-competitive inhibition pattern. However, the spectral changes observed upon reaction of the enzyme with PEA at pH 8.8 are fully superimposable to those observed at pH 8 (data not shown), providing no support for the hypothesis.

Irrespective of this, our data show that the enzyme has the ability, under certain *in vitro* conditions, to become much less sensitive to phosphate inhibition, while retaining almost optimal catalytic efficiency. If by chance (e.g., thanks to some post-translational modification) the behavior of the enzyme *in vivo* resembled more closely the alkaline

behavior shown here, inhibition of PEA phospho-lyase by cytosolic phosphate would be substantially negligible.

Conclusions

The human PEA phospho-lyase is a PLP-dependent enzyme with a peculiar evolutionary history [17, 20]. Its kinetic characterization described in this work has also highlighted some unusual features of this catalyst. For example, PEA phospho-lyase (unlike most of its PLP-dependent congeners) appears to disfavor the accumulation of covalent reaction intermediates. Furthermore, the enzyme active site discriminates ligands primarily based on charge, and is strongly biased towards binding small dianions. Finally, the enzyme is inhibited by common dianions like phosphate, but the pattern of inhibition changes abruptly and becomes less severe at alkaline pH. The mechanistic and structural basis for these behaviors will have to be addressed and clarified in future studies, for which the present work represents a necessary foundation.

MATERIALS AND METHODS

Materials

The human recombinant PEA phospho-lyase (His-tagged at the N-terminus) was produced and purified as previously described [63].

3-APP was from Wako Chemicals. Yeast alcohol dehydrogenase, PEA, MSu, ESu and all other reagents were purchased from Sigma-Aldrich.

Enzymatic assays

Solutions for the PEA phospho-lyase assay (200 μ l final volume) at the desired pH value contained: 25 mM buffer (triethanolamine-HCl or MES-NaOH), 100 mM KCl, 1 mM EGTA, 5 μ M PLP, 0.5 mg/ml bovine serum albumin, \sim 0.2 mM NADH, 50 units/ml ADH, in addition to PEA and PEA phospho-lyase (0,5 μ M). Reactions were carried out at 20° or 30°C, depending on the experiment, and the rate of acetaldehyde formation was measured by spectrophotometrically monitoring the disappearance of NADH at 340 nm. Data were analyzed by nonlinear least-squares fitting to the appropriate kinetic equation using Sigma Plot (Systat Software Inc.).

Inhibition studies

Reaction rates were monitored in the presence of phosphate and other inhibitory anions (added as sodium salts). Rates in the presence of 3-APP were determined from just the first minute of the kinetic time-courses, since 3-APP tends to slowly inactivate the enzyme by converting the cofactor to PMP [20].

Earlier studies [16, 17, 20] and preliminary controls indicated that at pH between 6 and 8 the anions tested behaved as simple competitive inhibitors, thus in this pH interval inhibition was usually assessed by keeping the substrate concentration constant (1 mM) and increasing the inhibitor concentration. Decreases in activity were then fit to the following equation, which assumes purely competitive inhibition:

$$\frac{v}{v_0} = \frac{K_I(K_M + [PEA])}{K_I(K_M + [PEA]) + K_M[I]}$$

(Eq. 1)

Where v is the observed reaction rate, v_0 is the rate in the absence of inhibitor, $[I]$ is the concentration of the anion and K_I is the respective inhibition constant. At pH higher than 8, however, we found that inhibition by phosphate and other anions was no longer purely competitive, thus we performed substrate titration experiments at different concentrations of inhibitor and fit the results to the general Eq. 2 [64]:

$$v = \frac{k_{cat}[E][PEA]}{K_M \left(\frac{1 + \frac{[I]}{K_I}}{1 + \frac{\beta[I]}{\alpha K_I}} \right) + [PEA] \left(\frac{1 + \frac{[I]}{\alpha K_I}}{1 + \frac{\beta[I]}{\alpha K_I}} \right)}$$

(Eq. 2)

where the modifying factors α and β describe, respectively, the effect of the inhibitor on K_M and on V_{max} .

pH dependence analysis

The pH dependences of K_M or K_I were usually fit to the following equation, which assumes variation of the parameter, in a given pH interval, depending on the ionization of a single group:

$$K = \frac{10^{-pK_a} + 10^{-pH}}{\frac{10^{-pH}}{K_1} + \frac{10^{-pK_a}}{K_2}}$$

(Eq. 3)

In this equation (which was obtained by rearranging Eq. 5.8 in ref. [21]), K is the parameter is under consideration, K_1 and K_2 are the limiting values of the parameter at low and high pH, respectively, while pK_a refers to dissociation of the ionizable group in the free enzyme or free ligand.

Spectrophotometric measurements

The changes in absorption ensuing after reaction of PEA phospho-lyase (9 μ M) with PEA and other ligands in 25 mM triethanolamine buffer (pH 8) were monitored using a Cary 400 spectrophotometer (Varian). Cuvette holders were thermostated at 20 or 30 °C, depending on the experiment.

Fluorometric measurements

Emission spectra were recorded using a spectrofluorometer (Perkin Elmer LS-50B) with the cell holder thermostated at 20°C.

Solutions for these experiments contained 25 mM 1,3-bis (tris (hydroxymethyl)methylamino)propane (Bis-Tris propane), 100 mM KCl, 1 mM EGTA, 5 mM tris(2-carboxyethyl)phosphine, 10% glycerol, pH 8.0. This solution was chosen among various different compositions as it best stabilized the fluorescence signal of the native enzyme.

The concentration of PEA phospho-lyase was 0.5-2 μM . Binding of ligands to the enzyme was assessed by monitoring the changes in fluorescence emission of PLP upon direct excitation of the cofactor at 410 nm, as previously reported for other PLP-dependent enzymes [32-36]. The excitation and emission slits were kept as wide as the instrument allowed ($\text{slit}_{\text{ex}}=15$ nm, $\text{slit}_{\text{em}}=20$ nm) to ensure maximum sensitivity.

Stopped-flow measurements

Fast kinetic measurements were carried out using a SX-18MV stopped flow apparatus (Applied Photophysics) equipped with a 75-watt Xenon lamp and alternatively coupled to a photomultiplier (Applied Photophysics) for single wavelength measurements or to an MS 125TM 1/8-m spectrograph and Instaspec II photodiode array (Lot-Oriel) for multi-wavelength measurements. The temperature of the loading syringes and of the stopped-flow mixing cell compartment was kept at 20°C with a circulating water bath.

Reactions were carried out in 25 mM triethanolamine buffer, pH 8. PEA phospho-lyase (typically 20 μM) was mixed with PEA or phosphate at the desired concentration. For rapid-scanning experiments, spectra of the reaction mixture (in the 320-480 nm interval) were collected every 2.5 ms with PEA; every 8 ms with phosphate. For both set ups the instrumental dead time was 1.5 ms.

Single wavelength traces (20000 data points, linear time scale) were collected at 340 and 425 nm in the presence of PEA and at 390 nm in the presence of phosphate, respectively. Kinetics were acquired for 100 ms and 1 second for PEA and for up to 100 s for phosphate. Single-wavelength kinetic traces were usually fit to Eq. 4.

$$A = A_0 + \Delta A \{1 - \exp(-k_{obs}t)\}$$

(Eq. 4)

where A and A_0 are the absorbance values at a given time and at time $t \rightarrow \infty$, respectively; ΔA is the amplitude of the exponential curve and k_{obs} is the observed rate constant. In cases when the time-course of the reaction was clearly biphasic, data were fit to the following biexponential function:

$$A = A_0 + \Delta A_1 \{1 - \exp(-k_{obs1}t)\} + \Delta A_2 \{1 - \exp(-k_{obs2}t)\}$$

(Eq. 5)

Singular value decomposition analysis

The time-resolved spectra data matrices were analyzed by singular value decomposition (SVD) [44, 45] using the program MATLAB 6.0 (The Mathworks, Inc. Natick, MA). In the SVD procedure, a given ($m \times n$) data matrix (the A matrix, where m is the number of wavelengths and n is the number of spectra collected), is resolved into a product of three matrices, usually named U , S , and V^T , as shown in Equation 6.

$$A=U \times S \times V^T$$

(Eq. 6)

The ($m \times n$) U matrix consists of n orthonormal eigenvectors; S is a square diagonal matrix, and V^T is a ($n \times n$) matrix whose rows are also orthonormal. The columns of U are spectral components that combine, each with a contribution weighted by its singular value, to yield every observed spectrum. For each U component, the time evolution is derived from the corresponding row in the V^T matrix. The main criterion for the selection of usable components is the magnitude of the singular values, the higher values being the meaningful ones.

The SVD procedure applied to our rapid scanning served two purposes. The first was to clean up the time-resolved spectra. To this end, the U columns corresponding to meaningful spectra and the respective V rows and S singular values were multiplied to rebuild a data matrix purged of components attributable to simple noise (this procedure however cannot completely remove the noise from the time-resolved spectra, as the individual U columns do not necessarily represent the spectra of pure components). A second purpose of the SVD was to gain a better understanding of the kinetic processes under observation. In particular, the U spectral components could serve to extrapolate the features of kinetic intermediates, while the rows of V^T representing their time evolution could be compared to single-wavelength data.

NaBH₄ treatment of the enzyme-PEA complex

Excess (~30 mg/ml) of sodium borohydride was added to three solutions (400 μ l each) containing 30 μ M PEA phospho-lyase. In the first sample, the enzyme was dissolved in just buffer (25 mM triethanola-

mine, 100 mM KCl, 1 mM EGTA). The second sample contained the same buffer supplemented with 50 mM 3-APP and NaBH₄ was added only after ascertaining that reaction of the enzyme with 3-APP had led to the full conversion of the PLP cofactor to PMP (the process required a few minutes) [20]. The third sample contained buffer plus 15 mM PEA; in this case, NaBH₄ was added ~5 seconds after mixing the enzyme with its substrate. Experiments were conducted at 30°C

After addition of sodium borohydride, the three samples were centrifuged and their absorption spectra were measured, to assess the complete disappearance of oxidized PLP. The solutions were dialyzed twice (at least 3 hours each time) against 100 ml of a solution containing 25 mM Tris (pH 8), 100 mM KCl, 1 mM EGTA and 6 M urea. At the end of dialysis, the samples were again centrifuged and their absorption spectra were recorded.

REFERENCES:

1. John, R. A. (1995) Pyridoxal phosphate-dependent enzymes, *Biochim. Biophys. Acta.* 1248, 81-96.
2. Eliot, A. C. & Kirsch, J. F. (2004) Pyridoxal phosphate enzymes: mechanistic, structural, and evolutionary considerations, *Annu. Rev. Biochem.* 73, 383-415.
3. Toney, M. D. (2011) Controlling reaction specificity in pyridoxal phosphate enzymes, *Biochim. Biophys. Acta.* 1814, 1407-18.
4. Mehta, P. K. & Christen, P. (2000) The molecular evolution of pyridoxal-5'-phosphate-dependent enzymes, *Adv. Enzymol.* 74, 129-184.
5. Percudani, R. & Peracchi, A. (2003) A genomic overview of pyridoxal-phosphate-dependent enzymes, *EMBO Rep.* 4, 850-854.
6. Jansonius, J. N. (1998) Structure, evolution and action of vitamin B6-dependent enzymes, *Curr. Opin. Struct. Biol.* 8, 759-69.
7. Schneider, G., Kack, H. & Lindqvist, Y. (2000) The manifold of vitamin B6 dependent enzymes, *Structure Fold. Des.* 8, R1-6.
8. Percudani, R. & Peracchi, A. (2009) The B6 database: a tool for the description and classification of vitamin B6-dependent enzymatic activities and of the corresponding protein families, *BMC Bioinformatics.* 10, 273.
9. Toney, M. D. (2014) Aspartate aminotransferase: an old dog teaches new tricks, *Arch Biochem Biophys.* 544, 119-27.
10. Faraci, W. S. & Walsh, C. T. (1988) Racemization of alanine by the alanine racemases from *Salmonella typhimurium* and *Bacillus stearothermophilus*: energetic reaction profiles, *Biochemistry.* 27, 3267-76.
11. Badet, B., Inagaki, K., Soda, K. & Walsh, C. T. (1986) Time-dependent inhibition of *Bacillus stearothermophilus* alanine racemase by (1-aminoethyl)phosphonate isomers by isomerization to noncovalent

slowly dissociating enzyme-(1-aminoethyl)phosphonate complexes, *Biochemistry*. 25, 3275-82.

12. Phillips, R. S., Demidkina, T. V., Zakomirdina, L. N., Bruno, S., Ronda, L. & Mozzarelli, A. (2002) Crystals of tryptophan indole-lyase and tyrosine phenol-lyase form stable quinonoid complexes, *J Biol Chem*. 277, 21592-7.

13. Phillips, R. S., Demidkina, T. V. & Faleev, N. G. (2003) Structure and mechanism of tryptophan indole-lyase and tyrosine phenol-lyase, *Biochim Biophys Acta*. 1647, 167-72.

14. Ikushiro, H., Hayashi, H., Kawata, Y. & Kagamiyama, H. (1998) Analysis of the pH- and ligand-induced spectral transitions of tryptophanase: activation of the coenzyme at the early steps of the catalytic cycle, *Biochemistry*. 37, 3043-52.

15. Sprinson, D. B. & Weliky, I. (1969) The conversion of ethanolamine to acetate in mammalian tissues, *Biochem. Biophys. Res. Commun*. 36, 866-70.

16. Fleshood, H. L. & Pitot, H. C. (1970) The metabolism of O-phosphorylethanolamine in animal tissues. I. O-phosphorylethanolamine phospho-lyase: partial purification and characterization, *J. Biol. Chem*. 245, 4414-20.

17. Veiga-da-Cunha, M., Hadi, F., Balligand, T., Stroobant, V. & Van Schaftingen, E. (2012) Molecular identification of hydroxylysine kinase and of the ammoniophospholyases acting on 5-phosphohydroxy-L-lysine and phosphoethanolamine, *J. Biol. Chem*. 287, 7246-55.

18. Davis, L. & Metzler, D. E. (1972) Pyridoxal-linked elimination and replacement reactions in *The enzymes 3rd ed.* (Boyer, P., ed) pp. 33-74, Academic Press, New York.

19. Tai, C. H. & Cook, P. F. (2001) Pyridoxal 5'-phosphate-dependent α,β -elimination reactions: mechanism of O-acetylserine sulfhydrylase, *Acc. Chem. Res.* **34**, 49-59.
20. Schioli, D., Cirrincione, S., Donini, S. & Peracchi, A. (2013) Strict reaction and substrate specificity of AGXT2L1, the human O-phosphoethanolamine phospho-lyase, *IUBMB Life.* **65**, 645-50.
21. Fersht, A. R. (1999) *Structure and Mechanism in Protein Science - A Guide to Enzyme Catalysis and Protein Folding*, Freeman & Co., New York.
22. Myller, A. T., Karhe, J. J., Haukka, M. & Pakkanen, T. T. (2013) The pH behavior of a 2-aminoethyl dihydrogen phosphate zwitterion studied with NMR-titrations, *J. Mol. Struct.* **1033**, 171–175.
23. Jungas, R. L. (2006) Best literature values for the pK of carbonic and phosphoric acid under physiological conditions, *Anal. Biochem.* **349**, 1-15.
24. Knitt, D. S. & Herschlag, D. (1996) pH dependencies of the *Tetra-hymena* ribozyme reveal an unconventional origin of an apparent pK_a, *Biochemistry.* **35**, 1560-70.
25. Johnson, L. L., Pavlovsky, A. G., Johnson, A. R., Janowicz, J. A., Man, C. F., Ortwine, D. F., Purchase, C. F., 2nd, White, A. D. & Hupe, D. J. (2000) A rationalization of the acidic pH dependence for stromelysin-1 (Matrix metalloproteinase-3) catalysis and inhibition, *J. Biol. Chem.* **275**, 11026-33.
26. Gillies, R. J., Liu, Z. & Bhujwalla, Z. (1994) ³¹P-MRS measurements of extracellular pH of tumors using 3-aminopropylphosphonate, *Am. J. Physiol.* **267**, C195-203.
27. Drewe, W. F., Jr. & Dunn, M. F. (1986) Characterization of the reaction of L-serine and indole with *Escherichia coli* tryptophan synthase via

rapid-scanning ultraviolet-visible spectroscopy, *Biochemistry*. 25, 2494-501.

28. Sterk, M. & Gehring, H. (1991) Spectroscopic characterization of true enzyme-substrate intermediates of aspartate aminotransferase trapped at subzero temperatures, *Eur. J. Biochem.* 201, 703-7.

29. Rossi, G. L., Mozzarelli, A., Peracchi, A. & Rivetti, C. (1992) Time course of chemical and structural events in protein crystals measured by microspectrophotometry, *Phil. Trans. Royal Soc. Lond. A.* 340, 191-207.

30. Hayashi, H., Mizuguchi, H. & Kagamiyama, H. (1993) Rat liver aromatic L-amino acid decarboxylase: spectroscopic and kinetic analysis of the coenzyme and reaction intermediates, *Biochemistry*. 32, 812-8.

31. Donini, S., Percudani, R., Credali, A., Montanini, B., Sartori, A. & Peracchi, A. (2006) A threonine synthase homolog from a mammalian genome, *Biochem. Biophys. Res. Commun.* 350, 922-8.

32. Goldberg, M. E., York, S. & Stryer, L. (1968) Fluorescence studies of substrate and subunit interactions of the β_2 protein of *Escherichia coli* tryptophan synthetase, *Biochemistry*. 7, 3662-7.

33. Federiuk, C. S. & Shafer, J. A. (1983) A reaction pathway for transamination of the pyridoxal 5'-phosphate in D-serine dehydratase by amino acids, *J. Biol. Chem.* 258, 5372-8.

34. Vaccari, S., Benci, S., Peracchi, A. & Mozzarelli, A. (1996) Time-resolved fluorescence of tryptophan synthase, *Biophys. Chem.* 61, 9-22.

35. Benci, S., Vaccari, S., Mozzarelli, A. & Cook, P. F. (1997) Time-resolved fluorescence of O-acetylserine sulfhydrylase catalytic intermediates, *Biochemistry*. 36, 15419-27.

36. Marchetti, M., Bruno, S., Campanini, B., Peracchi, A., Mai, N. & Mozzarelli, A. (2013) ATP binding to human serine racemase is cooperative and modulated by glycine, *FEBS J.* 280, 5853-63.

37. Toney, M. D. & Kirsch, J. F. (1993) Lysine 258 in aspartate aminotransferase: enforcer of the Circe effect for amino acid substrates and general-base catalyst for the 1,3-prototropic shift, *Biochemistry*. *32*, 1471-9.
38. Campanini, B., Schiaretti, F., Abbruzzetti, S., Kessler, D. & Mozzarelli, A. (2006) Sulfur mobilization in cyanobacteria: the catalytic mechanism of L-cystine C-S lyase (C-DES) from *synechocystis*, *J Biol Chem*. *281*, 38769-80.
39. Bisht, S., Rajaram, V., Bharath, S. R., Kalyani, J. N., Khan, F., Rao, A. N., Savithri, H. S. & Murthy, M. R. (2012) Crystal structure of *Escherichia coli* diaminopropionate ammonia-lyase reveals mechanism of enzyme activation and catalysis, *J Biol Chem*. *287*, 20369-81.
40. Kezuka, Y., Yoshida, Y. & Nonaka, T. (2012) Structural insights into catalysis by β C-S lyase from *Streptococcus anginosus*, *Proteins*. *80*, 2447-58.
41. D'Aguzzo, S., Gonzales, I. N., Simmaco, M., Contestabile, R. & John, R. A. (2003) Stereochemistry of the reactions of glutamate-1-semialdehyde aminomutase with 4,5-diaminovalerate, *J. Biol. Chem*. *278*, 40521-6.
42. Minelli, A., Charteris, A. T., Voltattorni, C. B. & John, R. A. (1979) Reactions of DOPA (3,4-dihydroxyphenylalanine) decarboxylase with DOPA, *Biochem. J*. *183*, 361-8.
43. Montioli, R., Cellini, B., Dindo, M., Oppici, E. & Voltattorni, C. B. (2013) Interaction of human Dopa decarboxylase with L-Dopa: spectroscopic and kinetic studies as a function of pH, *Biomed. Res. Int*. *2013*, 161456.

44. Henry, E. R. & Hofrichter, J. (1992) Singular value decomposition: Application to analysis of experimental data, *Meth. Enzymol.* 210, 129–192.
45. Henry, E. R. (1997) The use of matrix methods in the modeling of spectroscopic data sets, *Biophys. J.* 72, 652-73.
46. Miles, E. W., Houck, D. R. & Floss, H. G. (1982) Stereochemistry of sodium borohydride reduction of tryptophan synthase of *Escherichia coli* and its amino acid Schiff's bases, *J. Biol. Chem.* 257, 14203-10.
47. Erion, M. D. & Walsh, C. T. (1987) 1-Aminocyclopropanephosphonate: time-dependent inactivation of 1-aminocyclopropanecarboxylate deaminase and *Bacillus stearothermophilus* alanine racemase by slow dissociation behavior, *Biochemistry.* 26, 3417-25.
48. Rege, V. D., Kredich, N. M., Tai, C. H., Karsten, W. E., Schnackerz, K. D. & Cook, P. F. (1996) A change in the internal aldimine lysine (K42) in O-acetylserine sulfhydrylase to alanine indicates its importance in transamination and as a general base catalyst, *Biochemistry.* 35, 13485-93.
49. Goldberg, J. M. & Kirsch, J. F. (1996) The reaction catalyzed by *Escherichia coli* aspartate aminotransferase has multiple partially rate-determining steps, while that catalyzed by the Y225F mutant is dominated by ketimine hydrolysis, *Biochemistry.* 35, 5280-91.
50. Metzler, C. M., Harris, A. G. & Metzler, D. E. (1988) Spectroscopic studies of quinonoid species from pyridoxal 5'-phosphate, *Biochemistry.* 27, 4923-33.
51. Mozzarelli, A., Peracchi, A., Rovegno, B., Dale, G., Rossi, G. L. & Dunn, M. F. (2000) Effect of pH and monovalent cations on the for-

mation of quinonoid intermediates of the tryptophan synthase $\alpha_2\beta_2$ complex in solution and in the crystal, *J. Biol. Chem.* 275, 6956-62.

52. Roy, M., Miles, E. W., Phillips, R. S. & Dunn, M. F. (1988) Detection and identification of transient intermediates in the reactions of tryptophan synthase with oxindolyl-L-alanine and 2,3-dihydro-L-tryptophan. Evidence for a tetrahedral (*gem*-diamine) intermediate, *Biochemistry*. 27, 8661-9.

53. Karsten, W. E. & Cook, P. F. (2009) Detection of a *gem*-diamine and a stable quinonoid intermediate in the reaction catalyzed by serine-glyoxylate aminotransferase from *Hyphomicrobium methylovorum*, *Biochim. Biophys. Acta.* 1790, 575-80.

54. Hedstrom, L. (2001) Enzyme Specificity and Selectivity in *Encyclopedia of Life Sciences*, John Wiley & Sons, Ltd., Chichester. .

55. Tawfik, D. S. (2014) Accuracy-rate tradeoffs: how do enzymes meet demands of selectivity and catalytic efficiency?, *Curr. Opin. Chem. Biol.* 21C, 73-80.

56. Phillips, R. S. & Gollnick, P. D. (1989) Evidence that cysteine 298 is in the active site of tryptophan indole-lyase, *J. Biol. Chem.* 264, 10627-32.

57. Shao, L. & Vawter, M. P. (2008) Shared gene expression alterations in schizophrenia and bipolar disorder, *Biol. Psychiatry.* 64, 89-97.

58. Logotheti, M., Papadodima, O., Venizelos, N., Chatziioannou, A. & Kollis, F. (2013) A comparative genomic study in schizophrenic and in bipolar disorder patients, based on microarray expression profiling meta-analysis, *Sci. World J.* 2013, 685917.

59. Coghlan, S., Horder, J., Inkster, B., Mendez, M. A., Murphy, D. G. & Nutt, D. J. (2012) GABA system dysfunction in autism and related disor-

ders: from synapse to symptoms, *Neurosci. Biobehav. Rev.* 36, 2044-55.

60. Menzie, J., Pan, C., Prentice, H. & Wu, J. Y. (2014) Taurine and central nervous system disorders, *Amino Acids.* 46, 31-46.

61. Gonzalez, D. H., Iglesias, A. A. & Andreo, C. S. (1984) On the regulation of phosphoenolpyruvate carboxylase activity from maize leaves by L-malate. Effect of pH, *J. Plant .Physiol.* 116, 425-34.

62. Chen, G., Edwards, T., D'Souza V, M. & Holz, R. C. (1997) Mechanistic studies on the aminopeptidase from *Aeromonas proteolytica*: a two-metal ion mechanism for peptide hydrolysis, *Biochemistry.* 36, 4278-86.

63. Donini, S., Ferrari, M., Fedeli, C., Faini, M., Lamberto, I., Marletta, A. S., Mellini, L., Panini, M., Percudani, R., Pollegioni, L., Caldinelli, L., Petrucco, S. & Peracchi, A. (2009) Recombinant production of eight human cytosolic aminotransferases and assessment of their potential involvement in glyoxylate metabolism, *Biochem. J.* 422, 265-272.

64. Leskovac, V. (2003) *Comprehensive Enzyme Kinetics*, Kluwer, New York.

Enzyme-based fluorometric assay for the quantitative analysis of O-phosphoethanolamine in biological fluids

Davide Schirolì^a and Alessio Peracchi^{a,b}

^a Department of Life Sciences, Laboratory of Biochemistry, Molecular Biology and Bioinformatics, University of Parma, 43124 Parma, Italy.

^b Corresponding author. Phone: +39 0521905137 Fax: +39 0521905151.

Email: alessio.peracchi@unipr.it.

ABSTRACT

O-phosphoethanolamine (ethanolamine phosphate; PEA) is an intermediate of phospholipid metabolism and its levels in biological fluids are increased in some metabolic, genetic and psychiatric diseases. Determination of PEA is thus of relevance to diagnosis and monitoring of diseases. Standard detection methods of PEA levels are liquid-chromatography–mass spectrometry or capillary electrophoresis–mass spectrometry. Here we describe a rapid and inexpensive enzymatic assay for the detection of PEA levels. The assay is based on the conversion of PEA to acetaldehyde in the presence of the enzyme O-phosphoethanolamine phospho-lyase (PEA-PL), followed by oxidation of the aldehyde by aldehyde dehydrogenase, in parallel with the reduction of nicotinamide adenine dinucleotide (NAD⁺) to NADH. Determination of PEA concentration is based on the detection of stoichiometrically generated NADH. We tried to optimize the assay for the detection of PEA in blood, where the amine has typically a concentration in 1-4 μ M range. Our assay could satisfactorily quantitate this low amounts of analyte in a buffer-water system, but did not work in plasma, presumably due to interference by other components of the biological matrix. These results suggest that for successful application of the assay to blood and to other biological fluids an appropriate pre-processing of the sample will have to be developed.

INTRODUCTION

O-phosphoethanolamine (PEA) is involved in membrane homeostasis: it is an important metabolite of the glycerophospholipids biosynthetic pathway, the Kennedy pathway [1], and a junction between that and the synthesis of sphingolipids [2]. An abnormal PEA concentration can be associated to alterations in mitochondrial respiration [3, 4] and in brain cell metabolism [5-7].

PEA was also found to be altered in different biological fluids and tissues, as a consequence of a wide range of diseases and pathologies: in plasma during sepsis [8], in cerebrospinal fluid (CSF) as a consequence of cerebral injury (ischemia) [9, 10], in myometrium during pregnancy [11], in bronchoalveolar lavage (BAL) of individuals with asthma [12]. Moreover an elevated level of PEA in urine supports the diagnosis of a rare genetic disease, termed hypophosphatasia, caused by the deficiency of alkaline phosphatase [13]; urinary excretion of PEA was also shown to be increased in patients with frequent bone diseases (osteoporosis) and hypertension [14].

Recently a Japanese group also reported a lowered concentration of PEA in the plasma of subjects with major depression [15, 16]. Depression disorder is one of the most common pathologies in the developed countries, with approximately 10% of the entire population being affected during their lifetime. Depression is a complex multi-factorial disease that can have different causes and symptoms, and for psychiatrists it is often difficult to discern among different forms of this disease and between it and other similar pathologies. Therefore, if the claim of the Japanese group [15, 16] were substantiated by further studies, the plasmatic PEA level could represent a precious diagnostic

tool, complementing clinical examination to ensure maximal accuracy in the identification of depression.

Various methods for the measurement of PEA in biological fluids have been previously described, but they are expensive and time-consuming, like in the case of the mass spectrometry approach used by Kawamura et al. [15]. An enzymatic assay based on fluorescence or absorbance detection could be a rapid and user-friendly alternative to the complex and expensive techniques described.

Both to further investigate the data collected by the Japanese group and to achieve a fast and inexpensive enzymatic method to use in diagnostics, we tried to develop an assay for measuring the amount of PEA using PEA phospho-lyase (PEA-PL). This enzyme converts PEA to acetaldehyde, phosphate and ammonia. The aldehyde, in turn, can be further processed by a coupled NAD-dependent dehydrogenase, to yield an optical signal.

Blood was the elective fluid in which we decided to firstly develop the enzymatic assay. The normal blood concentration of PEA is around $4.0 \pm 2.0 \mu\text{M}$ in adults (a similar concentration of $6.0 \pm 1.1 \mu\text{M}$ is reportedly present also in CSF, while higher concentration are found in saliva and urine; <http://www.hmdb.ca/metabolites/hmdb00224>). This low concentration of PEA in plasma excludes the possibility to directly quantitate the dehydrogenase reaction by monitoring the absorption of NADH, since the formation or consumption of $4 \mu\text{M}$ NADH would imply an exceedingly small change in terms of absorbance ($\epsilon_{340} = 6220 \text{ M}^{-1}\text{cm}^{-1}$). For this reason we tried to develop an assay that was sensitive enough, using fluorescence and a PEA-PL-aldehyde dehydrogenase-diaphorase-resazurin coupled reaction, similar to those described in other cases [17, 18]. PEA-PL degrades PEA producing acetaldehyde,

reduced then by an aldehyde dehydrogenase. In the last step, diaphorase uses the NADH produced by the aldehyde dehydrogenase to transform resazurin into the highly fluorescent resorufin (Fig. 1).

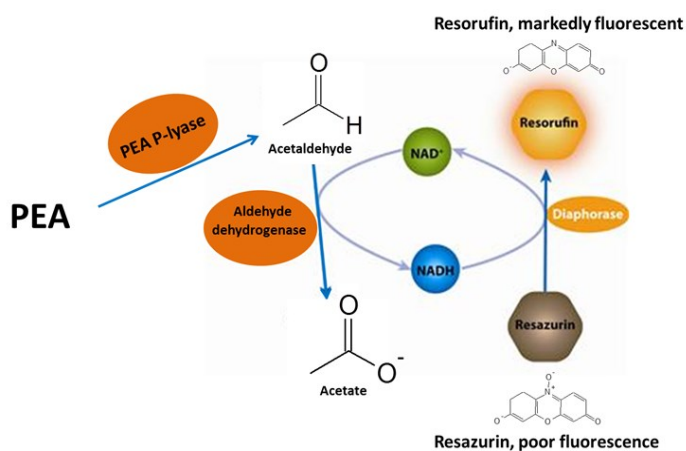


Figure 1: Reaction scheme of the fluorescence assay for PEA quantitation: PEA is initially converted to acetaldehyde by PEA-PL. Aldehyde dehydrogenase then oxidizes acetaldehyde to acetate while converting NAD⁺ to NADH, which in turn is used by diaphorase to reduce resazurin to resorufin. This latter compound is quantitated by measuring emission at 610 nm (excitation at 540 nm).

MATERIALS AND METHODS

Materials

The human recombinant PEA-PL (His-tagged at the N-terminus) was produced and purified as previously described [19]. Aldehyde dehydrogenase (from *Saccharomyces cerevisiae*) and diaphorase (from *Clostridium kluyveri*) were purchased from Sigma. Resazurin and all other chemical reagents were also from Sigma-Aldrich.

Plasma samples were obtained from the transfusional center of the local hospital (Ospedale Maggiore di Parma) and stored at -20°C .

Design of the resazurin-based fluorescence assay for PEA quantitation

The three-steps coupled enzyme reaction is shown in Fig. 1 and follows the direction described in the introduction. Buffer conditions, substrate and coenzyme concentrations were set to favor the conversion of PEA to acetaldehyde (catalyzed by PEA-PL) and then to acetate (by the action of aldehyde dehydrogenase), thus resulting in the accumulation of NADH.

In the third enzymatic step, NADH is used by diaphorase to reduce the poorly fluorescent resazurin, generating the highly fluorescent resorufin. Fluorometric detection is carried out with excitation at around 540 nm and emission at 610 nm [20].

Emission spectra were recorded using a spectrofluorometer (Perkin Elmer LS-50B) with the cell holder thermostated at 20°C . Solutions for these experiments contained 100 mM Hepes (pH 8), 100 mM KCl, 1 mM EGTA, 10% glycerol, 0.1 mg/ml Aldehyde dehydrogenase, 5 μM Resazurin, 100 μM NAD^{+} , 0.1 mg/ml diaphorase. The concentration of PEA phospho-lyase was 0.5–2 I M.

Deproteinization methods

The pre-treatments of plasma, used in this study to try to eliminate proteins and other interfering plasma components prior to PEA assay, have been described before.

Methanol-chloroform treatment and ultrafiltration (Vivaspin 500, cut-off 3000 MWCO) were performed essentially as described in [21]. Perchlorate denaturation of proteins was also carried out as described in [21] while proteinase K treatment followed the procedure in [17].

Expression and purification of ethanolamine kinase

The gene encoding ethanolamine kinase from *Trypanosoma brucei* (TbC/EK2) was cloned into pEt15bTEV, by Gibellini et al. [22]. *E.coli* BL21-C⁺ cells were transformed with the plasmid. To achieve protein expression, bacterial cultures were supplemented with IPTG and incubated at 30° C overnight. Afterwards, bacteria were collected by centrifugation and resuspended in a lysis buffer composed by 300 mM NaCl, 50 mM Tris-HCl pH 8, 5% Glycerol and 5 mM β -mercaptoethanol. The cells were homogenized by sonication.

The recombinant protein (carrying an N-term His-Tag) was purified from the soluble fraction of the cell lysate using an affinity cobalt-resin. After elution from the resin, the protein was dialyzed against a buffer similar to the lysis buffer, except that it contained DTT (1 mM) instead of β -mercaptoethanol. The final yield of soluble protein was about one third of that reported by Gibellini and co-workers [22]. This could be due to the different *E.coli* strain used for the expression.

PEA and ^{32}P -PEA production

The production of PEA by ethanolamine kinase (TbC/EK2) was assayed using a coupled assay with pyruvate kinase and lactate dehydrogenase [23]. The reaction mixture contained: 50 mM MOPS pH 7.8, 150 mM KCl, 6 mM MgCl_2 , 0.5 mg/ml BSA, 5 mM ATP, 20 mM ethanolamine, 1 mM phosphoenolpyruvate, pyruvate kinase and lactate dehydrogenase (the two enzymes are supplied in the same solution by Sigma-Aldrich). The concentrations of ATP and ethanolamine were saturating for TbC/EK2. The production of PEA was also occasionally tested using a coupled assay PEA-PL and alcohol dehydrogenase or also using TLC, where samples and controls were separated and stained with ninhydrin (data not shown).

Similar reaction conditions were also used to produce ^{32}P -labeled PEA, except that the reaction mixture also contained γ - ^{32}P -ATP (Perkin-Elmer). ^{32}P -PEA was separated from radioactive ATP and phosphate by thin layer chromatography (TLC) on silica plates (50% propanol/10% acetic acid). In preparative experiments, the position of ^{32}P -labeled PEA on the TLC plate was identified by autoradiography, after which the silica surface was scraped away and ^{32}P -PEA was eluted by centrifugation of the scraped powder in buffer solution.

Analytical thin layer chromatography

TLC was also used for analytical experiments, where ^{32}P -PEA (and its degradation products) was detected and quantitated in different kinds of samples. TLC was performed with different eluting solvents: methanol 50%, methanol/acetic acid 50%/10%, propanol/acetic acid 50%/10% and propanol/ammonium 50%/10%.

RESULTS

Optimization of buffer features and of reagent concentrations for the fluorometric PEA assay.

Conditions for the assay were initially optimized in buffered water. Several negative controls were performed in parallel in order to determine the best buffer, best pH and optimal concentrations of diaphorase, dehydrogenase and PEA-PL. The concentration of this last enzyme is quite critical, as we did not know its ability to catalyze reaction with low amount of substrate and also because it contains a fluorescent cofactor that could interfere with fluorescence measurement.

PEA-PL works at its best at pH 8 [24], similarly also aldehyde dehydrogenase has its best activity at the same pH value (product from Sigma-Aldrich 82884). Furthermore, other previously described assays based on the resazurin/diaphorase reaction were performed at pH 8 [18]. Thus we opted for this as the pH of choice for our assay. Between the different buffers tested (Triethanolamine, Tris, Bis-tris-propane and HEPES), HEPES at pH 8 gave the best results.

In the assay mixture, 5 μM resazurin was used, to approximate the highest concentration of PEA reportedly found in blood. As for PEA-PL, a concentration of 0.8 μM (0.04 mg/ml) gave the best compromise in terms of reaction velocity and PLP intrinsic fluorescence. Aldehyde dehydrogenase was used at 0.1 mg/ml and diaphorase also at 0.1 mg/ml. These two enzymes were ultrafiltered before being used, as they contain substances that increase the fluorescence of the baseline. Between the baseline and the measure we waited 15 and 30 min, fluorescence was however stable after 15 min. Temperature was set up at 20°C.

Serum sample was deproteinized in several different ways. Ultrafiltration has the advantage to avoid sample treatment with chemicals that

can alter its properties; on the other hand it could not be able to detach the analyte from the strong interaction with proteins or other components of the serum.

Other methods used were methanol-chloroform extraction [25], perchlorate denaturation of proteins [21]. We tried to use also proteinase K to degrade proteins [17].

Fluorescence assay: range of linearity of the readout and test of the assay on plasma ultrafiltrate supplemented with PEA.

The fluorescence signal arising from resorufin production (reaction conditions described in materials and methods) was shown to increase linearly with the amount of PEA, in the 0.5-10 μM range (Fig. 2A). Similar results were obtained in a lower range of PEA concentrations and with addition of 50% deproteinized (ultrafiltered) plasma (Fig. 2B). Otherwise any Δ Fluorescence was detected in a sample with 50% of ultrafiltrate, supplemented with 10 μM PEA just before the ultrafiltration, with respect to the negative control (sample containing ultrafiltrate not supplemented with PEA). Analogous results were obtained using all the different deproteinization methods (when plasma was treated with proteinase K and then ultrafiltered, it also seemed to acquire an inhibitory effect on the coupled enzymatic reactions – data not shown). An experiment using ^{32}P -PEA was then performed to understand if exogenous PEA is degraded prior or during ultrafiltration, so that it cannot be further detected by the assay.

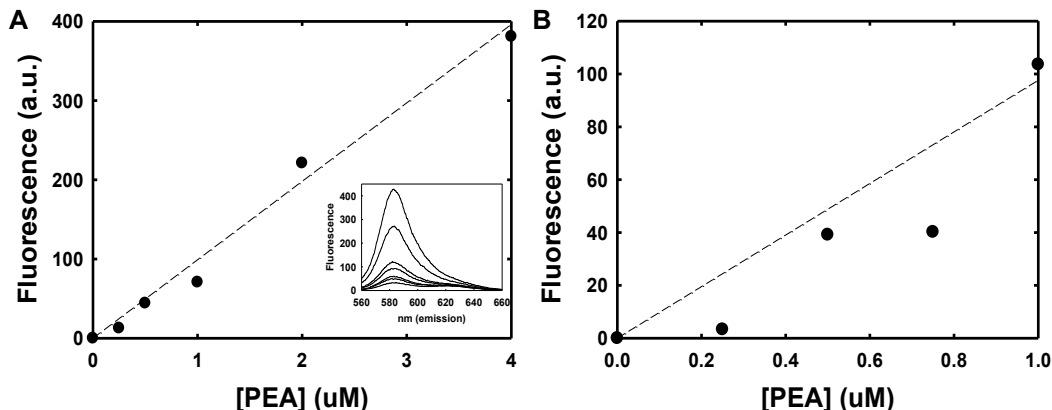


Figure 2: (A) Fluorescence assay performed as described in materials and methods between 0 and 4 μM PEA, the solid line is a linear regression correlating fluorescence and PEA concentration. (B) Fluorescence assay performed between 0 and 1 μM of PEA, in this case the reaction solution contained also 50% of ultrafiltered plasma. Correlation between the intensity of fluorescence and concentration of PEA was still observed but less satisfactory,

Assay with radioactive PEA: analysis of the deproteinization methods and of the fluorescence assay reaction, using ^{32}P -PEA.

^{32}P -PEA was produced using ethanolamine kinase [22]. First of all EK production was improved in order to obtain a good yield of soluble kinase; then transformation of EA to PEA was also optimized. Some components of the procedure (both for the enzymatic synthesis of PEA and for the purification of EK) were different respect to those used by Smith et al. (see material and methods and [22]).

Once selected the best condition to separate PEA from ATP and phosphate (TLC elution with propanol and acetic acid, Fig. 3A and 3B) we performed various analysis using ^{32}P -PEA. First of all we investigat-

ed whether the failure of the assay to function on the ultrafiltered plasma mirrored loss of PEA during the ultrafiltration process itself. In this case PEA was seen to pass through the filter, ^{32}P -PEA was in fact detected in the ultrafiltrate, with an estimated concentration similar to that observed in plasma (Fig. 3C and 3D). Moreover there was no detectable radioactivity (measured using Geiger counter, data not shown) retained by the filter. The different migration of ^{32}P -PEA in the sample above the filter the radioactive material in the ultrafiltrate with respect to is probably due to the interaction of PEA with the complex matrix of the untreated plasma.

Subsequently it was tested the reaction catalyzed by PEA-PL in a solution containing all the components used for the fluorescence assay and in the ultrafiltrate. Separation of the radioactive molecules in the reaction mixture was performed using different TLC conditions, in parallel with positive control (^{32}P -PEA hydrolyzed by alkaline phosphatase, to release radioactive phosphate) and negative controls (^{32}P -PEA in ultrafiltrate and in buffer). Results in this case were ambiguous (Fig. 4): ^{32}P -PEA was shown not to be degraded, or only partially, in solution containing buffer and PEA-PL (and the other components used also in the fluorescence assay), while the TLC pattern observed in solutions containing ultrafiltrate of plasma- ^{32}P -PEA (50% of the reaction solution) and PEA-PL (with buffer and all the components used in fluorescence assay) is similar to that observed in the solution containing ^{32}P -PEA and CIP. Moreover the TLC pattern of ultrafiltered plasma- ^{32}P -PEA and of ^{32}P -PEA in water and buffer resembles that of ^{32}P -PEA with PEA-PL and the other components of the reaction. Similar results were obtained using two different eluting solvents: propanol/acetic acid and methanol/acetic acid.

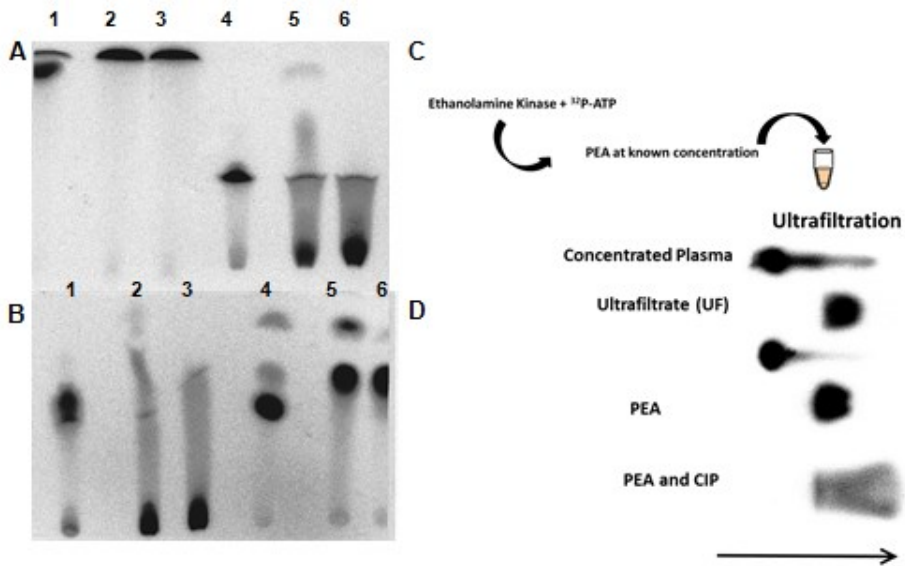


Figure 3: (A) TLC with eluent methanol of ^{32}P -PEA, EK + ATP and ATP (1,2 and 3). TLC with eluent 50% methanol/10% acetic acid of ^{32}P -PEA, EK + ATP and ATP (4,5 and 6). (B) TLC with eluent 50% propanol/10% acetic acid of ^{32}P -PEA, EK + ATP and ATP (1,2 and 3); TLC with eluent 50% propanol/10% ammonia of ^{32}P -PEA, EK + ATP and ATP (4,5 and 6). (C) Scheme of the ^{32}P -PEA experiment (D) TLC (50% propanol/10% acetic acid) of the different components of ^{32}P -PEA-Plasma ultrafiltration with two controls: PEA in buffer and PEA treated with alkaline phosphatase (CIP).

Conclusions.

We have set up a sensitive assay for the quantitation of PEA, which relies on the coupled reaction between PEA-PL, aldehyde dehydrogenase and diaphorase and which exploit the strong fluorescence signal arising from resazurin reduction. Our assay could satisfactorily quantitate micromolar amounts of PEA in a buffer-water system, but did not appear to work in plasma, despite application of ultrafiltration and other pre-processing procedures. This raises the possibility that either PEA-PL is inactivated by some plasma component, or that PEA is degraded or made unreactive by the plasma processing.

The control experiments using ^{32}P -PEA gave ambiguous results, which left open two different explanations:

PEA is degraded by PEA-PL in plasma. The paradoxically discordant TLC patterns obtained for the reaction of PEA-PL in buffered water (Figure 4A, first lane) and in buffer plus ultrafiltered plasma (Figure 4A, second lane) can be explained by the fact that radioactive PEA produced using EK could be contaminated by the presence of one or some inhibitors (phosphate, ethanolamine, inorganic ions etc.) that interfere with PEA-PL activity. In this case, components of the ultrafiltered plasma could neutralize the inhibitors. However, when ^{32}P -PEA was added to plasma prior to ultrafiltration, and then ultrafiltered, it did not react with the enzyme (data not shown).

PEA is not really degraded by PEA-PL and the TLC pattern of figure 4A-lane 2 is an artifact due to the interaction of PEA with some ultrafiltrate components. This is not however in accordance by the fact that PEA-serum negative control has a TLC pattern similar to that observed with PEA in buffer.

It seems then possible that PEA is degraded by PEA-PL, but the fact that fluorescence assay was not able to detect any Δ Fluorescence suggests that this assay cannot be used with this kind of sample, probably because the detection limit is close to the final PEA concentration in the deproteinized/ultrafiltered plasma.

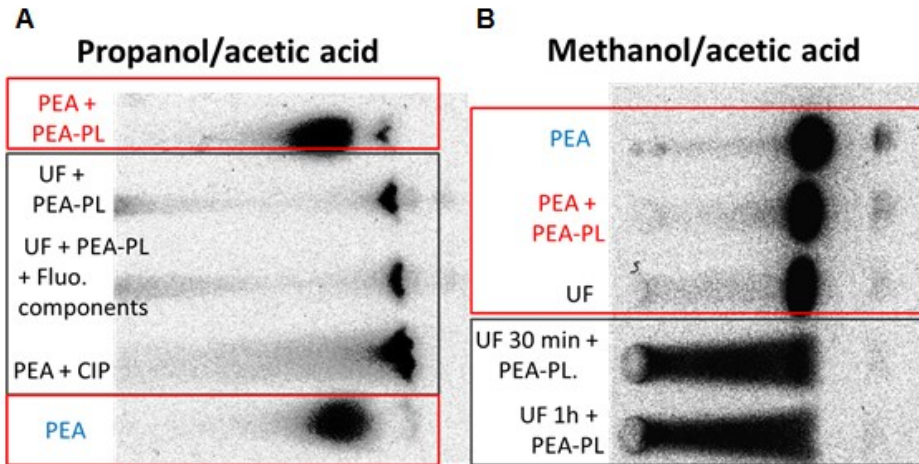


Figure 4: (A) TLC plate in propanol/acetic acid. The assay was performed in solutions containing all the components used in the fluorimetric assay. In the first red box the TLC pattern of a solution containing ^{32}P -PEA and PEA-PL. This pattern resembles that presented in the second red box where ^{32}P -PEA did not react with any enzyme. In the black box solutions containing ^{32}P -PEA-Plasma ultrafiltrate have a TLC pattern similar to that observed in solution with PEA and CIP. (B) TLC plate in methanol/acid acetic acid with two controls in the red box: ^{32}P -PEA in buffer and ^{32}P -PEA-Plasma ultrafiltrate without the addition of PEA-PL and a solution containing ^{32}P -PEA in buffer (not in the ultrafiltrate) and PEA-PL. In the black box ^{32}P -PEA-Plasma ultrafiltrate with the addition of PEA-PL, after 30 minutes and 1 hour.

In sum, our assay is seems currently not apt at measuring the very low concentration of PEA found in blood samples. It seems likely how-

ever that other methods for pre-treating and/or for concentrating may improve the situation. It may also be possible to apply this assay to samples having a different composition and with a higher concentration of PEA (e.g., the urine of patients with hypophosphatasia). Moreover this assay can be used for the detection of the activity of sphingosine-1-phosphate lyase, which has a key role in several processes, like inflammation [26], and for which some detection methods have been published during the last few years [5, 27-30]

REFERENCES:

1. Gibellini, F. & Smith, T. K. (2010) The Kennedy pathway--De novo synthesis of phosphatidylethanolamine and phosphatidylcholine, *IUBMB life*. **62**, 414-28.
2. Aguilera-Romero, A., Gehin, C. & Riezman, H. (2014) Sphingolipid homeostasis in the web of metabolic routes, *Biochimica et biophysica acta*. **1841**, 647-56.
3. Gohil, V. M., Zhu, L., Baker, C. D., Cracan, V., Yaseen, A., Jain, M., Clish, C. B., Brookes, P. S., Bakovic, M. & Mootha, V. K. (2013) Meclizine inhibits mitochondrial respiration through direct targeting of cytosolic phosphoethanolamine metabolism, *The Journal of biological chemistry*. **288**, 35387-95.
4. Modica-Napolitano, J. S. & Renshaw, P. F. (2004) Ethanolamine and phosphoethanolamine inhibit mitochondrial function in vitro: implications for mitochondrial dysfunction hypothesis in depression and bipolar disorder, *Biological psychiatry*. **55**, 273-277.
5. Kashem, M. A., Wa, C., Wolak, J. P., Grafos, N. S., Ryan, K. R., Sanville-Ross, M. L., Fogarty, K. E., Rybina, I. V., Shoultz, A. & Molinaro, T. (2014) A High-Throughput Scintillation Proximity Assay for Sphingosine-1-Phosphate Lyase, *Assay and drug development technologies*.
6. Zeise, M. & Lehmann, A. (1987) Phosphoethanolamine transiently enhances excitability of rat hippocampal neurons in vitro, *Journal of comparative physiology A, Sensory, neural, and behavioral physiology*. **161**, 461-7.
7. Bostwick, J. R., Abbe, R. & Appel, S. H. (1992) Phosphoethanolamine Enhances High-Affinity Choline Uptake and

Acetylcholine Synthesis in Dissociated Cell Cultures of the Rat Septal Nucleus, *J Neurochem.* **59**, 236-244.

8. Chiarla, C., Giovannini, I., Siegel, J. H., Boldrini, G. & Castagneto, M. (2000) The relationship between plasma taurine and other amino acid levels in human sepsis, *The Journal of nutrition.* **130**, 2222-7.

9. Phillis, J. W. & O'Regan, M. H. (2003) Characterization of modes of release of amino acids in the ischemic/reperfused rat cerebral cortex, *Neurochem Int.* **43**, 461-467.

10. Uchiyama-Tsuyuki, Y., Araki, H., Yae, T. & Otomo, S. (1994) Changes in the extracellular concentrations of amino acids in the rat striatum during transient focal cerebral ischemia, *J Neurochem.* **62**, 1074-1078.

11. Phoenix, J. & Wray, S. (1994) Changes in human and rat uterine phosphoethanolamine and taurine with pregnancy and parturition, *Exp Physiol.* **79**, 601-604.

12. Hofford, J. M., Milakofsky, L., Pell, S., Fish, J. E., Peters, S. P., Pollice, M. & Vogel, W. H. (1997) Levels of amino acids and related compounds in bronchoalveolar lavage fluids of asthmatic patients, *American Journal of Respiratory and Critical Care Medicine.* **155**, 432-435.

13. Cusworth, D. (1958) The Isolation and Identification of Phosphoethanolamine from the Urine of of Hypophosphatasia.

14. Licata, A. A., Radfar, N., Bartter, F. C. & Bou, E. (1978) The urinary excretion of phosphoethanolamine in diseases other than hypophosphatasia, *Am J Med.* **64**, 133-138.

15. Kawamura, N., Shinoda, K., Ohashi, Y., Ishikawa, T. & Sato, M. (2011) Biomarker for depression, method for measuring a biomarker for depression, computer program, and recording medium in, Google Patents,

16. Ohga, T. & Ohashi, Y. (2014) Method for measuring ethanolamine phosphate in, Google Patents,

17. Balss, J., Pusch, S., Beck, A.-C., Herold-Mende, C., Krämer, A., Thiede, C., Buckel, W., Langhans, C.-D., Okun, J. & von Deimling, A. (2012) Enzymatic assay for quantitative analysis of (d)-2-hydroxyglutarate, *Acta Neuropathol.* **124**, 883-891.

18. Guilbault, G. G. & Kramer, D. N. (1965) Fluorometric Procedure for Measuring the Activity of Dehydrogenases, *Analytical chemistry.* **37**, 1219-1221.

19. Donini, S., Ferrari, M., Fedeli, C., Faini, M., Lamberto, I., Marletta, A. S., Mellini, L., Panini, M., Percudani, R., Pollegioni, L., Caldinelli, L., Petrucco, S. & Peracchi, A. (2009) Recombinant production of eight

human cytosolic aminotransferases and assessment of their potential involvement in glyoxylate metabolism, *Biochem J.* **422**, 265-272.

20. Candeias, L., MacFarlane, D. S., McWhinnie, S. W., Maidwell, N., Roeschlaub, C. & Sammes, P. (1998) The catalysed NADH reduction of resazurin to resorufin, *J Chem Soc Perkin Trans 2*, 2333-2334.

21. Daykin, C. A., Foxall, P. J. D., Connor, S. C., Lindon, J. C. & Nicholson, J. K. (2002) The comparison of plasma deproteinization methods for the detection of low-molecular-weight metabolites by ¹H nuclear magnetic resonance spectroscopy, *Anal Biochem.* **304**, 220-230.

22. Gibellini, F., Hunter, W. & Smith, T. (2008) Biochemical characterization of the initial steps of the Kennedy pathway in *Trypanosoma brucei*: the ethanolamine and choline kinases, *Biochem J.* **415**, 135-144.

23. Roskoski Jr, R. (1983) Assays of protein kinase, *Methods in enzymology.* **99**, 3-6.

24. Schioli, D., Cirrincione, S., Donini, S. & Peracchi, A. (2013) Strict reaction and substrate specificity of AGXT2L1, the human O-phosphoethanolamine phospho-lyase, *IUBMB life.* **65**, 645-50.

25. Bligh, E. G. & Dyer, W. J. (1959) A rapid method of total lipid extraction and purification, *Can J BiochemPhysiol.* **37**, 911-917.

26. Serra, M. & Saba, J. D. (2010) Sphingosine 1-phosphate lyase, a key regulator of sphingosine 1-phosphate signaling and function, *Adv Enz Regul.* **50**, 349-362.

27. Bandhuvula, P., Fyrst, H. & Saba, J. D. (2007) A rapid fluorescence assay for sphingosine-1-phosphate lyase enzyme activity, *J lipid res.* **48**, 2769-2778.

28. Bandhuvula, P., Li, Z., Bittman, R. & Saba, J. D. (2009) Sphingosine 1-phosphate lyase enzyme assay using a BODIPY-labeled substrate, *Biochem Biophys Res Commun.* **380**, 366-370.

29. Reina, E., Camacho, L., Casas, J., Van Veldhoven, P. P. & Fabrias, G. (2012) Determination of sphingosine-1-phosphate lyase activity by gas chromatography coupled to electron impact mass spectrometry, *Chem Phys Lipids.* **165**, 225-231.

30. Billich, A., Beerli, C., Bergmann, R., Bruns, C. & Loetscher, E. (2013) Cellular assay for the characterization of sphingosine-1-phosphate lyase inhibitors, *Anal Biochem.* **434**, 247-253.

